A New Method of Calibrating Wireline Logs With Carbonate Core Measurements To Recognize Pay Zones

by

Varma Gottumukkala

Thesis

Submitted in Partial Fulfillment of the Requirements for the Degree of

Masters of Science in Petroleum Engineering

Department of Petroleum and Natural Gas Engineering

New Mexico Institute of Mining and Technology

Socorro, New Mexico 87801.

August 2002.

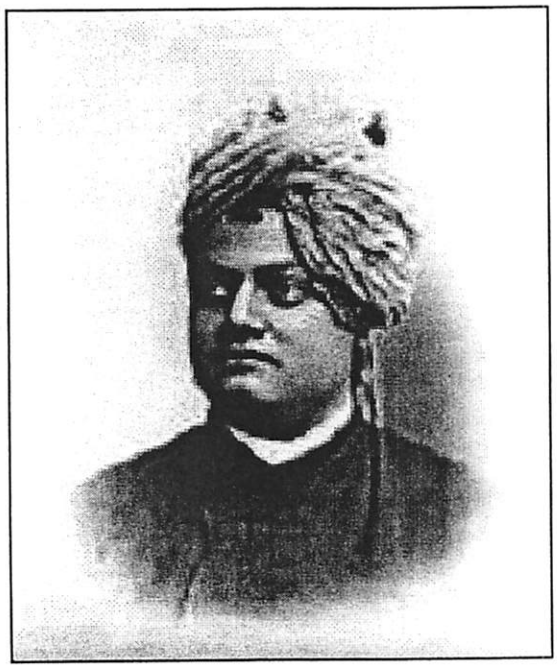

Swami Vivekananda

"The secret of religion lies not in theories but in practice
To be good and do good - that is the whole of religion"

"One may gain political and social independence, but if one is a slave to his passions and desires, one cannot feel the pure joy of real freedom"

-Swami Vivekanada

This work is dedicated to my loving parents **Koteswara Raju Gottumukkala, Rama Gottumukkala** and to my lovely fiancé **Aruna Varma**

- Varma Gottumukkala

ABSTRACT

Defining the initial water saturation in a dolomite reservoir in Southeast New Mexico was problematic and resulted in questions about possible oil left behind pipe after development. The application of Archie's equation was particularly suspect because of the variation in the resistivity of connate water samples. Cores and logs were available from six wells in the Dagger Draw Field and showed interstitial, fractured and vuggy porosity. A global prioritizing technique called fuzzy ranking was used to select log tracts to correlate with core measurements.

Selected log tracts then served as inputs to a neural network to develop multivariate correlations with the core measurements. The cores defined bulk volume oil, bulk volume gas, bulk volume water and aspect ratio. The focus of this research is the estimates of bulk volume oil, gas and water. Optimal neural network architectures were developed for each of the six available well datasets. All architectures were designed to maintain a ratio of neural network weights to samples ratio less than 0.5.

Each network was blind tested against the remaining five datasets. One of the datasets with 200 whole core measurements was found to be particularly robust and was used to generate BVO logs in fourteen partially cored and un-cored wells in the field.

The statistical properties sum, average, and standard deviation calculated with the BVO, BVG and BVW logs correlated with the initial oil, gas and water-producing rates. Thus a new method to recognize behind pipe pay zones in a dolomite/carbonate reservoir and estimate the first years oil-producing rate was developed. The method has particular utility in finding bypassed pay for recompletion projects [7].

ACKNOWLEDGEMENTS

I am indebted to my research advisor, Mr. Bill Weiss, Head of Reservoir Evaluation and Advanced Computational Technologies group, Petroleum Recovery Research Center for providing continuous guidance, encouragement and financial support through out this work. I would also express my gratitude to him for always being available for assistance.

I would like to thank my academic advisor Dr. Thomas Engler for his support and always encouraging me with his discussions, and my committee member Dr. Her-Yuan Chen for his guidance and thought provoking class room discussions. Apprecitaion is also extended to Dr. Ronald Broadhead for providing the geological information and encouraging discussions.

I would like to thank all faculty members of Petroleum and Natural Gas Engineering Department and Petroleum Recovery Research Center for their excellent support through out my studies.

Thanks to all my friends for their support and happy moments.

TABLE OF CONTENTS

LIST OF FIGURES

LIST OF TABLES

NOMENCLATURE

a : Empirical constant based on lithology

BVO : Bulk Volume Oil

BVG : Bulk Volume Gas

BVW : Bulk Volume Water

f,v : Activation function

F : Formation volume factor

in1 : Input variable 1

in2 : Input variable 2

m : Empirical constant of the matrix

n : Total no of records

r : Correlation Coefficient

R_w : Water resistivity

R_t : Total resistivity of the formation

S_w : Water Saturation

S_o : Oil Saturation

S_g : Gas Saturation

S, STD: Standard Deviation.

wl : Weights

$_i$: Desired output for pattern I

$\bar{x}$: Mean

$\overline{Y}$: Average

y_i : Network output for pattern i.

ϕ : Porosity

CHAPTER I

Introduction

The Dagger Draw field is located on the margin of the North West shelf basin and Delaware Basin in Southeast New Mexico. It is one of the most productive oil fields in New Mexico. In 1996 oil production was 14% of New Mexico's total annual production.

The location of the Dagger Draw field is shown in Figure 1.1. The Dagger Draw field boundaries are restricted by the following geological features.

- Huapache Monocline (South west)
- North west shelf Basin (North)
- Delaware Basin (East)
- Indian Basin (South)

Upper Pennsylvanian (Cisco/Canyon) and lower Wolfcamp carbonates of the Dagger Draw field are the most productive zones of oil and gas. Since its initial development the upper Pennsylvanian (Cisco/Canyon) section has contributed significant amount of gas production in Southeast New Mexico, and is anticipated that it will continue to do so for many more years.

More than 1.846 TCF of gas had been produced since 1990, from the 26 designated reservoirs in the play with production greater than 5 BCF. But, by the end of twentieth century only one third of the 1800^{+} original producing wells were active, and an increase of development activity was underway, which indicates much more oil and gas remains to be produced from this play.

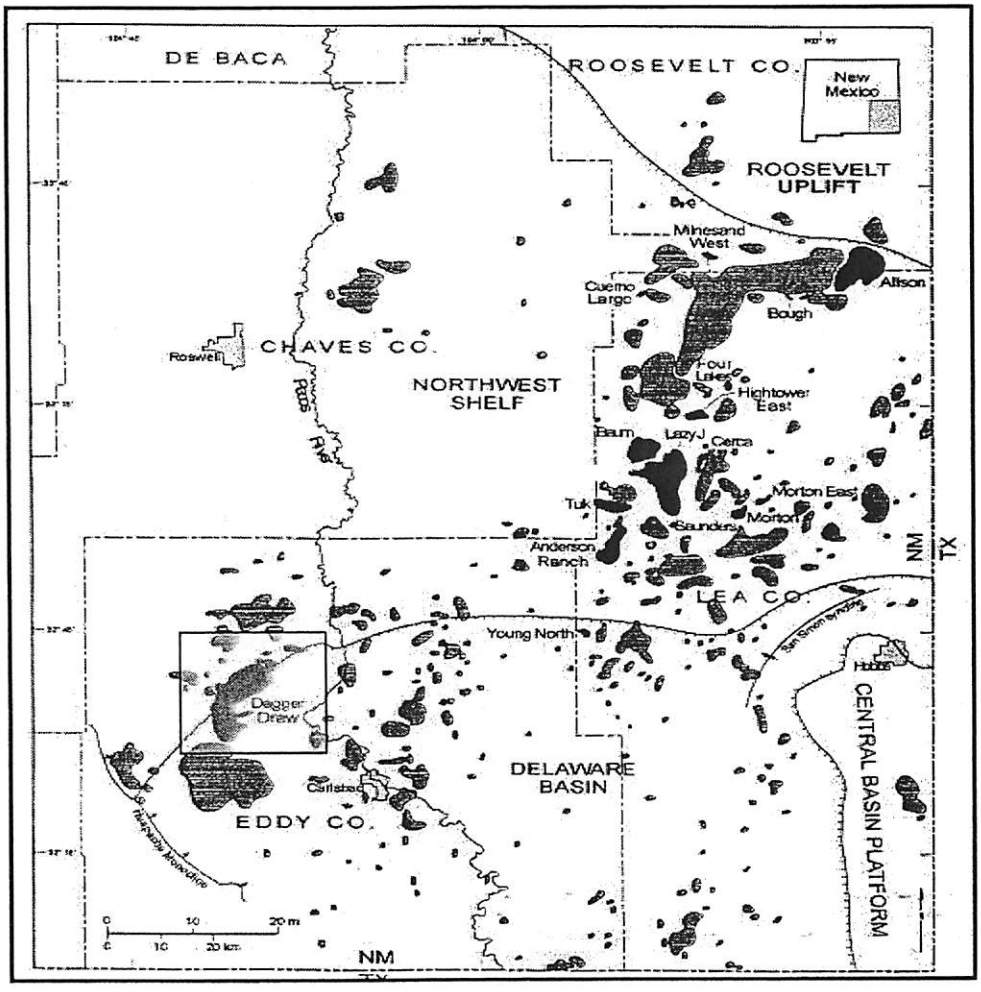

Figure 1.1: Upper Pennsylvanian lower Wolfcamp oil and gas fields in Southeast New Mexico and study area.

1.1 Dagger Draw Production History

Dagger Draw field when discovered consisted of two distinct fields (Dagger Draw North and South) Dagger Draw North was discovered in 1964. When first produced the annual production of the discovery well was only 6000 bbl of oil, after that the well was shutin and the field was abandoned in 1965. The discovery of the Dagger Draw South Field was in 1971, when two additional wells were drilled. In 1973, three more wells were drilled and started producing. Only 17 producing wells were drilled since 1979 and development in both fields was slow.[2]

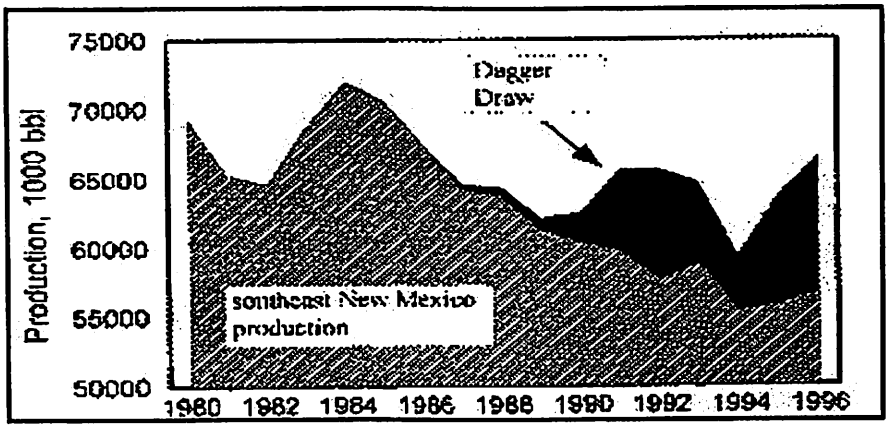

Figure 1.2: Plot showing the Dagger Draw production during 1980-1996

In 1988 the operators initiated a redevelopment plan by extending the field with new step out wells. This redevelopment resulted in the removal of the boundaries between the two fields, thus producing from a common reservoir. The annual production rate increased from approximately 200,000 bbl in 1987 to a peak of 9.8 million bbl in 1996 and by the end of 1997 only 399 wells were productive. The annual production rate from 1980 to 1996 is shown in the Figure 1.2. During those years New Mexico's oil

resources were depleting and at that stage Dagger Draw contributed significantly to maintain production.[2,3]

Initially wells were drilled on the structurally high parts of the field. The development of the field was based on the structural entrapment of oil. It was not until redevelopment, that the stratigraphic nature of the trap became apparent. The Dagger Draw Field trap is formed by a dolomitized shelf margin carbonate bank complex. Algal mounds along the dolomitized bank trend produced the best porosity. Using borehole-imaging logs, the redevelopment of the field was spurred.[2,3]

At first, it was thought that the combination of low porosity and high production was caused by brecciated or fractured reservoir. But, conventional porosity logs indicated that porosity was less than 7% through out the reservoir. With initial production rates greater than 2000 bbl/day a good reservoir permeability was estimated. The bore-hole imaging logs that were run in 1980's indicated that a large percentage of the porosity is formed by a network of interconnected secondary vugs, which are unable to be detected by conventional porosity logs.[2,3]

Subsequent reevaluation of the reservoir generated redevelopment that transformed Dagger Draw into the most productive field in New Mexico. Dagger Draw Field has a water to oil ratio of 3.7:1, due to this, disposal of large volumes of production water became expensive. Inspite of the high costs associated with water disposal, down-

hole pumps were used to produce sufficient volumes of fluid to render the field economic.

Development of the upper Pennsylvanian reservoir includes two geographic areas in Southeast New Mexico: one is North Lea, East Chaves, and Roosevelt Counties and the other is West Eddy County. These two geographic areas in the upper Pennsylvanian reservoir have distinct reservoir qualities; the Northeast region characteristically produces associated gas, water and large quantities of oil from a system of relatively thin (10ft -35ft) intervals, but laterally extensive shelf limestone's ranging from 5900 to 11500 ft deep.

Conversely, the upper Pennsylvanian formation of Eddy County produces large quantities of both associated and nonassociated gas, water and lighter condensate, from higher relief, shelf-margin dolomite banks found at depths ranging from 6600 to 9600ft and exemplifies a complex reservoir.

These shelf margin dolomite banks generally are stratigraphically bounded by tight shelf limestones and shale's but again are commonly situated over older, influenced upper Pennsylvanian carbonate deposition, and also influences the recent day productive behavior.

A strong hydrodynamic water drive that is induced from the Huapache monocline provides the trap for the Indian basin/Dagger draw complex. Because of this water drive

the gas/oil/water contacts which are spread along the axis of the dolomite bank were tilted and thus complicated the fluid relationships in structurally lower parts of the reservoir.[2,3]

1.2 Geology

Oil fields in the Canyon and Cisco section (Pennsylvanian: Missourian and Virgilian) and in the lower Wolfcampian (Permian) occur primarily in shelf and shelf margin carbonates on the Northwest shelf of the Permian Basin and Delaware basin, which was relatively shallow during the late Pennsylvanian and earliest part of Permian. Most of the fields are located in Northeast Lea, Eddy Counties and in Southern Roosevelt County.

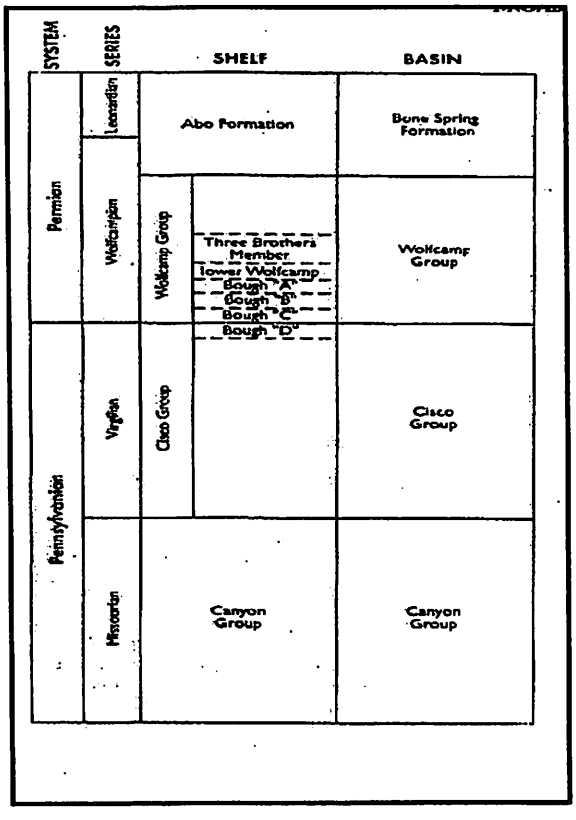

Figure 1.3: Stratigraphic column of upper Pennsylvanian and Wolfcampian rocks

These oil fields produce from the lower part of the Wolfcamp carbonates (Permian), Canyon group (Pennsylvanian: Missourian) and Cisco group (Pennsylvanian: Virgilian). Most of the production is from Canyon and Cisco groups (upper Pennsylvanian) in the Northern Eddy County and minor production from the lower Wolfcamp Figure 1.3.[2]

Oil fields formed by shelf margin dolomite banks are found in back bank shelf limestones and their depth to production interval ranges from 6,600 to 9,600 ft. These reservoirs with relatively thin zones of interconnected vugs exhibits high permeability, and therefore have excellent productive capability.[2,3]

1.3 Trap Mechanism

The Dagger Draw Field is formed by a combination trap (stratigraphic/hydrodynamic). The trapping mechanism is stratigraphic in nature, with lateral and vertical seals formed by impermeable shales and shelf limestones. The reservoir consists of a dolomitized shelf-margin carbonate bank in the Canyon and Cisco groups (upper Pennsylvanian). As a result of dolomitization, vuggy and intercrystalline pores within the algal mounds were formed, where the predominant lithology is dolomitized algal boundstones which forms a reservoir.

The dolomite bed is sealed by impermeable shales and shelf limestones (Figure 1.4). The net pay thickness of the dolomite bed is approximately 75 ft and the gross thickness exceeds 380ft along the depositional axis of the carbonate banks. Although,

primary trapping mechanism is stratigraphic, structural trap appears to locally influence productivity and a dynamic water drive tilted the oil-water contacts from the Southwest to the Northeast.[2]

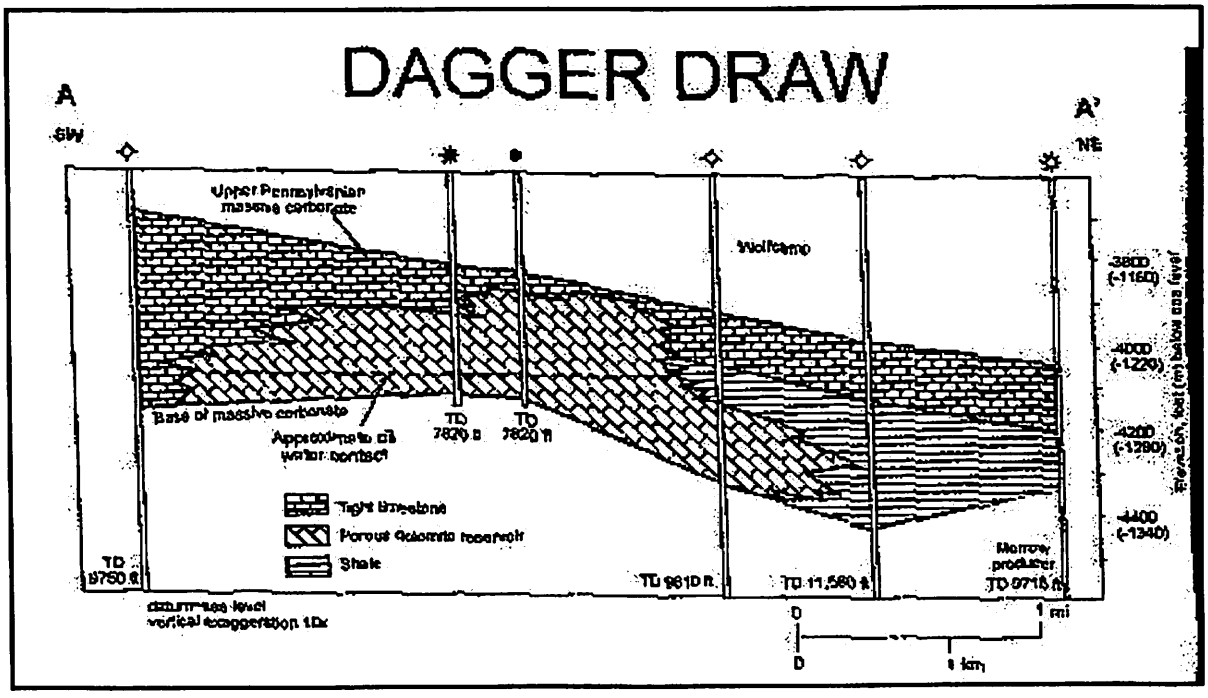

Figure 1.4: East-West structural cross section through Dagger Draw Field, showing productive facies and shale limestones seal.

1.4 Reservoir Properties

Conventional log porosities were quite low (< 7%), for most of the upper Pennsylvanian dolomites, but their productive capabilities exhibit good permeability. This has been commonly thought as a result of brecciation and well developed reservoir fracturing, but as a result of information obtained from the borehole imaging tools, most of the porosity present is interconnected secondary vugs which was not recognized earlier either by coring or other porosity measurements.

The Northwest updip back reef shelf limestones of the dolomite trend are also productive, but are generally less permeable than the dolomite facies and produce dry gases. Most part of Eddy County had been designated as a tight formation due to tight nature of the limestones, and low porosities in both dolomites and limestones.[3]

CHAPTER II

Neural Networks and Fuzzy Tools

Neural Network is a kind of artificial intelligence technology, which mimics the characteristics of biological neurons. Artificial neural systems or neural networks acquire, store, and utilize knowledge by learning just like human information processing system. The knowledge embedded in the artificial neural systems can be recalled in response to the presented information.[4]

There are several types of neural networks. The choice of the neural network depends on the problem requirements and data availability. A Back Propagation Network (BPN) could be used, if it is desired to predict the response of a new well from the time it is put on production, and then on. A Recurrent Network (RN) could be used if variations in the flow rates are expected, for example due to changes in operating pressures. It is desirable to use a BPN when the rate profiles of all the wells are smooth and monotonous. Recurrent Networks are effective in predicting highly randomized cases, but are more complex and take longer to train than a BPN.[5]

The Back Propagation Neural Network is the one, which is most widely used for engineering purposes. A schematic diagram of the back propagation neural network is shown in Figure.2.1.

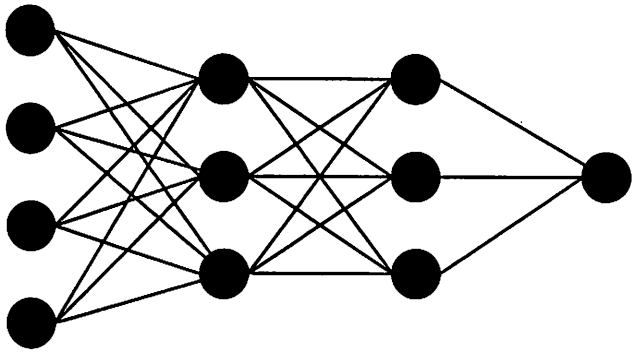

Figure 2.1: Structure of Back Propagation Neural Network.

2.1 Neural Network Architecture

The neural network usually consists of at least three layers. They are input layer, hidden layer and output layer. Each layer has a number of neurons or nodes represented by black circles in Figure 2.1. Each input neuron contains actual data introduced to the network externally. Depending on different applications, the hidden layer between the input layer and the output layer can be one or more than one.[1]

Each neuron in the output layer gives a response to the input data set provided. The neurons between layers are interconnected by different paths called weights. These weights determine how a particular set of inputs be sent to neurons in hidden layers through the connections established and so on, from hidden layer to neurons in the output layer. Training the neural network determines the number of weights.[5]

Establishment of a neural network is to train the neural network by adjusting the connections of the neurons (weights) between input, output and hidden layers, so that the

network can give desired output sets for given input data. During training, the weights are randomized between the ranges of 0 to 1. The input data matrix is multiplied by the weights connecting the input layer and the hidden layer to produce a new matrix. A transfer function is used to transfer this matrix to another matrix, which is the output of the middle layer neurons.

The obtained matrix is multiplied by the weights associated with the middle-output layer to generate a new matrix. Similarly a transfer function is used to transfer the matrix from the middle layer to output layer neurons. An example of the matrix multiplication is shown below in Figure 2.2.

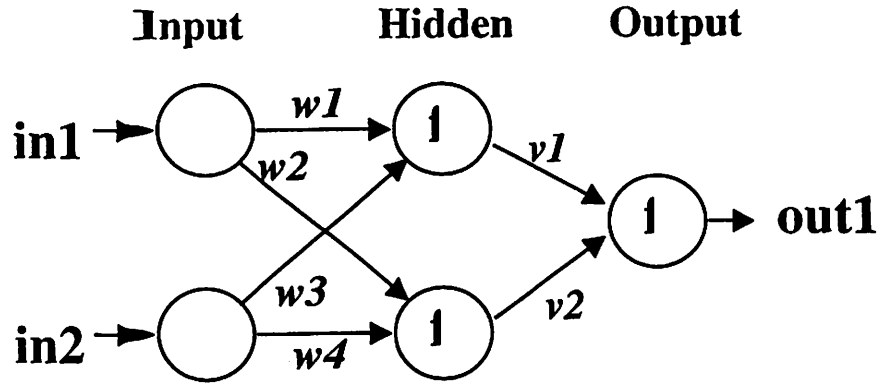

Figure 2.2: A fully connected three-layer feed-forward neural network with two neurons in both the input and hidden layers and one in the output layer

$$out1 = f(v_1 \times f(w_1 \times in1 + w_3 \times in2) + v_2 \times f(w_2 \times in1 + w_4 \times in2)) \quad (2.1)$$

$$\textit{where } f \textit{ represents the activation function, } f(x) = \frac{1}{1+\exp(\alpha x)} \quad (2.2)$$

The obtained output results are compared with the desired outputs to calculate the discrepancy. The weights are updated based on the discrepancy from output layer to input layer (Back Propagation Network) until a specified convergence criterion is satisfied for all input data sets and desired output sets.[5]

During training, the network is processed with N patterns where N is the number of logs. Each training well may have several different input-output relations for several times. During this process of training, the disparity of the output value is computed after a selected number of passes, and is compared against a user defined convergence criterion like the correlation coefficient. The higher the correlation coefficient the better the convergence which means the training can be terminated and the network is ready to predict. The accuracy of the trained network is evaluated by the mathematical functions in equation 2.1 and 2.2, which are used to calculate the correlation coefficient.

$$\overline{Y} = \sum_i \frac{y_i}{n} \tag{2.3}$$

$$r^2 = 1 - \frac{\sum_i (x_i - y_i)^2}{\sum_i (x_i - \overline{Y})^2} \tag{2.4}$$

The correlation coefficient is given by

$$r = \sqrt{r^2} \tag{2.5}$$

Where n is the number of patterns or records, x_i is the desired output for pattern i, y_i is the network output for pattern i, and $\bar{Y}$ is the average of the output values produced by the network. The two parameters (r^2 and r) are computed for both training and testing portion of the data file.[9]

The closer the correlation coefficient is to 100%, the better the network gets trained. A 100% correlation can never be achieved, but in practice the network usually trains to 90-95% correlation. Once the network is trained, we can use this trained file to predict unknown outcomes for given values of input parameters. If the disparity is greater than the convergence criterion desired, then the weights (connections) are updated and training is continued. The network has the same architecture during predicting and training stages.

Neural Network approach has several advantages. It does not require an explicit functional relationship between the input and output variables. It can be trained, to learn from past available data by history matching and approximate the nonlinear relationships to any degree of accuracy. It is applicable to multivariate systems also. One of the significant drawbacks of neural network approach is that, the input-output nodes of at least one particular data set should be provided before training. The number of input variables and type of input variables, which are going to be used to train the neural network cannot be easily determined from neural network analysis.

2.2 Guidelines for Placing Training Wells:

The goal is to develop a network with the minimum number of training wells, which is capable of generating accurate predictions. The neural network performs a non-linear interpolation between the logs of the training wells in order to predict the production rate profiles of the new well. Thus, it is important to ensure that the locations of the training wells do not result in an extrapolation process. Hence, the reservoir must be delineated by training wells.[5]

The wells that are going to be used for training must be placed near external boundaries and internal discontinuities, and they must sample the open regions of the reservoir. In addition, training wells should be placed near some existing wells to provide a characteristic interference correlation, while constructing the network.

2.3 Input-Output Selection Criteria and Limitations of Neural Networks

During the field development study, the key questions to be addressed are as follows:

1) What are the variables that we would like to predict? Include only those variables in the output.
2) What are the input variables that effect the output variables chosen? Are these input variables measurable and are effected by time? For example, the block pressure has an effect on the production of the well drilled. Therefore, it must be excluded from the input sets.

3) There are two types of technical barriers that today's neural networks face: (a) the inability to handle large amounts of data records.(and as a result rely on sampling), (b) the inability to deal with a large number of data fields (due to network suffocation).[5]

2.4 Fuzzy Tools

Fuzzy logic, expert systems, neural networks, and genetic algorithms are some of the efficient ways to handle problems that are rife with ambiguity. Although each method handles the uncertainty in different ways, they are part of the third generation technologies that will have an immense influence on the way we do things in future. If you use a blend of these technologies, the results are sometimes better than the sum of their parts.

For instance, combining the computational power of neural networks with the symbolic level of processing conveyed by fuzzy logic for selecting the input data sets, results in a synergy that improves speed, fault tolerance, and adaptiveness.

Fuzzy logic is a mutlivalued logic that allows for degree of set membership (e.g poor, intermediate, good, and excellent). In fuzzy logic, the three logic operations AND, OR and NOT return a degree of membership rather than a traditional Boolean values (TRUE (1), FALSE (0)). The fuzzy logic improves the human ability to reasoning and makes use of approximate data to find precise solutions.

The three main distinguisable features of fuzzy logic are (a) use of symbolic variables "in place of" or "in addition to" instead of numeric variables (b) characterization of simple relation between variables by using fuzzy condition statements and (c) characterization of complex relations by fuzzy algorithms. These features are currently being exploited for dynamic use of neural networks for pattern classification and in the design of neuro-fuzzy learning control systems.[4]

Fuzzy ranking is a tool used to select variables that are globally related. We find this as an excellent tool to select neural network inputs by filtering the noise in the dataset. The following fuzzy membership equation defines the first step in the filtering process. These fuzzy tools are used to fuzzify data for selecting appropriate inputs.[10]

$$\text{Fuzzy Membership Function, } F_i(x) = \exp\left(-\left(\frac{x_i - x}{b}\right)^2\right) \times y_i \qquad (2.6)$$

Figure 2.3 illustrates the application of the fuzzy membership function to a totally random dataset "with out a trend" and a correllatable dataset "with trend" noise added in both cases. The points defined by the fuzzy membership function are then used to generate fuzzy curves (defuzzyfication), shown in Figure 2.5 and defined by:

$$\text{Fuzzy Curve Function, } FC(x) = \frac{\sum_{i=1}^{N} F_i(x)}{\sum_{i=1}^{N} \frac{F_i(x)}{y_i}} \qquad (2.7)$$

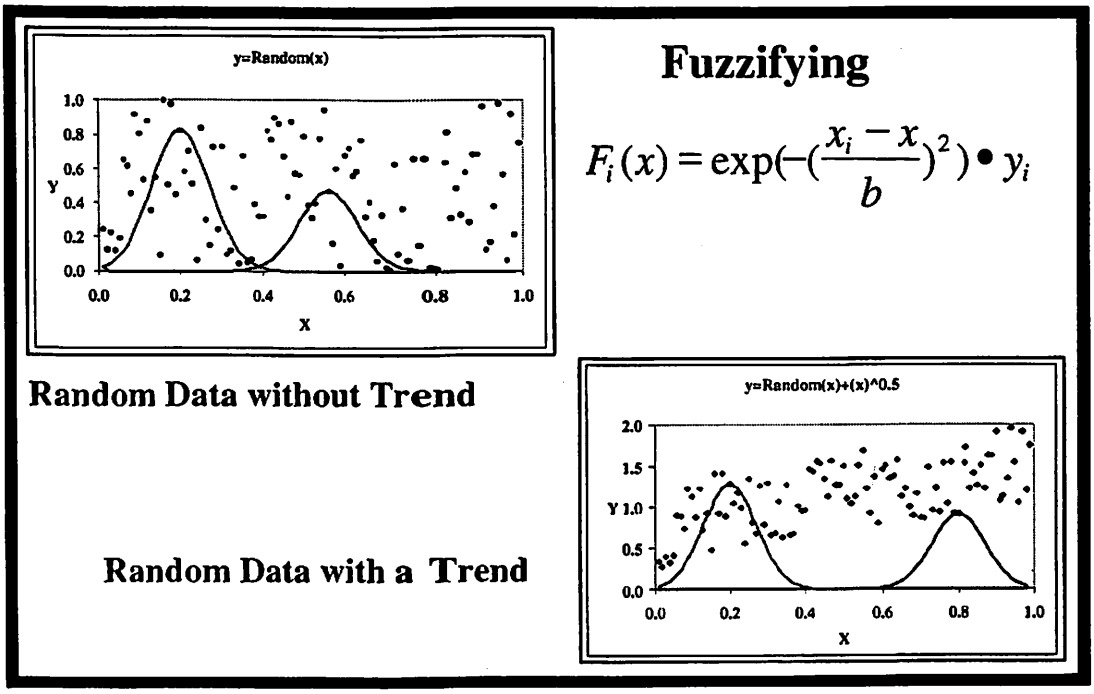

Figure 2.3: Fuzzifying a totally random dataset and a random dataset that includes a trend.

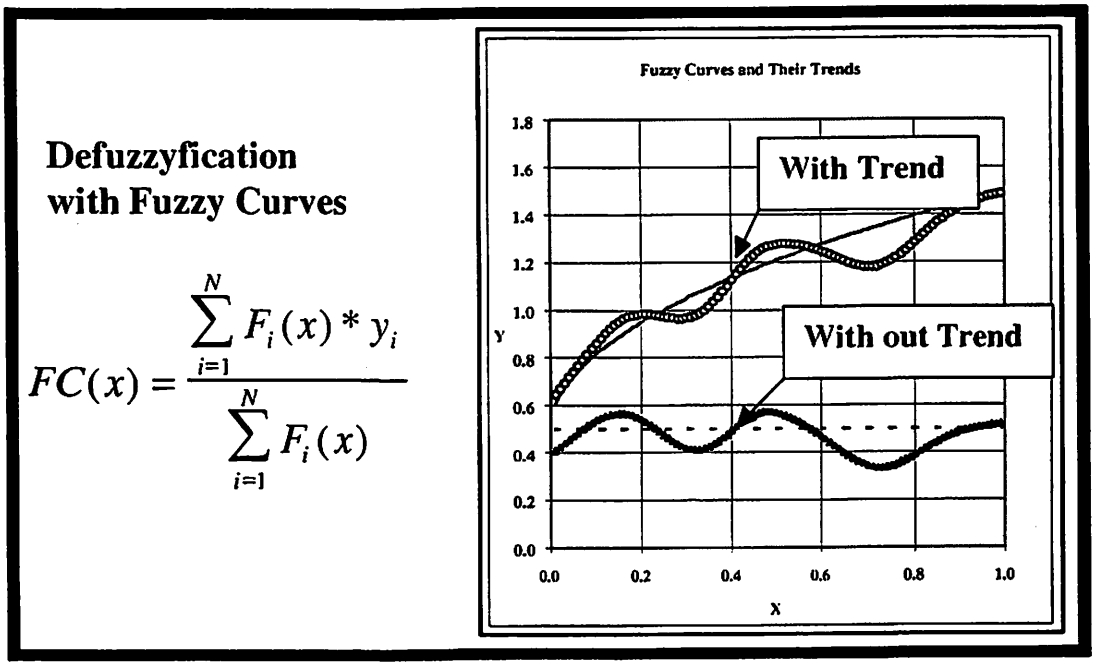

Figure 2.4: Fuzzy curves with trend and with out trend.

The fuzzy curve that resulted from the random dataset "without a trend", plots as a straight line (Figure 2.4), where Y is constant as X increases and is of no value in regression analysis. However, the noisy dataset "with trend" imposed shows that there is a correlation upwards and to the right between X and Y.[7]

Thus, a fuzzy curve can be used to find variables that correlate in a noisy dataset. Of course real datasets are more complex than those seen in the Figure 2.3. This ranking technique is referred to as single stage fuzzy ranking; more recently a two-stage fuzzy ranking process was developed to enhance the ranking procedure.

CHAPTER III

Predict Online and Log Responses

Predict online is the interface for neural network simulator, used to develop correlations between the well logs and core data. The Stuttgart Neural Network Simulator (SNNS) is actually an MLP (Multi Layer Perceptron) neural network software present on a remote server. A typical neural network can have any number of inputs and outputs but "Predict Online" has only one output. The complexity of the hidden layers of the network is a user defined parameter.[11]

The network typically requires two types of input files. One is for training, and the other for predicting the results after training. The training file uses the available log data and core data as inputs. This file contains input values of all known patterns. This file will be used to train the neural network and later again to test the network for best correlations. The output of the training and testing process is the trained network.

In general we use well logs (geophysical logs) as input variables, and core data as output variables to train the neural network. Well logs provide information about the lithology, presence of hydrocarbons, porosity, permeability and resistivity of the formation. They also provide information to map the isopach, isolith and the net pay thickness of the reservoir zone. Geophysical logs are simple and economical to obtain

reservoir information; more over they provide continuous and accurate data of the formation for each 0.5ft interval other than the core data. There are several different types of logs like SP log, G-Ray log, Resistivity log, Density Porosity log, Neutron Porosity log, Photo Electric Factor log, and Sonic log. Following is a brief introduction to each of these logs.

3.1 Caliper Log

Caliper log measure the bore hole diameters and evaluate borehole environment for logging measurements. It also identifies mudcake depositions and estimates hole volume to determine cement volume requirements, component formations to set packers and provide position data for dip meter interpretations.

The main advantage of caliper log is, it also reads the anisotropic mechanical properties of the formation. The more vuggy and loose the formations, the more fluctuation we see in the log readings.[6]

3.2 Spontaneous Potential Log (SP Log)

The SP log works on the principle of difference in electric potential between the fixed electrode at the surface and the movable electrode in the borehole. SP log performs well in a borehole with fresh mud and salty mud but not in empty or cased holes because a conducting media is needed to measure the potential difference. The main function of the SP log is, it allows us to distinguish between shale and clean formation. If the

potential on the log scale is positive then it is most likely a shale, if it is negative it should be clean formation.[6]

SP log can be used to calculate the water resistivity and water saturation of the formation using Archie's law when provided with mud filtrate resistivity

$$F = \frac{a}{\phi^m} \tag{3.1}$$

Archie's equation:

$$S_w = \sqrt{\frac{F * R_w}{R_t}} \tag{3.2}$$

Where F =Formation volume factor
R_w=water resistivity
R_t = Total resistivity of the formation
ϕ = Porosity

3.3 Gamma-Ray log (GR Log)

The Gamma Ray log is a continuous measurement of the natural radioactivity emanating from the formation, it does not have any fixed source in the tool that emits G-Rays, but it has a detector. The sensitive detectors present on the tools count the number of G-Rays per unit time. Principle isotopes emitting radiations are Potassium-40, Uranium and Thorium. These isotopes are much highly concentrated in clays thus radioactivity in shales is very high.

Air drilling increases the logging response for a G-Ray tool, because there is no media, which obstructs the tool from detecting the gamma rays. In general, the more is the G-Ray count, higher probability of shale.[6]

3.4 Resistivity Log

The Resistivity is defined as the resistance offered by a substance per unit area and length. Resistivity and conductivity are inversely related. Hydrocarbons are bad conductors of electricity. So greater resistivity indicates a presence of hydrocarbons.

The Resistivity logs are classified as tow types Induction logs and Lateral logs. The Induction log tool has one source electrode and one monitor electrodes, where as in a lateral arrangement we will have two monitor electrodes, the source electrode sends some electric signals through the formation and the monitor electrode detects the returned signals. These Resistivity logs are further classified into three types depending on the depth of investigation Shallow, Medium and Deep. By using Resistivity logs, the presence of hydrocarbons can be detected. The higher the resistivity, the more probability for a presence of hydrocarbons.[6]

3.5 Sonic Log

The Sonic log is used to find the presence of hydrocarbons and mainly porosity. The Sonic log transmits sound waves through the formation, sound travels faster in solid than liquid and gas media. Basic Sonic log will have one transmitter and two detectors

laterally arranged. By measuring the time required for the sound waves to travel through the formation, the porosity can be calculated.

Transient time is defined as the time difference between the source and receiver. So, the more the time is, the higher probability for a presence of liquid or gas rather than solid media. If the transient time is less the porosity is less, which means the formation is compacted without any pore spaces.[6]

3.6 Density Porosity Log

The Density Porosity Log is used to measure the porosity of the formation. This works on the same principle as a G-Ray log, but here we will have a source electrode which emits gamma rays, the emitted rays loose their energy when obstructed by the formation and scatters, these scattered gamma rays travel through different directions in the formation and some of them are absorbed by the formation.

So higher reflection of G-Rays means the rock is porous.In the presence of shale, the detector can only measure very less amount of gamma rays returning back, as the presence of shale absorbs the gamma rays from the source. We can calculate the porosity of (limestone, sandstone, dolomite) if we know the bulk density and the mud filtrate density of the formation using this log.[6]

3.7 Neutron Porosity Log:

The Neutron Porosity Log is used to measure the porosity of the formation. The Neutrons emitted from the radioactive source collides the formation and looses energy

primarily depending on hydrogen concentration because hydrogen is of the same size as neutron and looses around 67% energy per collision made by a neutron.

Hydrogen looses more energy with a collision than any other atom. If there is a presence of hydrocarbons in the formation, the neutrons coming back to the detector will be less as most of them loose their energy by colliding with the hydrogen atoms in the formation. Depending on the type of collision and the depth of investigation two types of Neutron Porosity logs are used Sidewall Neutron Porosity log (SNP) and Compensated Neutron Porosity log (CNL). Compensated Neutron Porosity log is most widely used because of its deeper depth of investigation and can be used in both open and cased hole logging.[6]

3.8 Photo Electric Factor Log (PEF Log)

The Photo Electric Factor log distinguishes the mineralogy of the formation regardless of porosity and fluid type. PEF is a strong function of the matrix and formation. Basing on the Pe (PEF) values the lithology of the formation is determined.[6]

Lithology	Pe Index
Quartz	1.81
Calcite	5.08
Dolomite	3.14
Anhydrate	5.05

Table 3.1: Photoelectric factor values for lithology of the formation.

3.9 Log Responses for Different Types of logs Based on Porosity

The following table shows log responses for different geophysical logs based on porosity and lithology of the formation.

Well Logs	Type of Response	Porosity/Water Saturation
SP log	Positive Potential	Less Porous, High shale content
Gamma Ray	High G-ray Count	Less Porous, Probably shale
Resistivity	High Resistivity	Low water saturation
Sonic	Large transit Time	Porous
Density Porosity	Low G-ray Count	Less Porous, Probably shale
Neutron Porosity	Less Neutron count	Porous, Presence of Hyd
Photo electric Factor	High PEF Index	Cal/Anhyd based on other logs

Table 3.2: Probable variations of well logs with porosity and saturation.

CHAPTER IV

Digitization

4.1 Procedure to Digitize Log Data

The available log data obtained from the wells should be digitized in order to train the neural network as "Predict Online"(neural networks interface) accepts only ASCII format files. The log data is usually available in the form of X-Y plots. This has to be digitized to get the data into (x, y) co-ordinates or ASCII format file; this process of converting plotted X-Y values to (x, y) co-ordinates is called Digitization. Digitization produces a text file in ASCII format. The software used for digitizing logs is "NDS Neural Log".

The first step in the process of digitizing is to scan the available well log data in the zone of interest, usually production interval using "NDS Neural Log" software. Starting with the software first click on the "Fax Scan" option, the user will be prompted with the "Fax Scan" window as shown in Figure 4.1.

Create a file as desired mostly the well name and the log type we are digitizing, in the "Projects" menu and select the "Images" option prompted in the next window and click "Scan". It is important to note that the maximum character length for the file name

cannot be greater than "8". Once the desired section of the log was scanned, we can stop the scanning by clicking the cancel button.

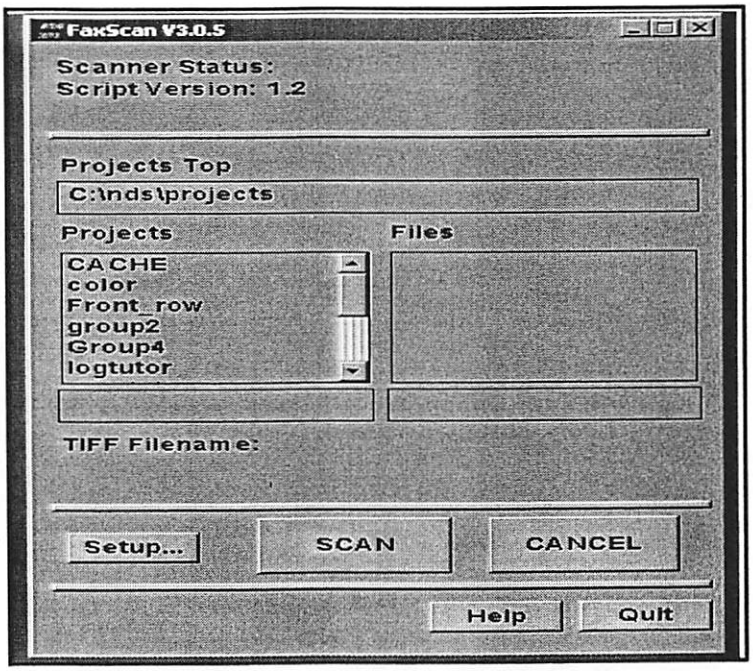

Figure 4.1: Scanner pop up window for "NDS Neural Log" software

To digitize the scanned image file click "create" then a pictorial view of the log that was scanned, will be displayed as shown in Figure 4.2. We can adjust the image to a convenient size by clicking the zoom "+ or –" at the bottom left hand corner. Then provide the maximum and minimum depths of the zone of interest in the column provided on the top right hand corner and mention the units.

Now, we need to provide the left and right values of the log, for porosity logs the left and right values varies in between 0.01 to 0.5, these values vary depending on the type of log we choose to digitize. Select the left and right values from the log header and

input those values in the columns provided on the bottom right hand corner by clicking on the log.

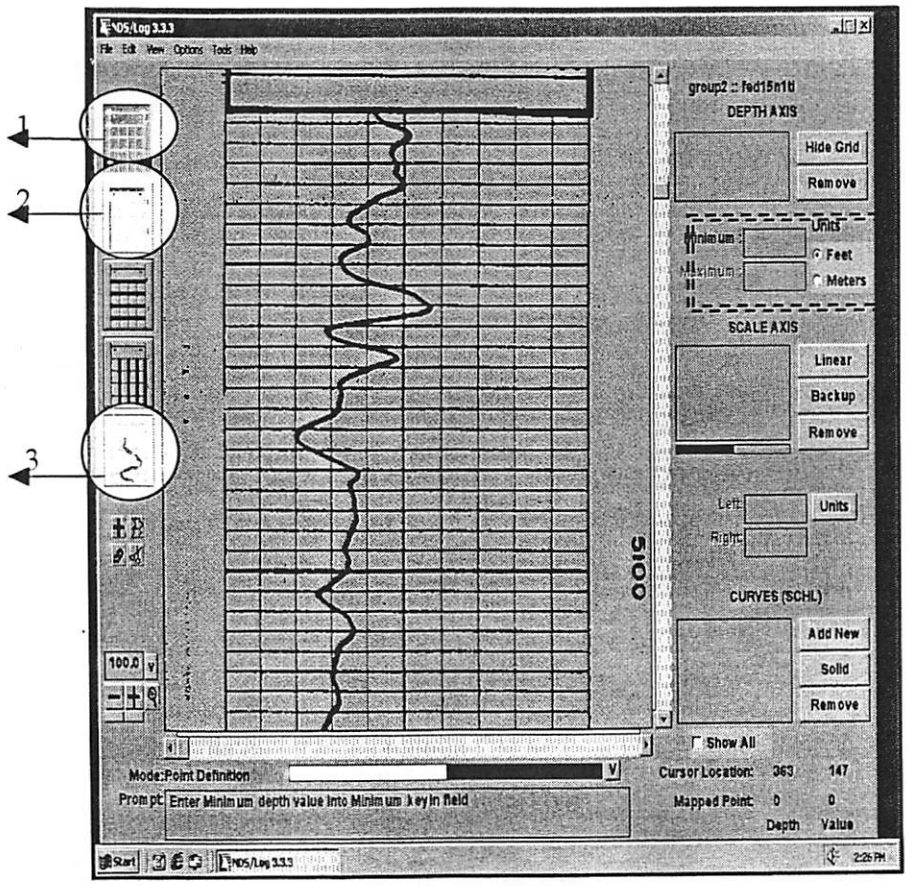

Figure 4.2: Window showing the scanned log using "NDS Neural Log"

The left and right values should also be plotted physically by using the mouse cursor ("+"), on the image log created after scanning. These markings should be done just above the marked minimum depth. Make sure that button "1" in Figure 4.2 always appears to be dark during these operations.

Once the maximum and minimum values of the log values and the depths are inputted, gridding should be done to provide an equal spacing between each and every

interval, click on button "2" Figure 4.2 and put the cursor at the minimum depth line and click, you will see an yellow grid line, go for the next grid line by clicking on the left and right hand corner of the digitized log depending on the interval you specify. If you want to grid spacing manually you can do that, but it takes more time. To avoid this, click on the grid lines that already plotted and click the right hand mouse button, gridding will be done automatically.

Now start digitizing the log, click on the button '3' (Figure 4.2) and place the cursor on the curve starting from the minimum depth, keep tracing the curve within the zone of interest, the software takes the numerical values of the log and saves the data in ASCII format. The digitization should be continuous. After tracing the curve save the file as digit file from the file menu, where the data is stored in an ".las" file. Convert this ".las" file format to "Spread sheet" format for better viewing and to generate fuzzy curves.

4.2 Fuzzy Ranking

The fuzzy curves are generated to select the best input logs for training the neural network, all the available log data cannot be inputted to train the network as neural network cannot hold large data files. A ranking procedure is defined to select the inputs. Rank is defined as the sum of the normalized range produced by the fuzzy curve and the correlation coefficient obtained from the trend line. The fuzzy directory automatically produces the normalized range which is stored in the system files.

Range is defined as the difference between the maximum and the minimum normalized values of the fuzzy curve. The higher the range the better the log can be used for our training, because it represents the noiseness of the data and at the same time the correlation coefficient should also be high.

If the fuzzy curve range is high and the correlation coefficient is good, means that the logs has a good correlation with the independent variable, formation parameters (core data).

As "Predict Online" uses a maximum of four input logs. We have to apply the fuzzy ranking procedure described above to select the best-input logs. In order to select the best logs for training, fuzzy curves were plotted for different logs (Appendix A), the higher the rank, the better the log that can be used for training.

4.3 Procedure to Generate Fuzzy Curves

Copy the fuzzy directory to your system "C" drive. The directory should contain "Fc.dat, X.dat; Y.dat; fuzzy.exe and fuzzytest.xls". Assemble the data you want to plot a fuzzy curve in a spreadsheet. The variables you want to rank typically a well log , seismic attribute, or a statistical indicator should go on the X-axis; the variables that you want to predict go on the Y-axis like the production data. Count the number of data pairs we want to plot the fuzzy curve for by using @count from the Excel spreadsheet.

Normalize both the X-axis and Y-axis variables of the fuzzy curve data using $(V-V_{min})/(V_{max}-V_{min})$ where V is the variable. Copy the normalized X-axis and Y-axis variable to two different notepads and save as X.data and Y.data respectively in the fuzzy directory.

Now open MS-DOS prompt and change the directory to fuzzy "cd fuzzy" then you will be prompted with "C:\fuzzy", then type "fuzzy" on the command line.Fuzzy will prompt you for the number of data pairs, enter the number of data pairs and hit "Enter" on the key board. Now open Fc.dat (text file) in the fuzzy directory.Since Fc.dat is not an Excel format, open it through Excel, the text import wizard will pop up asking for "space and delimitation" click on those to import Text file to Excel format.

You should be in an Excel file called Fc.dat, copy the range and the fuzzy curve data to another work sheet and save it. Then go back and close the Fc.dat (when excel asks you if you want to save say no). Construct an X-Y scatter chart from the data obtained. Add a suitable trend line, and click r^2 value display then you will get the correlation coefficient value. Sum the normalized range and the correlation coefficient to get the rank.

Once the fuzzy curves are plotted, select the logs, which has high ranking with consistent correlation coefficient and high normalized range. Use those logs for training the "Neural Network". A plot of the fuzzy curve for Deep Lateral Log (LLD) with Bulk Volume Oil is shown in Figure 4.3.

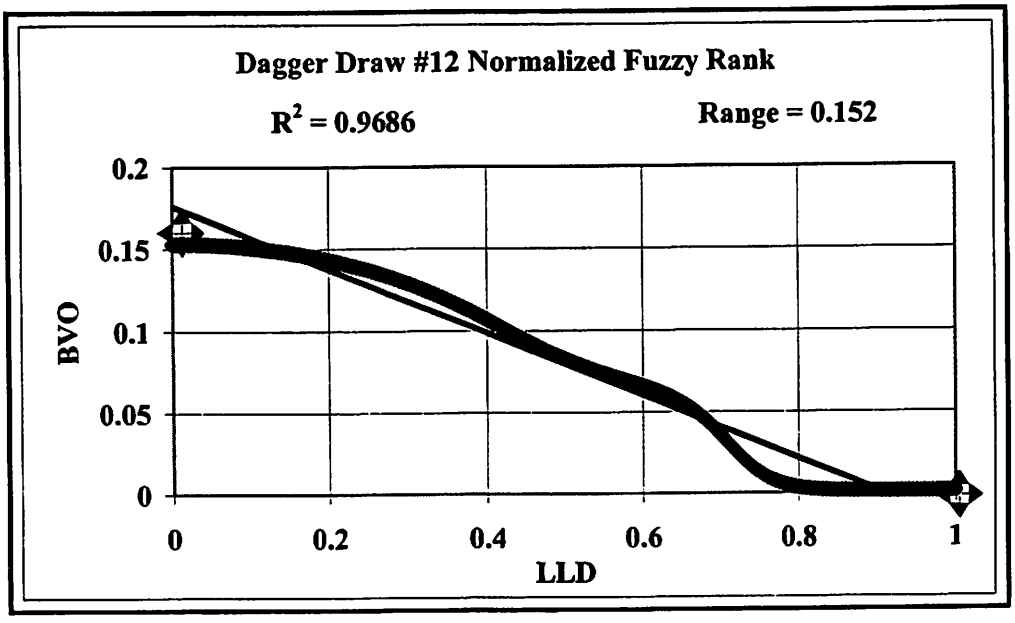

Figure 4.3: An example of a fuzzy curve with LLD and BVO

Range = 0.152-0.0 = 0.152

CHAPTER V

Neural Network Training and Predictions

Predict Online is the interface to the actual neural network simulator that is used for training the network and predicting. A set of input values and corresponding output values are provided to the neural network for training. The user then defines the number of weights and nodes between the input and output values by using different architectures. The neural network then iterates or back propagates the values assigned to the weights until a multivariate equation is produced which approximately matches the output values.

A correlation coefficient is used to gauge the "goodness" of the match or the "goodness" of the neural network training. In this cases log values are the inputs and core measurements are the output. Once the "goodness" is satisfactory, a trained network can be used to predict core measurements in the non-cored wells, given log data as input.

Since "Predict Online" does not have direct access to the input files present on the local system, all computations are performed on the server. The neural network "Predict Online" interface is shown in the flow chart (Figure 5.1). A login created by the server administrator is required to access files on the remote server. The resulting

"predicted" files are automatically generated.

Files, which are smaller than 32kb only, can be viewed directly; other files have to be downloaded from the server to the client system before they can be opened for viewing. To access predict online form client system, you need to have "java policy" file which gives permission to view the applet window on the server.

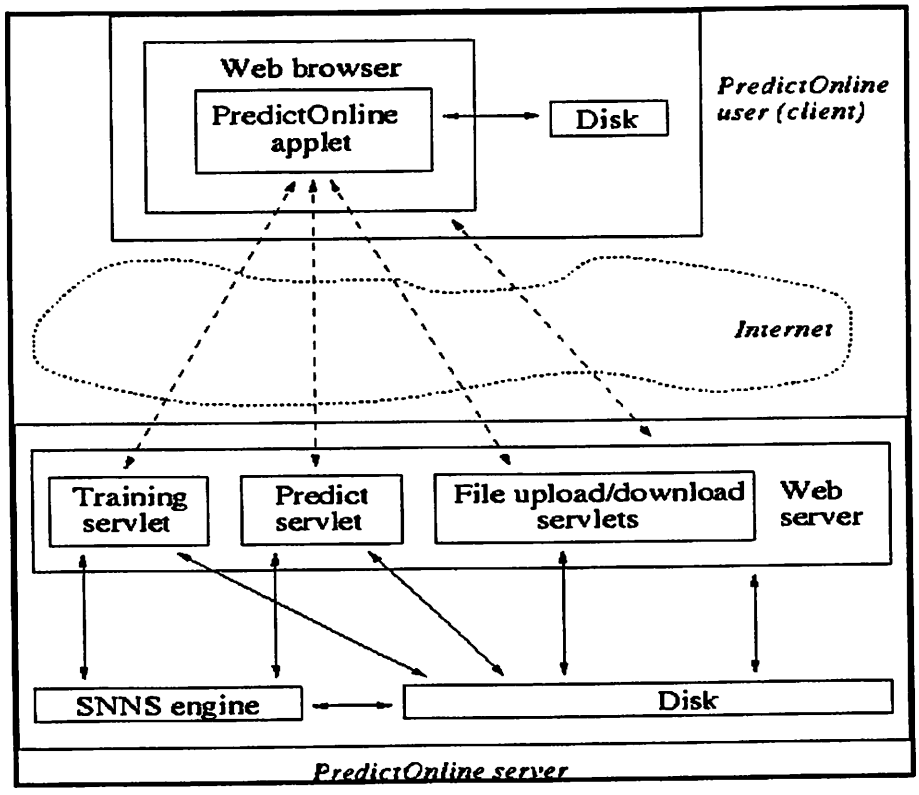

Figure 5.1 Shows the flow chart of Predict online user interface with neural network simulator

5.1 Application of Neural Network Simulator as a Client

Open the browser as http://ford.nmt.edu/Predictonline6. Click on the "login" button. The user will be prompted for a login name. If you already have login enter it and click "ok", if not contact the system administrator to create a new login.

Once successfully logged in to the server, a window will be prompted (Figure 5.2) asking you to create a project name and to upload the training files. Make sure that the project name shouldn't contain any spaces. All the projects and files pertaining to particular user are stored under the user login. Access to these files and projects are granted exclusively to that particular user alone.

If you are already an existing user, click on a particular project from the list and you can view all the files associated with that project, if not create a new project and start uploading the files for training and predicting. Its also important to note that all files present under the data files list will automatically be displayed in the predict file list.

In order to train the network, select the desired data file that the network is to be trained and provide with an architecture, where the number of weights should be always half less than the number of records. The first and the last entries of the architecture need not be entered, as they are the number of inputs and outputs. The output value for each pattern always remains to be one; the input may vary depending on the different type of logs we use to train the network basing on the fuzzy curve analysis. The user enters numbers separated by space in "ARCH" field provided on the top right hand corner.

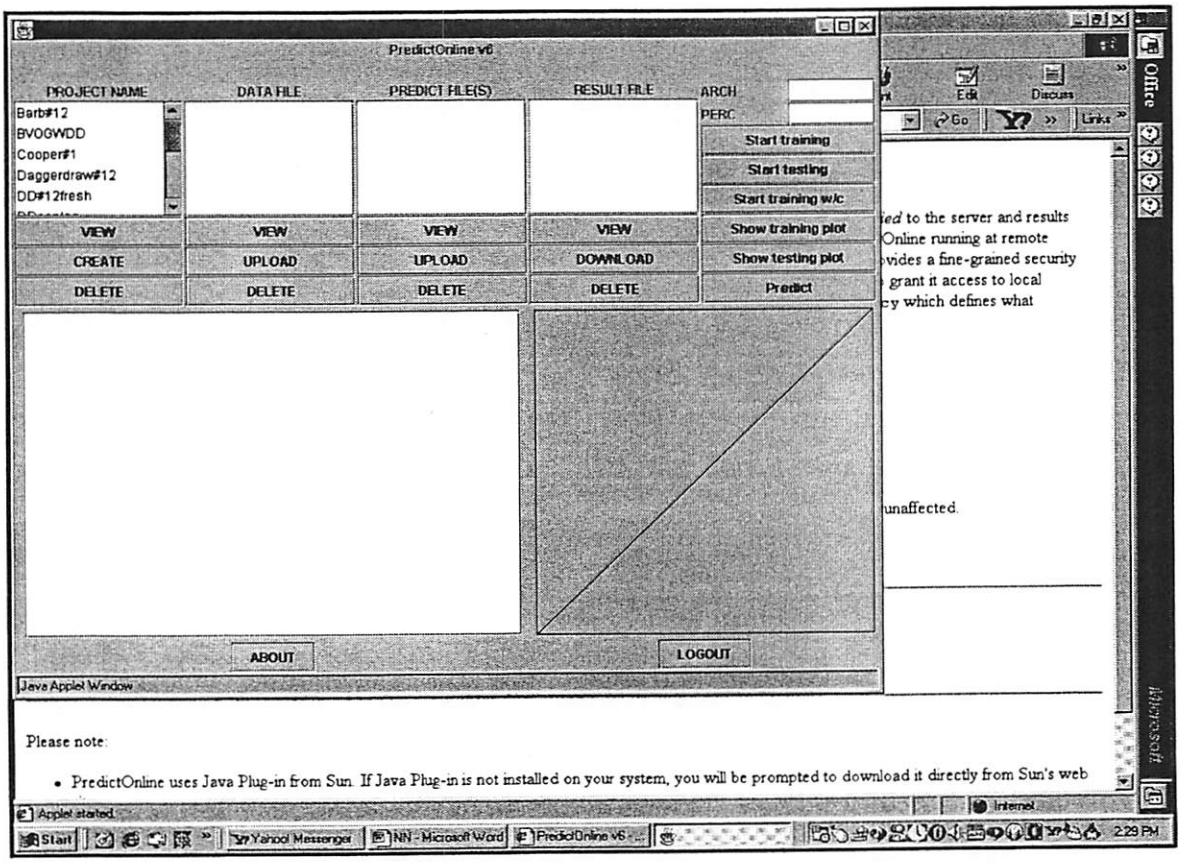

Figure 5.2: A view of the predict online window

In order to train the network we have two options, one is regular training and the other is training with cross validation, for regular training "PERC" value should be zero. "PERC" is the percentage of the number of records to the total available records the network uses for training. Upload the files to be trained and then click the "Start Training" button. To obtain good training correlation we have to keep on changing the architecture as explained earlier, once we obtain a good training correlation of around 80% or more, we can stop training and start to predict the results.

To test whether our training is perfect or not, provide "PERC" column with either 10% or 20%, this will randomly select 10% of all the values that are trained and tests the

data. If the network is trained well we will have the testing correlation to be same as training correlation.

In training with Cross-Validation, "PERC" column should be provided with a value other than zero during training process, the network randomly chooses values for both training and testing and generates a testing and training correlation. When these correlations are nearly equal and are above 80%, the network is ready to predict and the training is terminated.

It is better to do a regular training than training with cross validation since regular training uses all the input values provided for training network instead of choosing randomly as in training with cross validation. If desired select a particular file and click "show Plot" the training and testing plots can be viewed as shown in Figure 5.3, Y-axis represents the actual outputs and X-axis represents the desired outputs.

Once the network is trained, upload the predict files from the client system to the server, after uploading click on the particular file you want to predict in the predict file column and then click "Predict" button. The results will be automatically displayed in the "result' column with a "_ result" file extension. Care should be taken if a desired prediction is required from a particular training file or a trained network. The "result" files can be downloaded to the client system and can be converted to Excel spreadsheets. The application of this new technology is demonstrated with original data from the Dagger Draw Field.

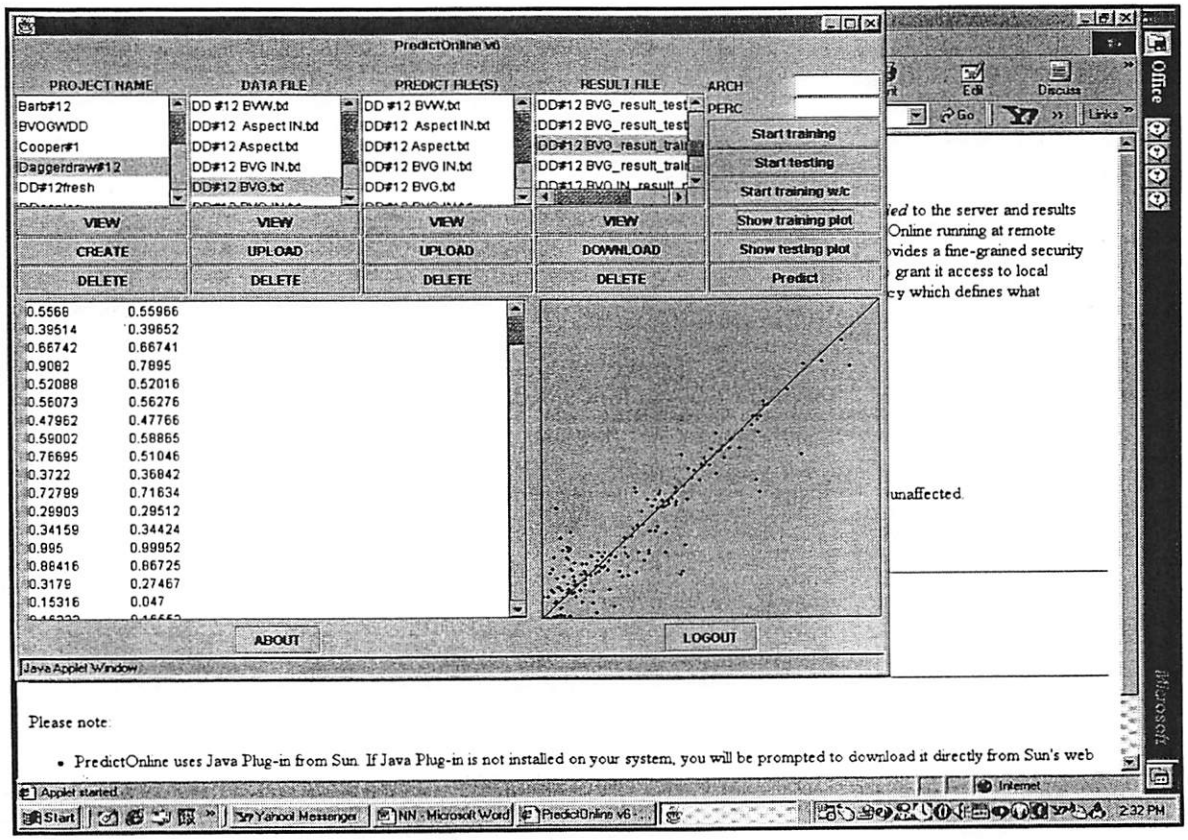

Figure 5.3: A window showing the training, testing and predicted results of the Neural Network along with the training plot.

Chapter VI

Results and Discussions

6.1 Dagger Draw Field

Dagger Draw field is located in Southeastern Eddy County, New Mexico. It is a shelf margin carbonate bank complex. Conventional log analysis is complicated by the vuggy nature of the rock .The present application of Neural Networks used data from six wells in the field. The following are the wells.

Well Name	Section	Township	Range
1. Dagger Draw # 12	30	19S	25E
2. Barbara # 1	18	19S	25E
3. Ocotillo # 1	10	20S	24E
4. Cooper # 1	1	20S	24E
5. Marathon Federal # 5	19	21S	23E
6. Saguaro # 8	14	20S	24E

To start predicting the oil, gas and water production rates from the non-cored wells, a neural network has to be established using the available input data (Well Logs and Core saturation values of oil, gas and water). The Bulk Volume of Oil, Gas and Water are calculated from the core saturations values by using the following equations

$$\text{BVO (Bulk Volume Oil)} = (1 - S_w) * \phi \quad (6.1)$$

$$\text{BVG (Bulk Volume Gas)} = (1 - S_w - S_o) * \phi \quad (6.2)$$

$$\text{BVW (Bulk volume Water)} = S_w * \phi \quad (6.3)$$

The obtained Bulk Volume Oil, Gas and Water along with the geophysical logs (G-Ray, PEF, LLS, LLD, MSFL, Dphi, Nphi, Caliper), were used as training input data sets for establishing a neural network. Geophysical logs provide information about the formation, formation temperatures and physical properties like porosity, resistivity, type of formation whether it's shale, sandstone or a carbonate including borehole diameter.

Well Logs (Geophysical logs) are digitized as explained earlier using "NDS Neural Log" to convert the graphical X-Y plot data to (x,y) numerical data so that we can input this digitized data to train neural network. These logs vary for each and every well depending upon the formation, but there will be a correlation existing between the logs and the formation, if all the wells belong to the same reservoir.

After obtaining the digitized data, fuzzy curves were plotted to select the best input logs for training the network. The greater the rank of the fuzzy curve the better the log works for predicting results. After selecting the logs we start with our training by inputting the digitized log data along with Bulk Volume Oil, Gas and Water values calculated from the core data.

The logs of all the six wells were digitized and the fuzzy curves were plotted Appendix-A. The ranks of all the logs of Dagger Draw #12 well are shown in Table 6.1.

Log	R^2	CC	Range	Rank
Caliper	0.612	0.782	0.291	1.073
Gamma	0.617	0.786	0.064	0.850
LLD	0.051	0.226	0.068	0.293
LLS	0.871	0.933	0.098	1.031
MSFL	0.318	0.564	0.097	0.661
N Phi	0.008	0.089	0.089	0.179
PEF	0.790	0.889	0.092	0.981
D Phi	0.444	0.666	0.213	0.879

Table 6.1: Table showing the fuzzy ranks of different well logs of Dagger Draw #12 Bulk Volume Oil

6.2 Training of Six Wells to Choose the Best Network for Predictions

6.2.1 Dagger Draw #12

The Dagger Draw #12 is located in Section 18 T 19 S, R 25 E of the North Dagger Draw Field. Pay zones in the Dagger Draw upper Pennsylvanian interval consist of fractured, vuggy dolomites sealed by non-porous limestone. A typical suite of eight logs is shown in Figure 6.1.

The log suite consists of gamma ray, caliper, density and neutron porosity, micro, shallow and deep resistivity and photoelectric logs. The dense limestone zones within the dolomite are readily identified by the shift in the Pe log from 3 (dolomite) to 5 units, plus the absence of separation in the resistivity logs. In this well, the pattern of the dolomite pay zones is readily identified.

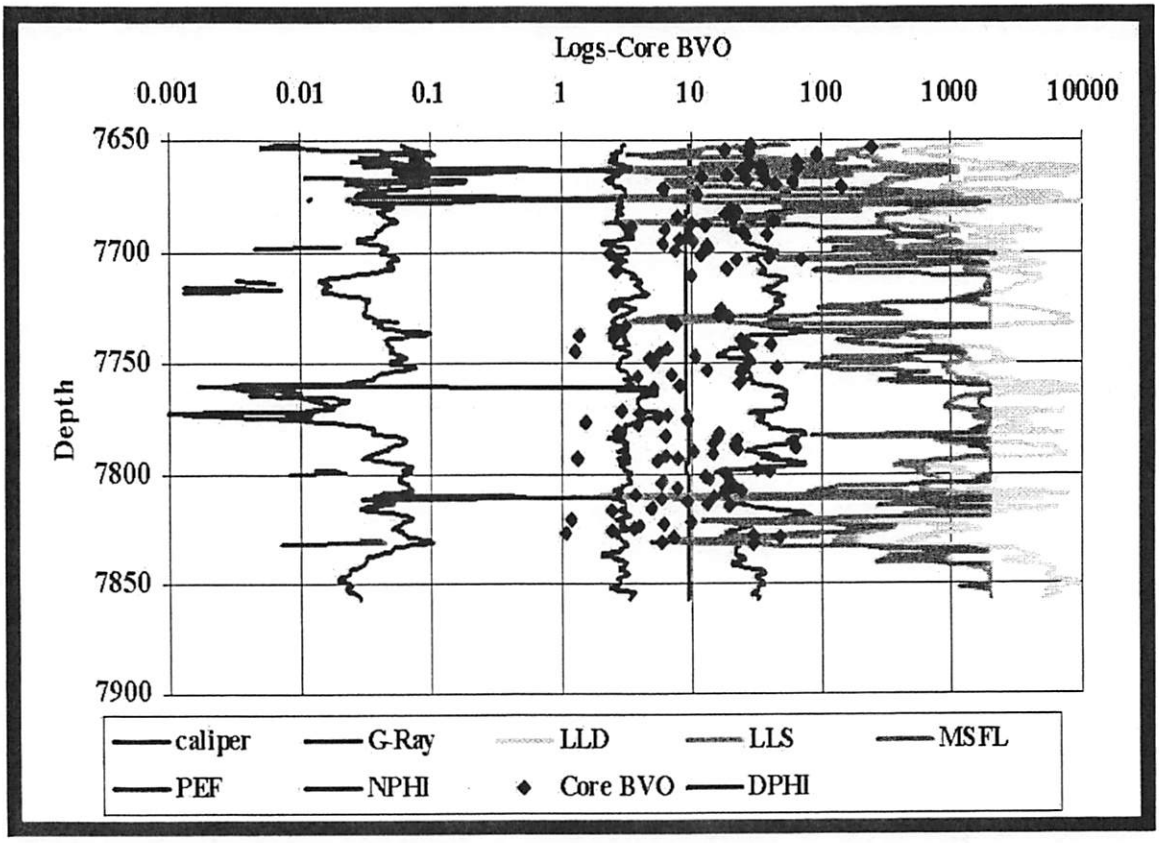

Figure 6.1: Suite of eight logs of Dagger Draw #12

Single stage fuzzy ranking was used to identify the relationship of the eight logs with bulk volume oil (BVO). The distribution of the 200 laboratory measurements is shown in Figure 6.1. No attempt was made to account for flushing that may have occurred during recovery of the core.

The fuzzy curve shown in Figure 6.2 has a y-axis range (difference between maximum and minimum fuzzy values) of 0.157. A straight line fit to the fuzzy curve has a correlation coefficient of 0.960. In this case the sum of the range and the correlation coefficient establishes the rank.

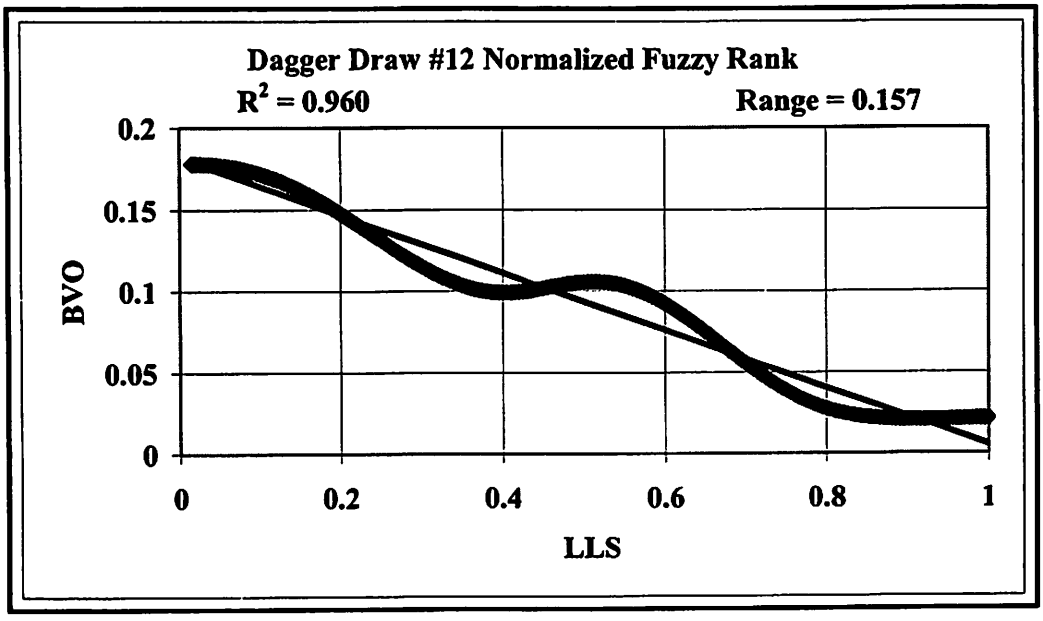

Figure 6.2: The shallow resistivity log correlates with the fuzzy BVO values.

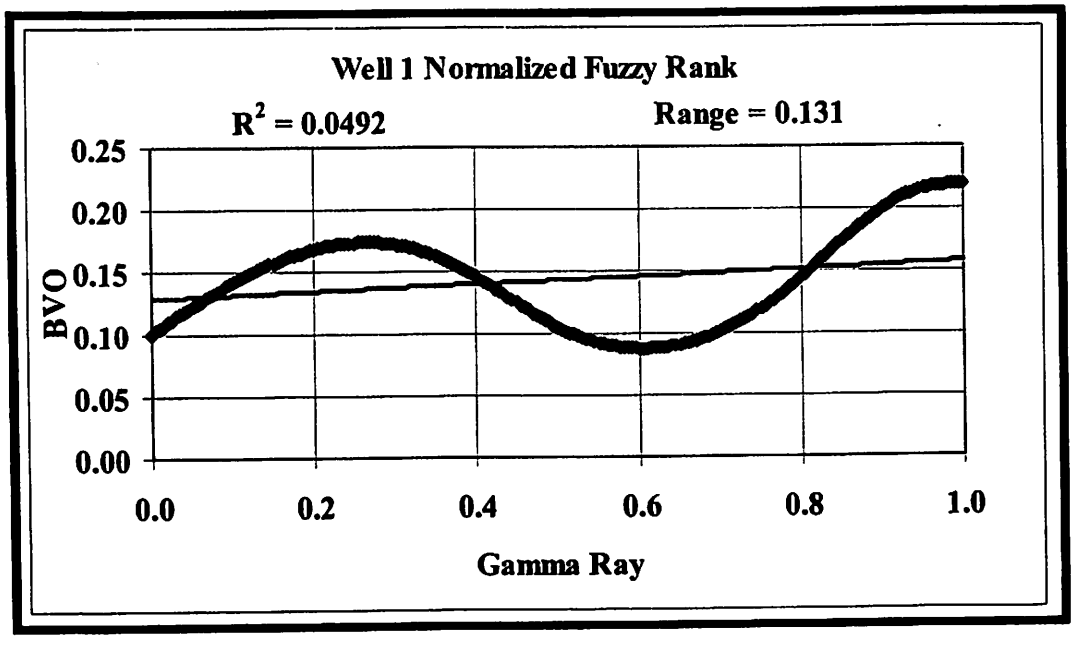

Figure 6.3: The gamma ray log does not correlate with BVO

The gamma ray fuzzy curve in Figure 6.3 has very little correlation with Bulk Volume Oil. Table 6.1 gives the fuzzy ranks of all the logs in Dagger Draw #12. Both Pe and Φ_D include a density measurement and the ranking is similar. Density porosity was used in the neural network training because the "range" is significantly greater than the "range" of the Photoelectric log.

Various logs of Dagger Draw #12 have been provided, based on the fuzzy ranking, the following logs were selected Caliper, LLS, Dphi and trained with core BVO values as output. The training starts with an architecture of 3-1-1-1 where "3"(Caliper, LLS, Dphi)is the number of inputs used, "1-1"(Architecture) is the number of hidden layers and "1"(Core BVO) is the number of outputs, till a good correlation coefficient is obtained.

For 8-4 architecture(3-8-4-1), the training correlation obtained was 0.95, and when tested the correlation was 0.90. Since the testing and training correlation coefficient are nearly equal, we can use this trained file for predictions. When this trained file was used to test, for intervals which don't have core Bulk Volume Oil (BVO)data, the results are shown in Figure 6.4 where the predicted and actual values match.

Applying fuzzy tools to select the input logs for predicting Bulk Volume Water (BVW) values with no core data, the following logs Caliper, LLS, Dphi (Appendix D) were selected for training and when trained with 6-4 architecture (3-6-4-1), the training

correlation and testing correlation were 0.93 and 0.88 respectively. When tested using this trained file the results are shown in Figure 6.6 .

To train the network for predicting the Bulk Volume Gas (BVG) the following logs are selected PEF, LLS, Dphi, using fuzzy ranking, and when trained with 6-4 architecture(3-6-4-1) the training and testing correlations were 0.92 and 0.90 respectively. The results are shown in the Figure 6.5.

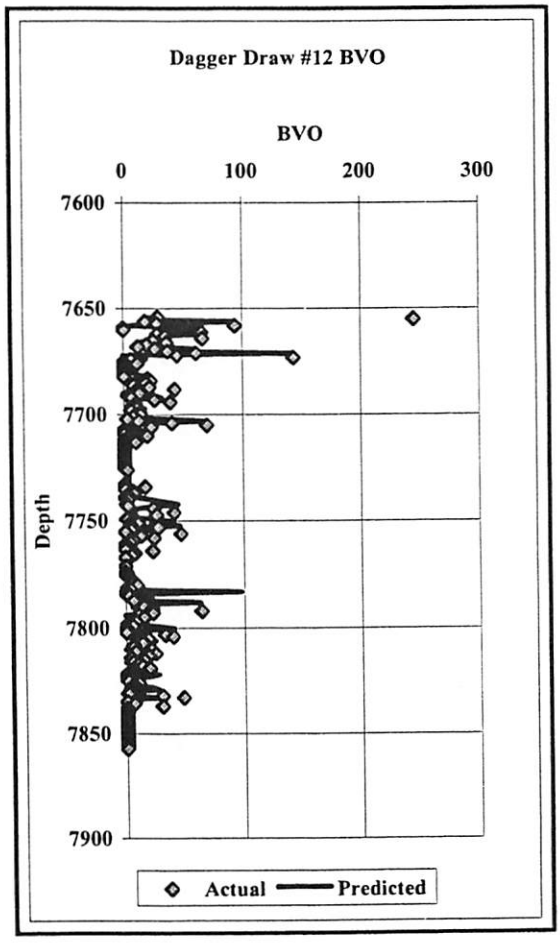

Figure 6.4: Actual Vs Predicted values of Dagger Draw #12 Bulk Volume Oil

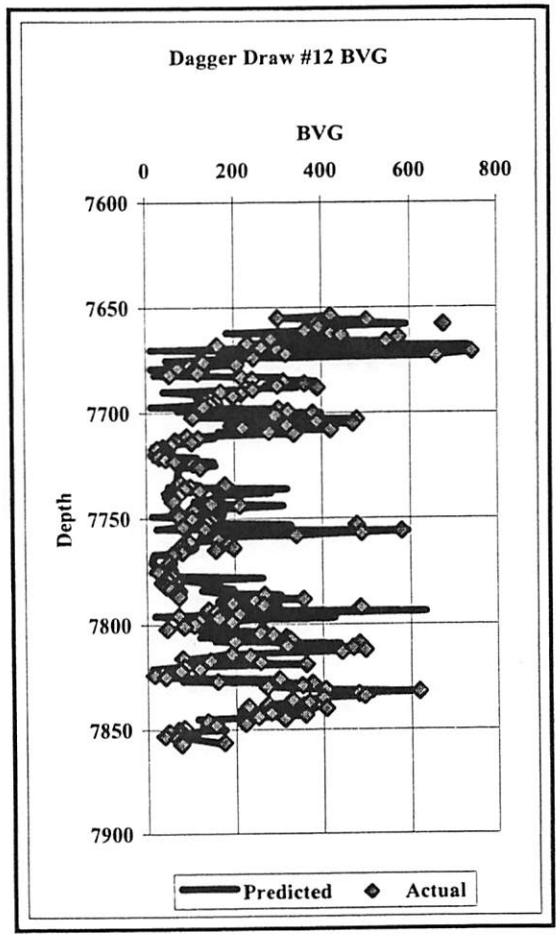

Figure 6.5: Actual Vs Predicted values of Dagger Draw #12 Bulk Volume Gas

In the same way the input logs selected to train the network for aspect ratio were Caliper, G-Ray , Dphi and the architecture used was 6-4(3-6-4-1). The training correlation coefficient was 0.78; the predicted aspect ratio values were compared with the actual values and are shown in the Figure 6.7.

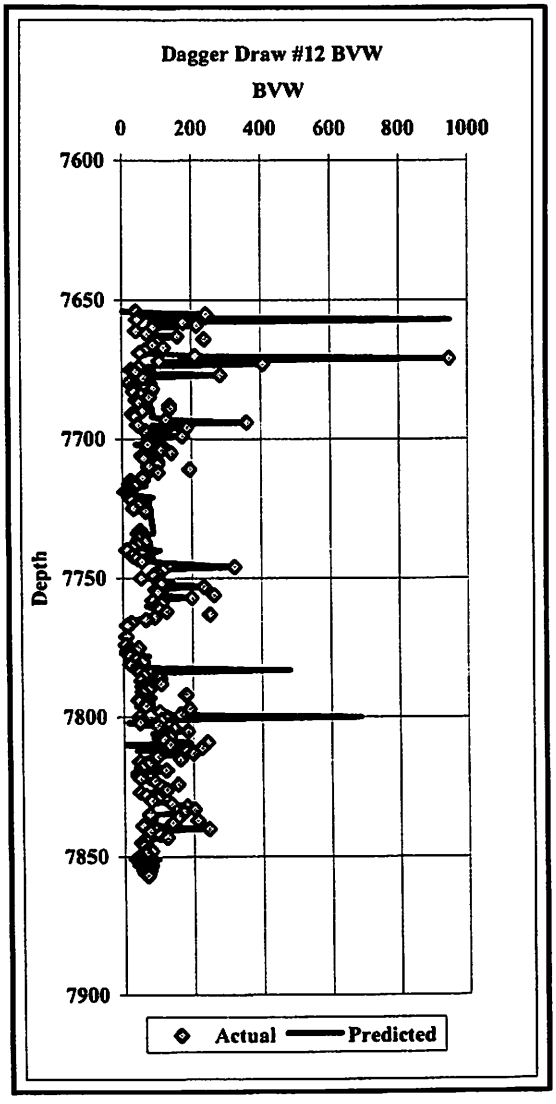

Figure 6.6: Actual Vs Predicted values of Dagger Draw #12 Bulk Volume Water

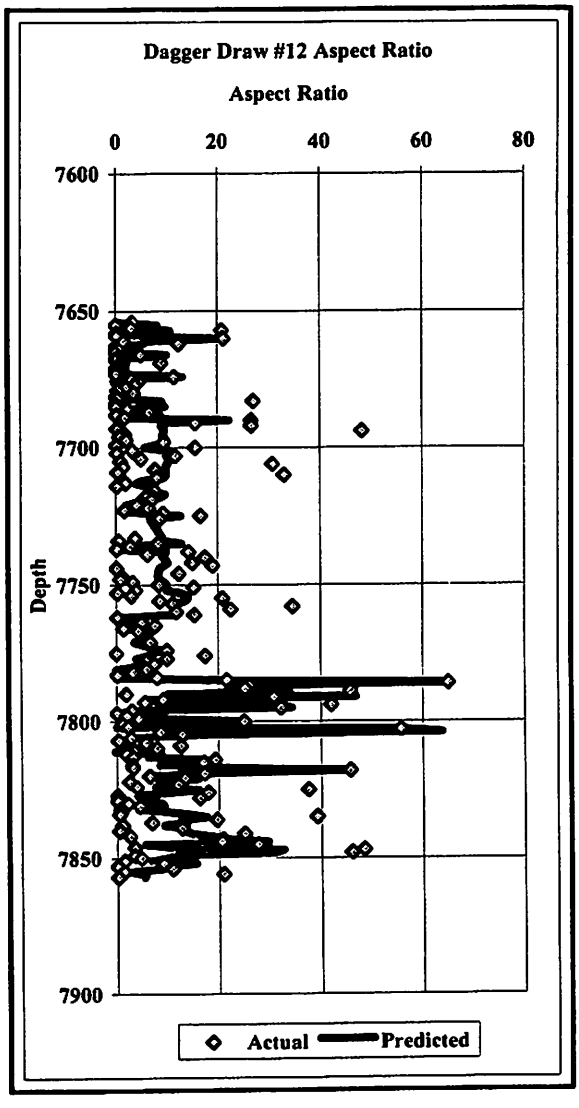

Figure 6.7: Actual Vs Predicted values of Dagger Draw #12 Aspect ratio.

As we can see from all the pseudo logs developed, the Bulk Volume Oil, Gas, Water and aspect ratio values matches with the core data between the intervals 7650ft to 7850ft. So, there is a probability that we can use this trained network for developing log correlations, this network can be used for predicting the Bulk Volumes of all the wells in the Dagger Draw field.

6.2.2 Marathon Federal # 5

Marathon Federal #5 is located in Section 19 T 21 S, R 24 E of South Dagger Draw. To predict the Bulk Volume Oil for Marathon Federal #5 the GR, Caliper and LLS logs were selected using the same principle of fuzzy ranking as previously discussed. These digitized logs were used to train the neural network for predicting Bulk Volume Oil of Marathon Federal #5. The training and testing correlations when trained with 6-4(3-6-4-1) architecture were 0.90 and 0.85 respectively. This trained data was used to predict the Bulk Volume Oil. (Figure 6.8)

Using the same technique of fuzzy ranking, Caliper, LLS , DPHI were selected to train the network for Bulk Volume Gas with 6-4(3-6-4-1) architecture. The network trained to 60%, and the predicted values obtained were plotted against the actual BVG in Figure 6.9. From the plot it can be seen that between the interval from 7500ft to 7530ft the history matching was good, but from 7720ft to7770ft the predicted values are fluctuating from the actual core data, therefore the prediction was poor.

G-Ray, MSFL, Dphi; were selected to train the network for predicting Bulk Volume Water with 6-4(3-6-4-1) architecture and 0.72 training correlation coefficient, the predictions were not bad except for an interval between 7750ft to 7760ft. Figure 6.10

.

Finally Caliper, G-Ray , Dphi were selected to train the network for aspect Ratio with 70% trained network. The architecture used for building this network was 6-4(3-6-4-1). The predictions of the aspect ratio were poor between the intervals 7730ft to 7770ft (Figure 6.11). So this trained network was eliminated from any further use because of poor training and predictions.

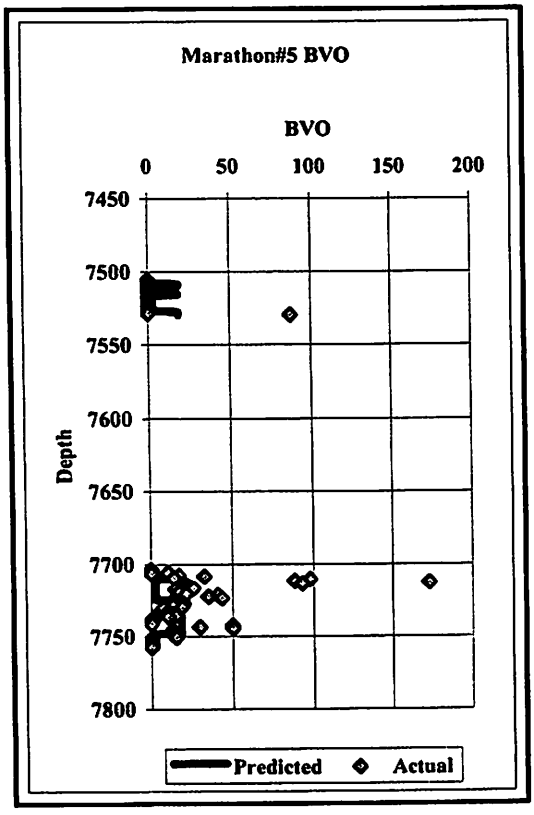

Figure 6.8: Actual Vs Predicted values of Marathon # 5 Bulk Volume Oil

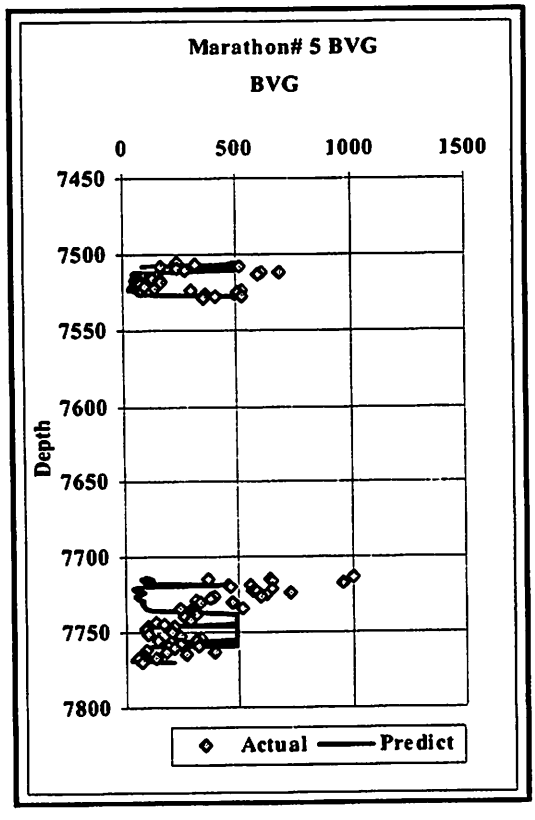

Figure 6.9: Actual Vs Predicted values of Marathon # 5 Bulk Volume Gas.

From all the pseudo logs that were developed for the Marathon # 5, the networks used for predicting the Bulk Volume Gas and aspect ratios can be eliminated as predicted values don't match with the actual values, and the training correlation coefficients were also less. Since, the Bulk Volume Oil and Water values of Marathon # 5 are also not well trained as compared to Dagger Draw # 12; it is not proposed to use the Marathon # 5 trained network for log correlations.

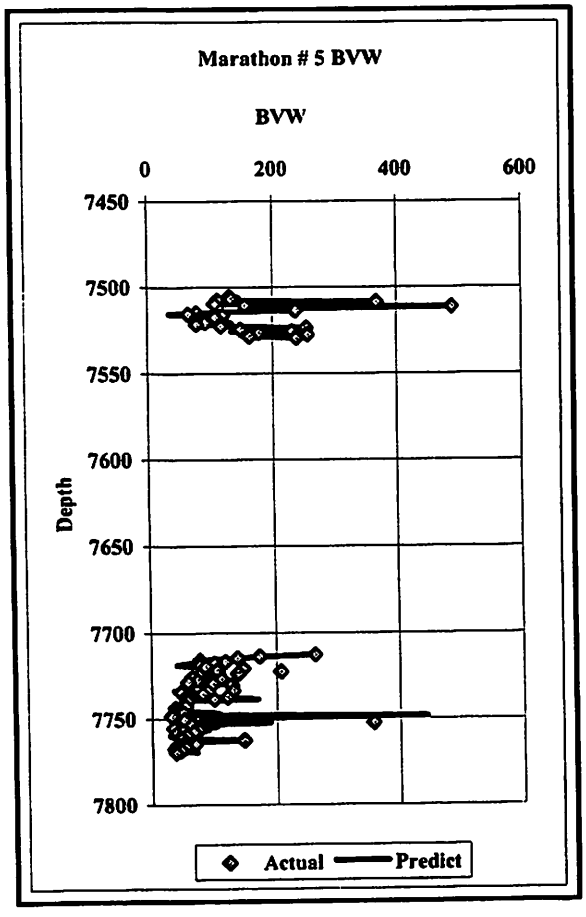

Figure 6.10: Actual Vs Predicted values of Marathon # 5 Bulk Volume Water

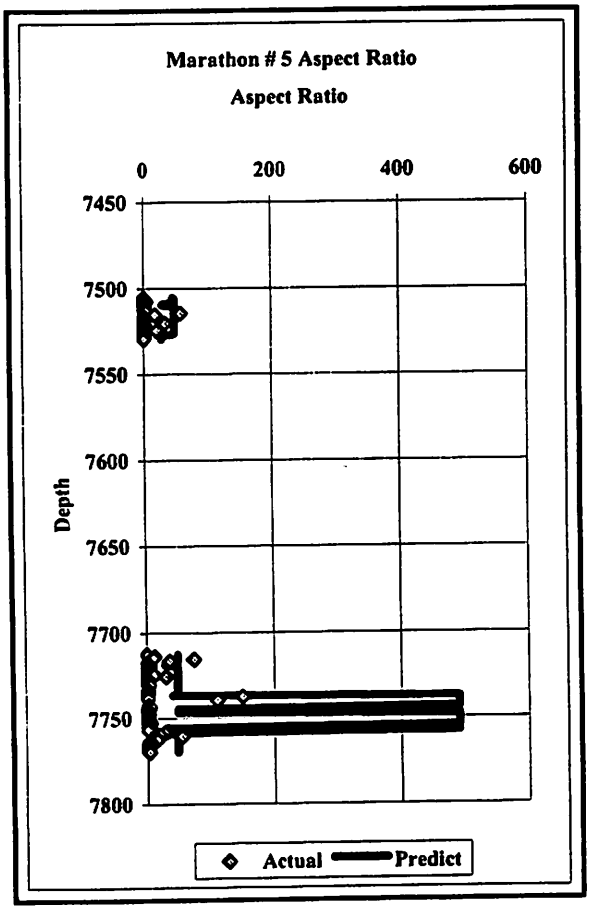

Figure 6.11: Actual Vs Predicted values of Marathon # 5 Aspect ratio.

6.2.3 Saguaro #8

The Saguaro # 8 is located in Section 14 T 20S, R 24 E in the South Dagger Draw. Caliper, MSFL, Nphi; were selected as input logs to train the network with 6-4(3-6-4-1) architecture for Bulk Volume Oil of Saguaro #8, the training correlation was 0.73. As we see from the plot Figure 6.12 the history matching of the Bulk Volume Oil is good except for an interval of 10ft which has minor fluctuations.

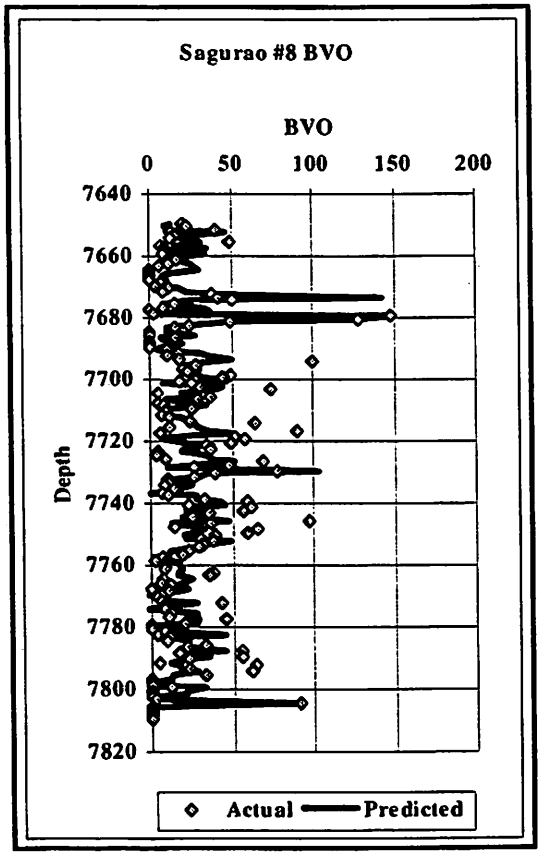

Figure 6.12: Actual Vs Predicted values of Saguaro # 8 Bulk Volume Oil

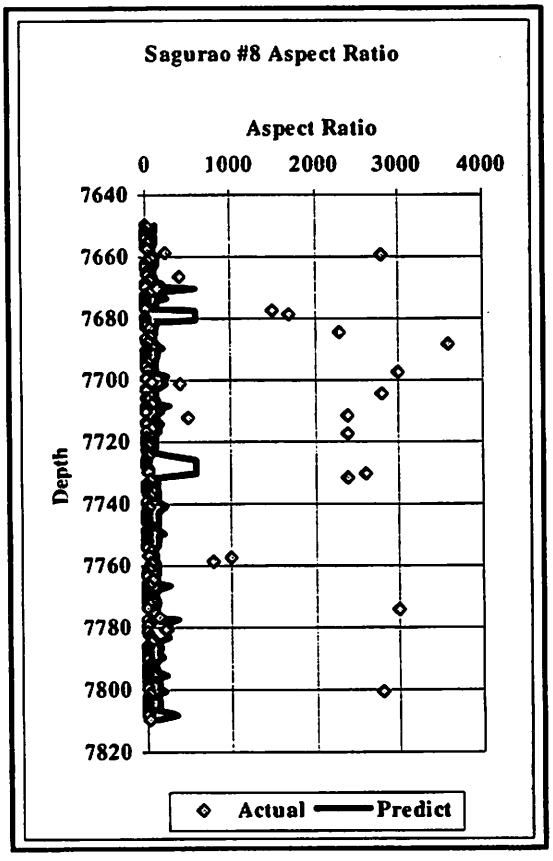

Figure 6.13: Actual Vs Predicted values of Saguaro # 8. Aspect ratio

In the same way the logs selected for predicting Bulk Volume Gas were Nphi, Caliper, Dphi and when trained with 8-4(3-8-4-1) architecture the training was up to 70%, the predicted values are almost constant with slight fluctuations, but still didn't

match with the actual core values, between the intervals 7650ft to 7810ft (Figure 6.14). The history matching wasn't good, nor was the training. For predicting the Bulk Volume Water and aspect ratio the following logs were selected; LLS, PEF, Nphi and LLD, MSFl ,Dphi. respectively. These when trained with 6-4(3-6-4-1) architecture trained to 50% and 80% .

As we see from the pseudo logs Figure 6.13 the aspect ratio predictions were poor. Also, the predicted Bulk Volume Water value always remained constant between the interval 7650ft-7810ft and has poor history matching (Figure 6.15). This is because of the poor training correlation and these networks can no more be used for developing log correlations.

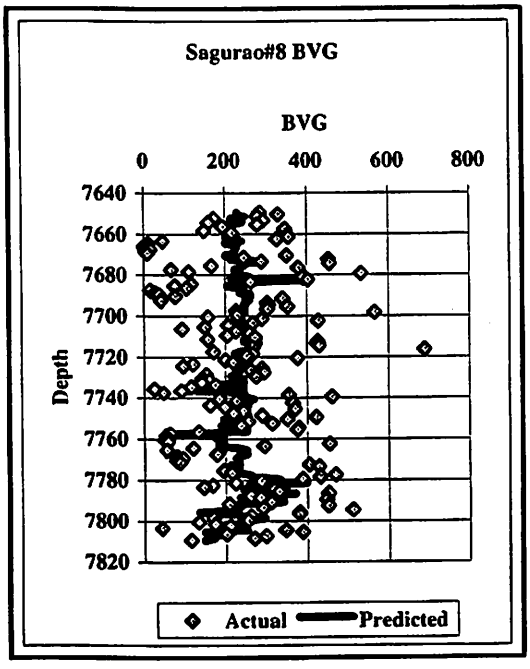

Figure 6.14: Actual Vs Predicted values of Saguaro # 8 Bulk Volume Gas

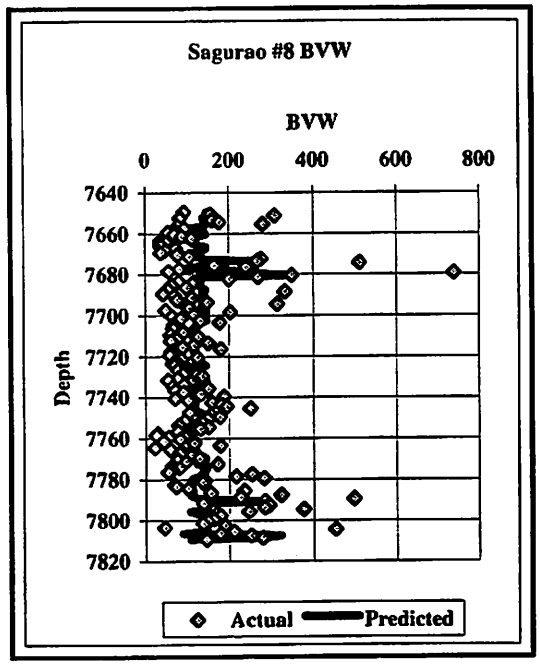

Figure 6.15: Actual Vs Predicted values of Saguaro # 8 Bulk Volume Water.

6.2.4 Barbara # 12

The Barbara #12 is located in Section 18 T 19 S, R 24 E of North Dagger Draw Field. Caliper, PEF, Nphi; were selected as input logs to train the network for predicting the Bulk Volume Oil of Barbara #1, the training correlation was 0.30, and as we see from the pseudo log in Figure 6.16 the network predicted high Bulk Volume Oil values which doesn't match with the actual values, this is the because of the poor training correlation (30%).

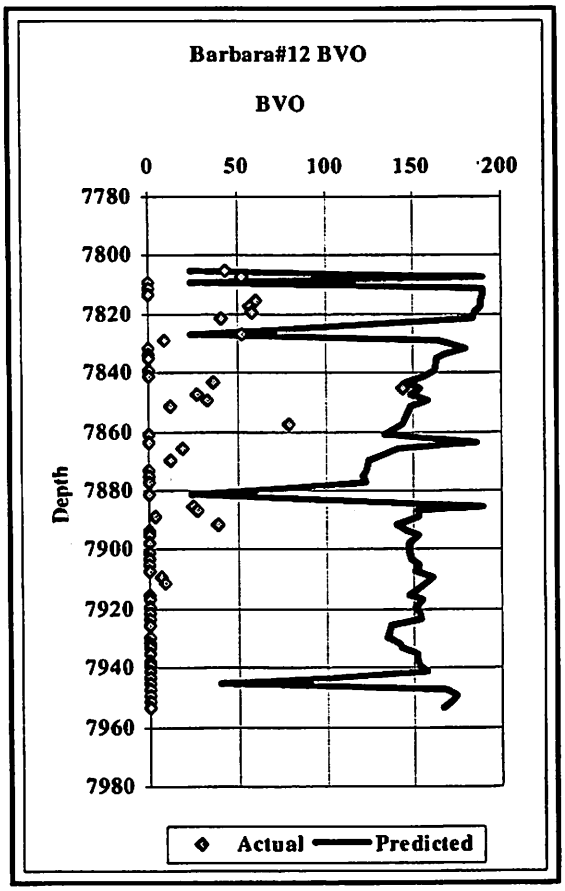

Figure 6.16: Actual Vs Predicted values of Barbara # 12 Bulk Volume Oil

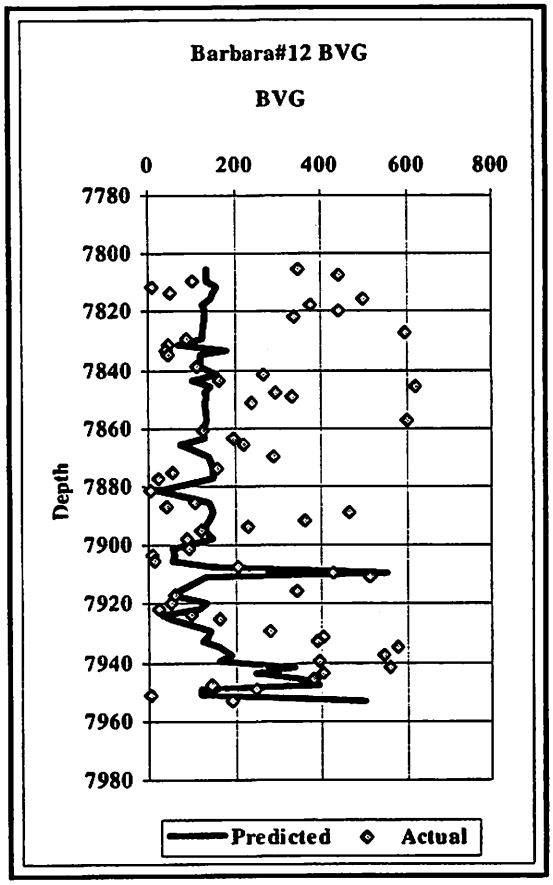

Figure 6.17: Actual Vs Predicted values of Barbara #12 Bulk Volume Gas.

In the same way, the logs selected for predicting the Bulk Volume Gas and Water are Nphi, LLS ,Dphi; and LLD, MSFL, Nphi respectively. The network when trained with 4-2 (3-4-2-1) architecture, has 55% and 76% correlation respectively. As evident from the pseudo logs Figure 6.17 the predicted Bulk Volume Gas values are always less than the actual values, while the history matching for Bulk Volume Water matched well with the actual values Figure 6.18. However still the network is not as well trained as Dagger Draw #12. Therefore, this network was also eliminated .

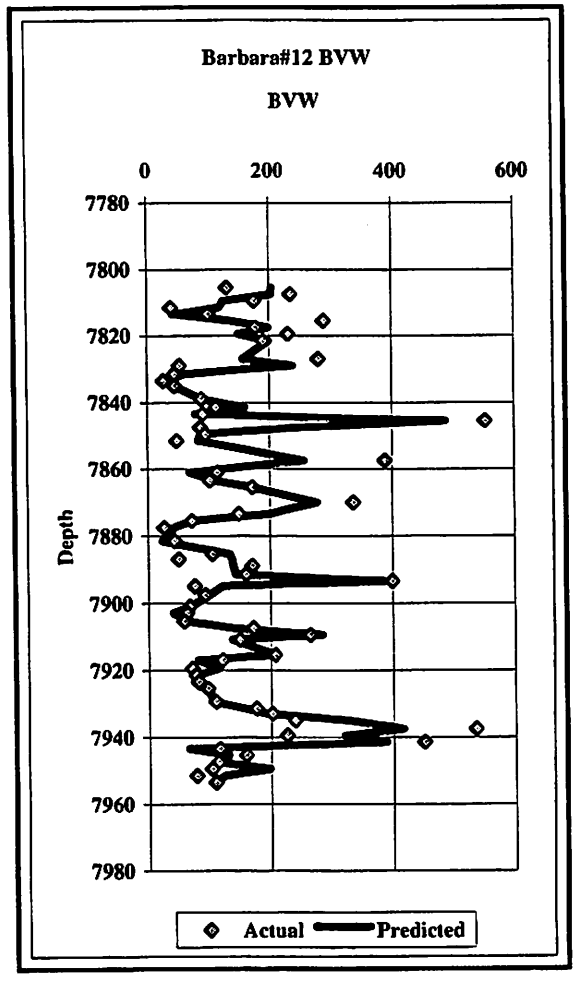

Figure 6.18: Actual Vs Predicted values of Barbara # 12 Bulk Volume Water

Since none of the pseudo logs had good history matching, this data cannot be used to develop log correlations and all of them were eliminated.

6.2.5 Cooper #1

Cooper # 1 is located in Section 1 T 20S R 24 E of the South Dagger Draw field. G-Ray, LLS, Dphi; were selected as input logs to train the network for predicting the Bulk Volume Oil of Cooper #1, when trained with 4-2(3-4-2-1) architecture the correlation coefficient was 0.85, Figure 6.19, there is an excellent history match between the actual Bulk Volume Oil and the predicted values.

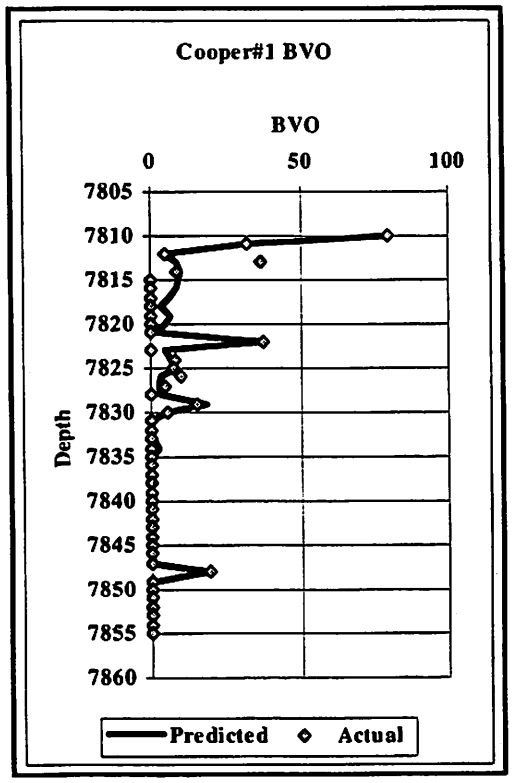

Figure 6.19: Actual Vs Predicted values of Cooper # 1 Bulk Volume Oil

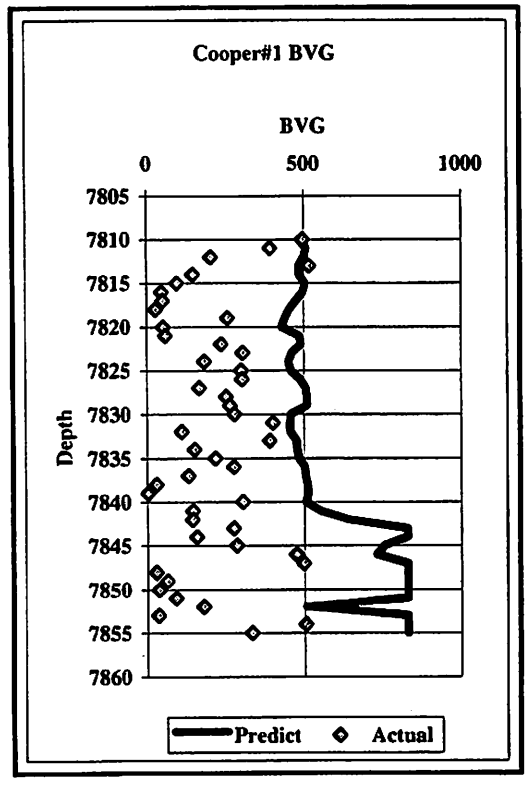

Figure 6.20: Actual Vs Predicted values of Cooper #1 Bulk Volume Gas.

This trained network can be used for developing log correlations, but has less data point when compared to Dagger Draw #12.

In the same way the logs selected for predicting Bulk Volume Gas, were Nphi, LLS ,G-Ray and when trained with 3-2(3-3-2-1) architecture ,the network was trained to 65%. As evident from the pseudo log in Figure 6.20, there is no good match between the predicted Bulk Volume Gas values and the actual values, so this network was eliminated. Nphi, LLS, G-Ray; were selected for training the network to predict the Bulk Volume Water values, the correlation coefficient was 0.81 when trained with 6-4(3-6-4-1) architecture. The history matching is good as evident from the pseudo log in Figure 6.21. There is a probability that this network can be used for predicting the Bulk Volume Water of the non-cored wells; however due to few core data points (55), this network cannot be used to develop log correlations.

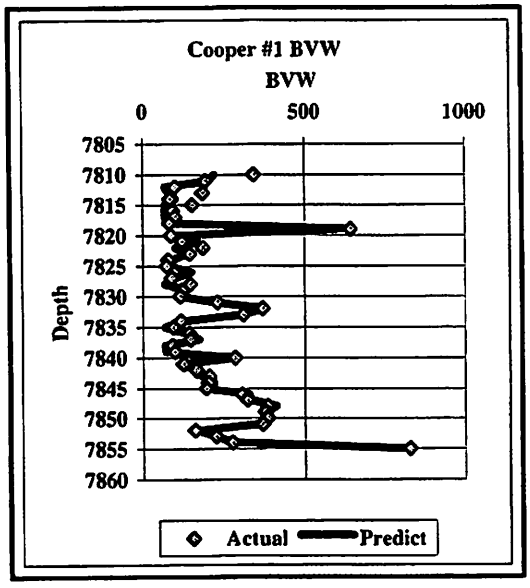

Figure 6.21: Actual Vs Predicted values of Cooper # 1 Bulk Volume Water

6.2.6 Ocotillo # 8:

The Ocotillo # 8 is located in Section 10 T 20 S, R 24 E of South Dagger Draw. NPhi, LLS, Dphi were selected as input logs to train the network for predicting the Bulk Volume Gas of Ocotillo # 8. The training correlation was 0.68 when trained with 6-4(3-6-4-1) architecture. This well was a dry hole, it didn't produce any oil during its earlier stages of production. So, there is no possibility of developing a network to predict the oil rates. As we can see from the pseudo log Figure 6.22 the predicted values match better with the actual values in the bottom of the interval than the top of the interval.

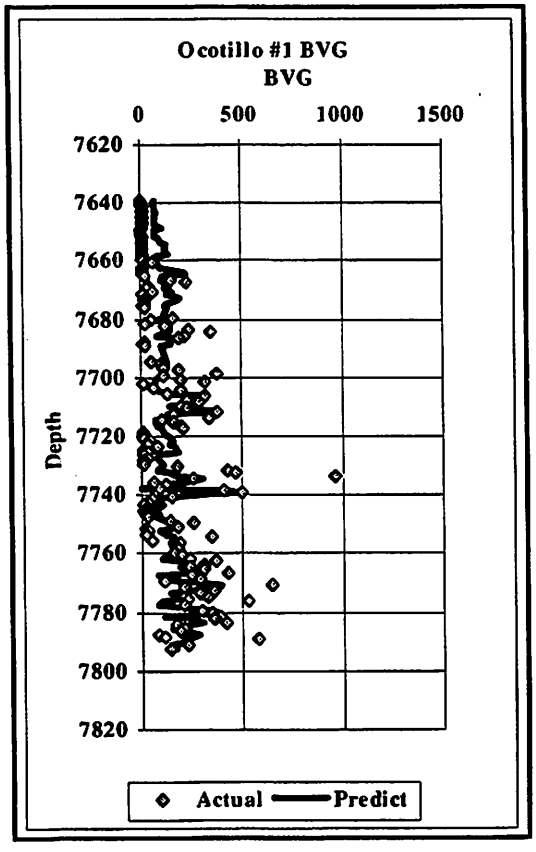

Figure 6.22: Actual Vs Predicted values of Ocotillo # 1 Bulk Volume Gas

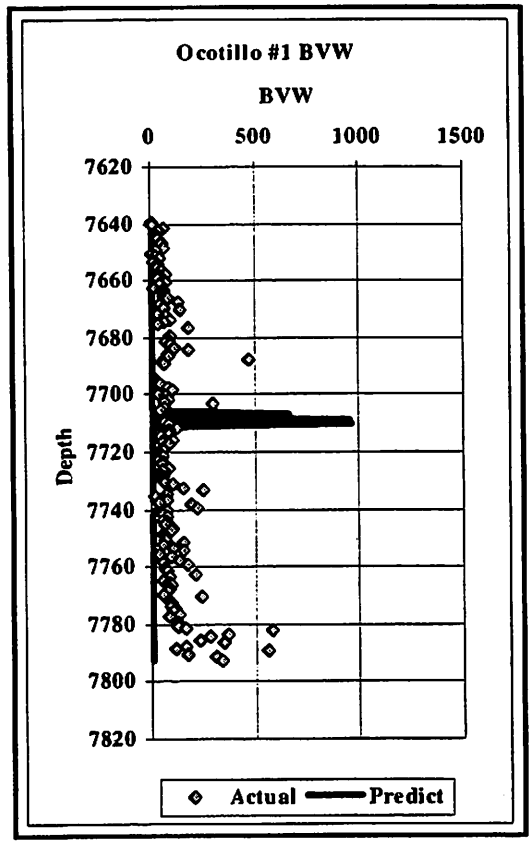

Figure 6.23: Actual Vs Predicted values of Ocotillo # 1 Bulk Volume Water.

In the same way the logs selected for predicting the Bulk Volume Water were Caliper, PEF, Nphi; the correlation coefficient when trained with 6-4(3-6-4-1) architecture was 60%. The predicted Bulk volume Water values were almost constant except for the interval between 7705ft to 7715ft and never matched with the actual values (Figure 6.23). So, this network was also eliminated because of poor training correlations.

As evident from all the pseudo logs developed, only Dagger Draw #12 has the best training and history matching results. Saguaro # 8 also had good training and predicted results for Bulk Volume Oil, Gas and Water, but the predicted values remain less correlated with the actual values. So, the Dagger Draw #12 trained network was selected to develop log correlations.

6.3 Predictions based on the trained Dagger Draw#12 network

A multivariate correlation was developed using three top ranked logs (caliper, shallow resistivity and density porosity) as inputs to a neural network with the laboratory values of Bulk Volume Oil from corresponding core data as the output. The goodness (correlation coefficient was 90%) of the neural network training is shown in a log format in Figures 6.4, 6.5, 6.6.

Cores from six wells are included in the database. The caliper, shallow resistivity and density porosity logs from each well were used as input and the respective core values of bulk volume oil were used as output.

Over training was minimized by considering the weights-to-records ratio to be always less than 0.5. This robust architecture was blind tested by predicting Bulk Volume Oil, Gas, Water and aspect ratio of the remaining five wells and log correlations were developed. The predicted results of the remaining five wells when blind tested are explained below.

6.3.1 Barbara#1 Predictions using Dagger Draw #12 Trained Network

The logs used for predicting the Bulk Volume Oil, Water of Barbara #1 were Caliper, LLS, Dphi; and for predicting the Bulk Volume Gas and Aspect Ratio are PEF, LLS, Dphi and Caliper, G-ray, Dphi logs respectively which produced best training results.

All these logs were selected irrespective of the fuzzy ranking procedure because here we are trying to establish a log correlation between the Dagger Draw #12 and the remaining five wells; therefore, the logs used will follow the same pattern as those used for developing the Dagger Draw #12 trained network. However, these logs are the individual logs of Barabara #1.When these logs are inputted and predicted for Bulk volume Oil, Gas and Water using the Dagger Draw#12 trained network, the results predicted were in good agreement to the actual core measurements Figures 6.24, 6.25, 6.26.

The architecture of this network always remains constant as we are using a trained network (Dagger Draw #12) to predict the results of all the remaining wells.

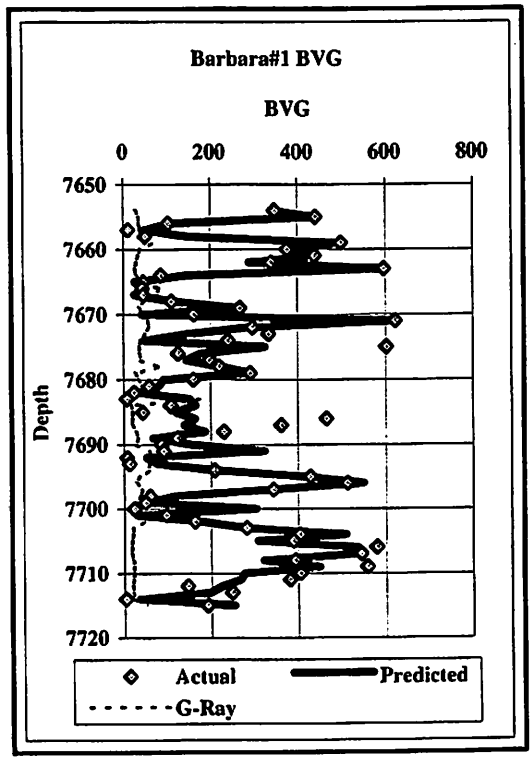

Figure 6.24: Actual Vs Predicted values of Barbara # 12 Bulk Volume Gas based Dagger Draw #12 trained network

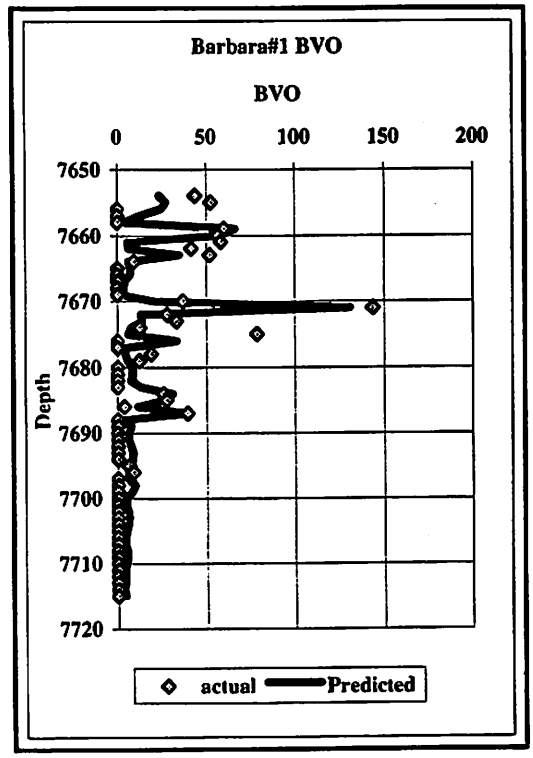

Figure 6.25: Actual Vs Predicted values of Barbara # 12 Bulk Volume Oil based Dagger Draw #12 trained network

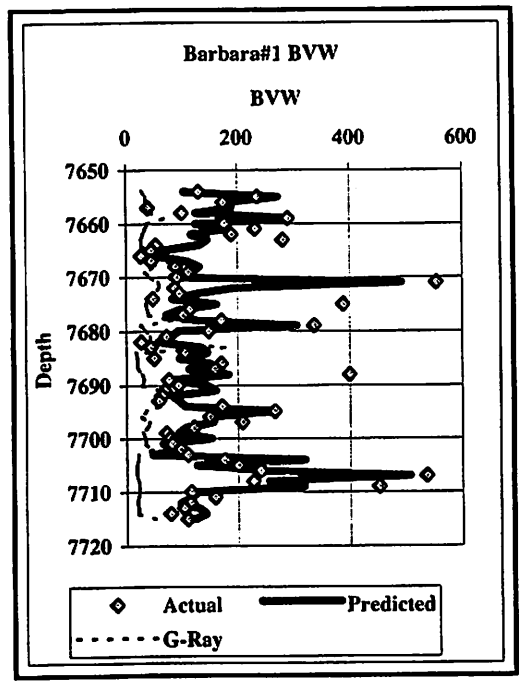

Figure 6.26: Actual Vs Predicted values of Barbara # 12 Bulk Volume Water based Dagger Draw #12 trained network

As we can see from the three-pseudo logs that were developed, the Bulk Volume Oil, Gas and Water values almost match with the core measurements.

6.3.2 Marathon #5 Predictions using Dagger Draw #12 Trained Network

To predict the Bulk Volumes Oil, Gas, Water, and aspect Ratio of Marathon #5 the Dagger Draw #12 log patterns were used since there exists good correlations established between the logs and the core measurements. Caliper, LLS, Dphi; which produced best training results for Dagger Draw #12 were used to predict the Bulk Volume Oil, Water of Marathon #5. To predict the Bulk Volume Gas again the same log patterns (PEF, LLS, Dphi) as used by Dagger Draw # 12 were used, and to predict the aspect ratio values Caliper, G-Ray, Dphi were used.

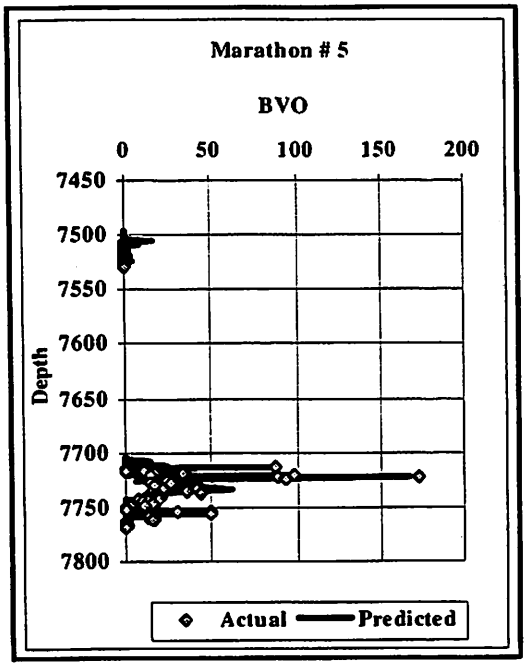

Figure 6.27: Actual Vs Predicted values of Marathon # 5 BVO (DD #12 Network)

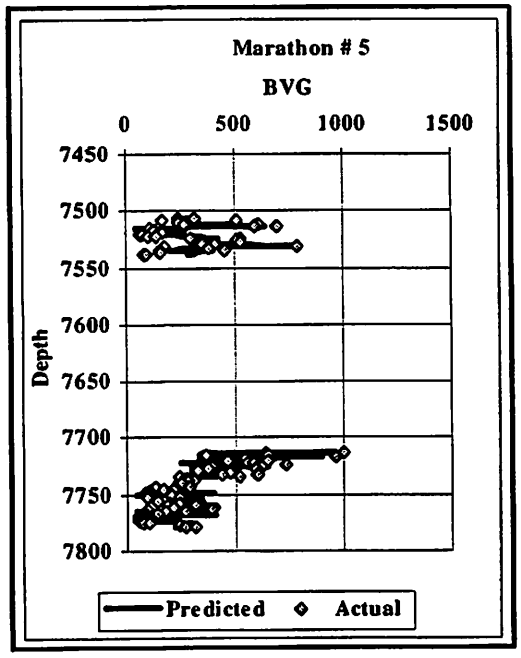

Figure 6.28: Actual Vs Predicted values of Marathon # 5 BVG (DD#12 Network)

As we can see from the pseudo logs, there was an excellent history match between the predicted and the actual values Figures 6.27, 6.28, 6.29, 6.30. For the intervals between 7550ft to 7700ft no core measurements were taken, nor the log data was available.

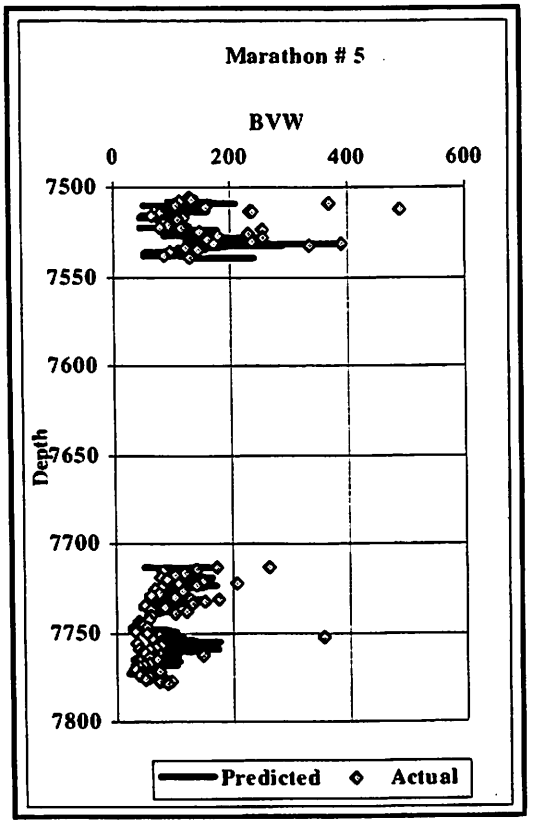

Figure 6.29: Actual Vs Predicted values of Marathon # 12 Bulk Volume Oil based Dagger Draw #12 trained network

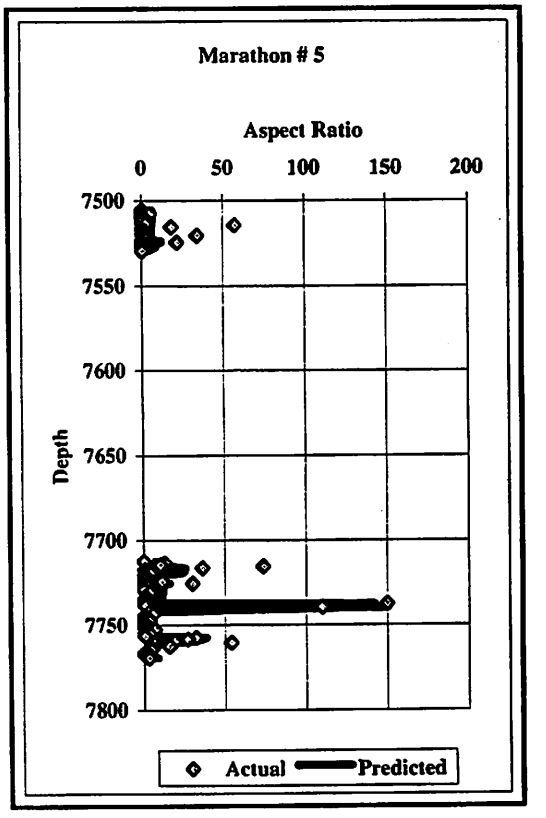

Figure 6.30: Actual Vs Predicted values of Marathon # 5 Aspect ratio based Dagger Draw #12 trained network

6.3.3 Saguaro #8 Predictions using Dagger Draw #12 Trained Network

Using the same trained network of Dagger Draw #12, and following the same log patterns the Bulk Volume Oil, Gas, Water and Aspect ratio of the Saguaro # 8 have been predicted and results were compared to the actual core measurements.

It is evident from the logs Figures 6.31, 6.32, 6.33, 6.34 that there is one to one correlation between the Dagger Draw #12 trained network and the Saguaro # 8 as the results predicted were good with the actual values.

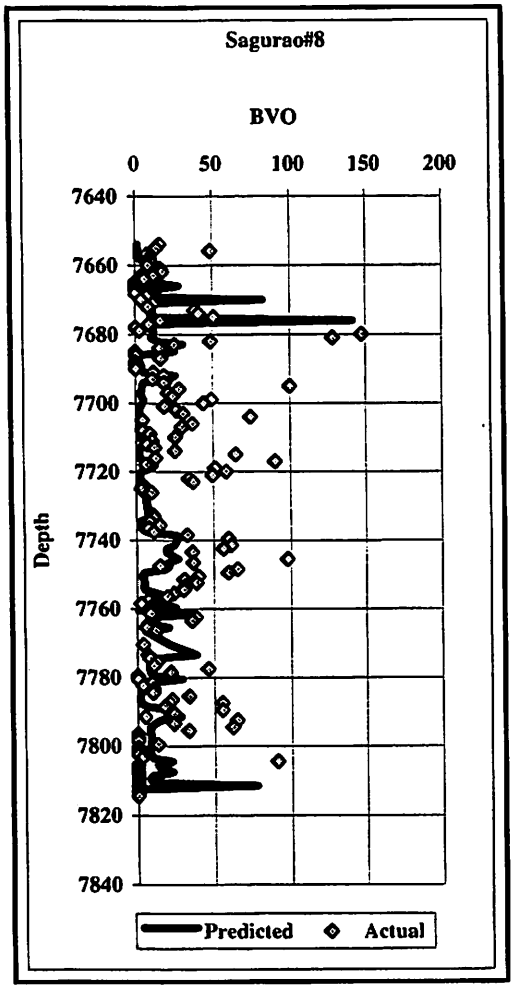

Figure 6.31: Actual Vs Predicted values of Saguaro # 8 Bulk Volume Oil based on Dagger Draw #12 trained network

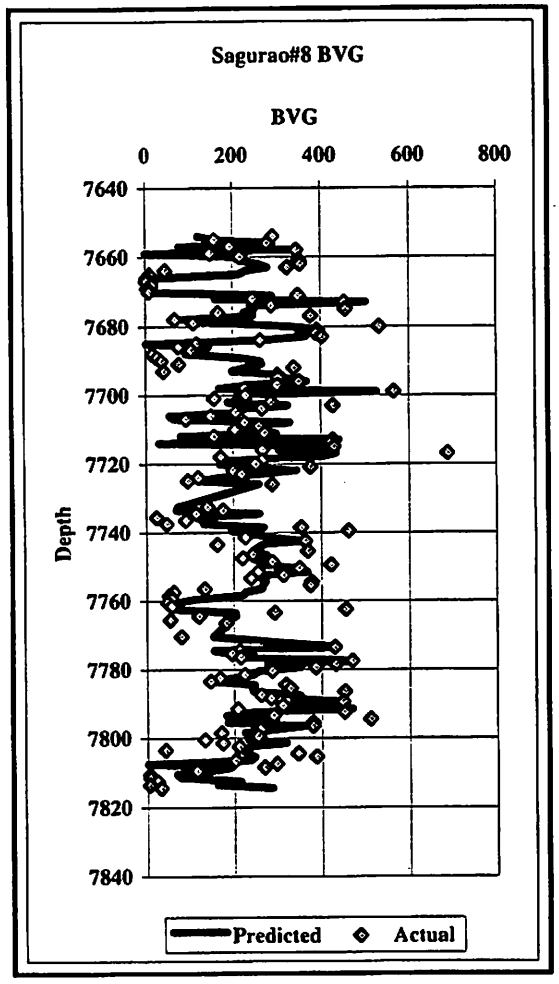

Figure 6.32: Actual Vs Predicted values of Saguaro # 8 Bulk Volume Gas based on Dagger Draw #12 trained network

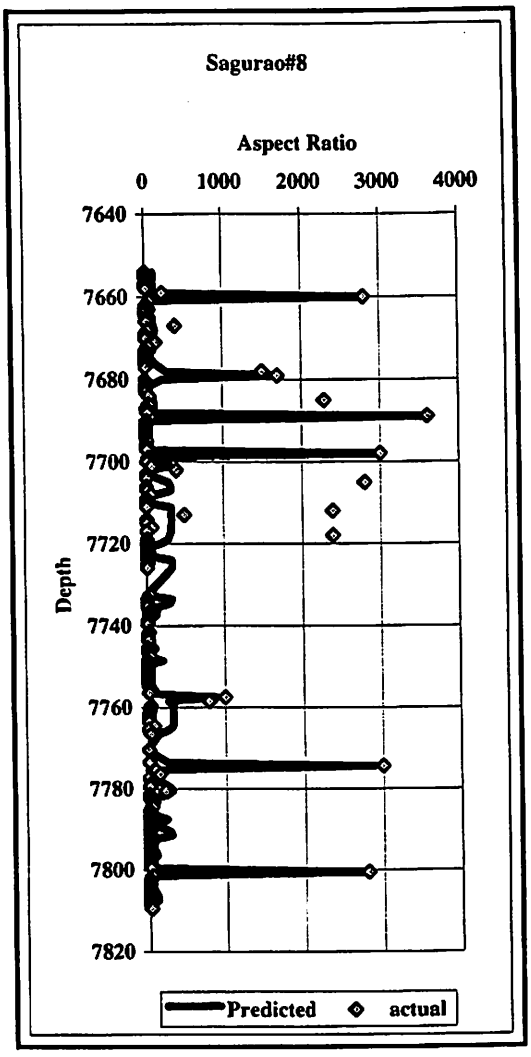

Figure 6.33: Actual Vs Predicted values of Saguaro # 8 Bulk Volume Water based on Dagger Draw #12 trained network

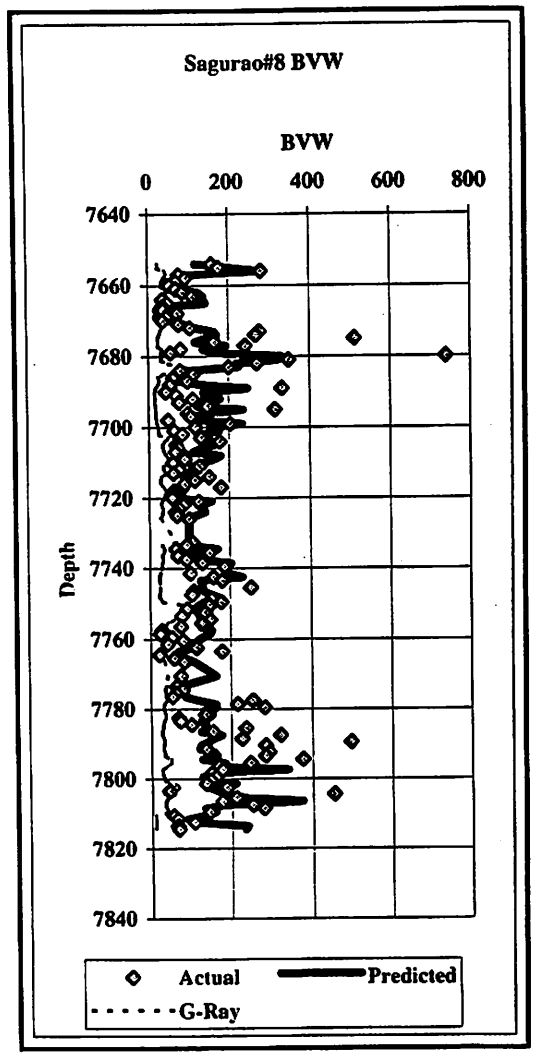

Figure 6.34: Actual Vs Predicted values of Saguaro # 8 Aspect ratio based on Dagger Draw #12 trained network

6.3.4 Cooper #1 Predictions using Dagger Draw #12 Trained Network

Using the Dagger Draw #12 trained network and following the same log patterns the Bulk Volume Oil, Gas and water of Cooper #1 are predicted. The results when compared with the predictions based on the individual logs, shows that the there is a good history matching. As an example if we compare the Bulk Volume Gas predicted values of the two different networks that we have created, Figure 6.35 show that the predicted

values don't match with the actual core measurements. In the same case using a well trained network (Dagger Draw #12) produces the best results as evident from Figure 6.36.

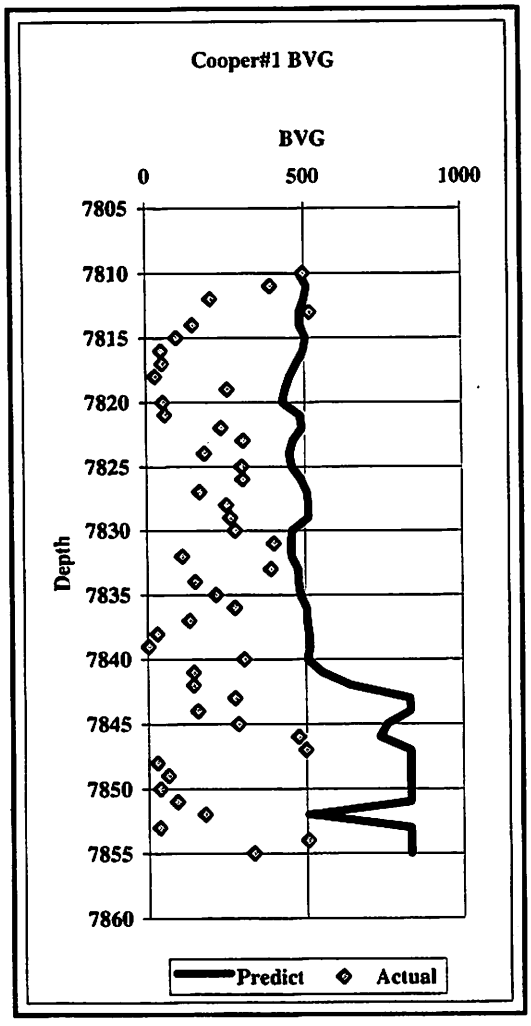

Figure 6.35: Actual Vs Predicted values of Cooper # 1 Bulk Volume Gas based on its Individual Network

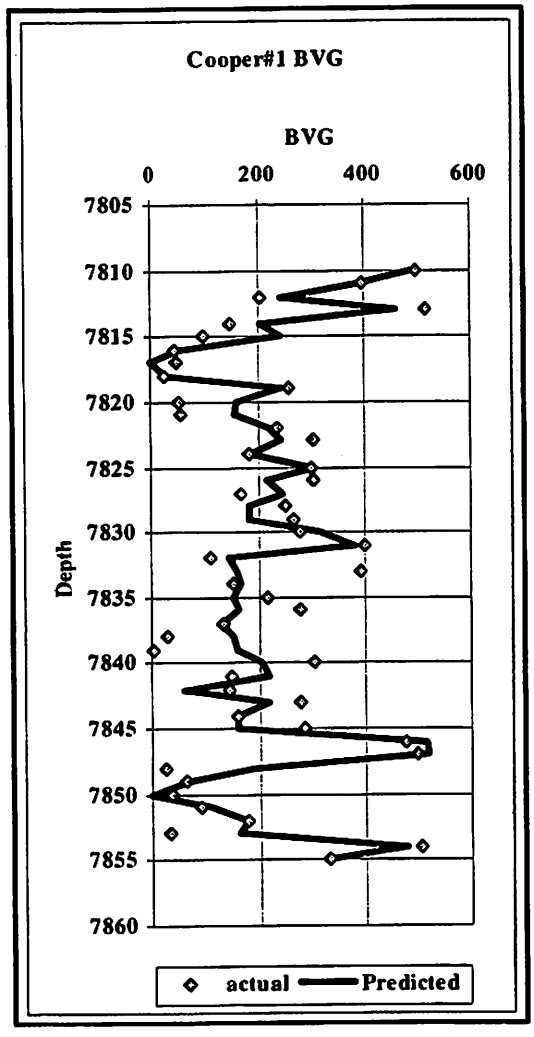

Figure 6.36: Actual Vs Predicted values of Cooper # 1 Bulk Volume Gas based on Dagger Draw #12 trained network

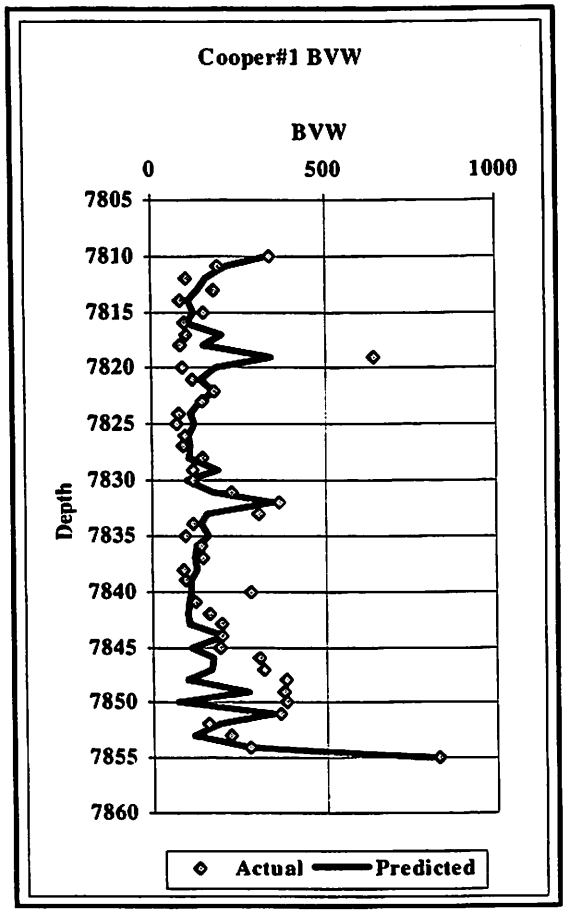

Figure 6.37: Actual Vs Predicted values of Cooper # 1 Bulk Volume Water based on its Dagger Draw #12 trained Network

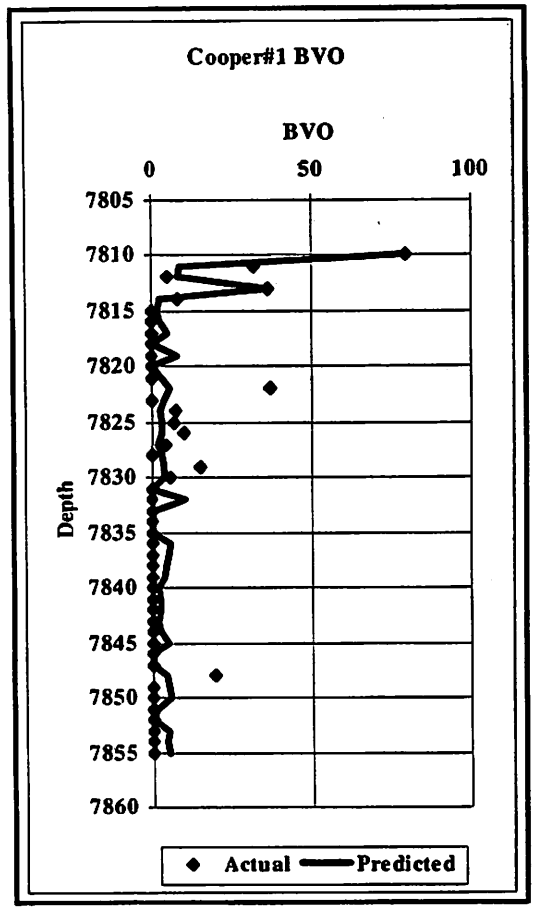

Figure 6.38: Actual Vs Predicted values of Cooper # 1 Bulk Volume Gas based on Dagger Draw #12 trained network

The Bulk Volume Water and Oil predictions are also good Figures 6.37, 6.38. Although the predictions with Bulk Volume Oil doesn't show much difference but still Dagger Draw #12 is the best trained network as it has a good correlation between the logs and the core measurements.

6.3.5 Ocotillo # 8 Predictions using Dagger Draw #12 Trained Network

This is a dry hole, thus there is no oil production in this well when the past history data was used to train the network, but we can see in Figure 6.40 oil being predicted. This is because Ocotillo#1 produced in later years. In the same way the history matching of the predicted Bulk Volumes of Gas is also good. Figure 6.39

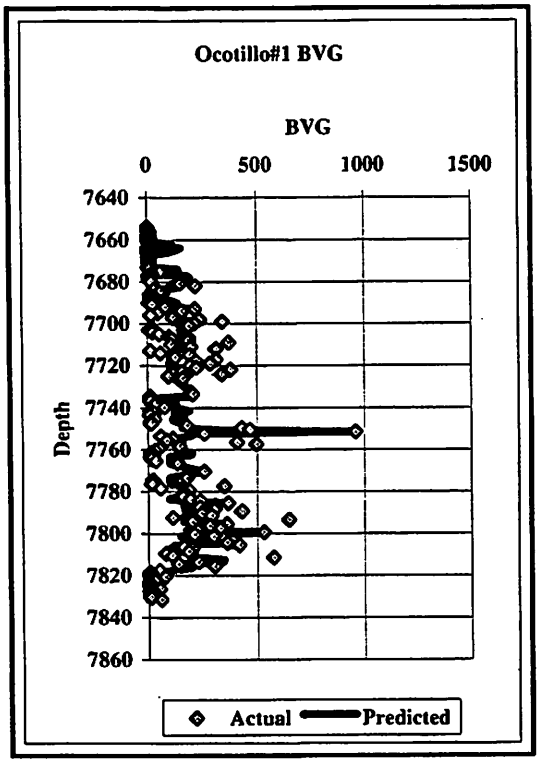

Figure 6.39: Actual Vs Predicted values of Ocotillo # 1 Bulk Volume Gas based on Dagger Draw #12 trained network

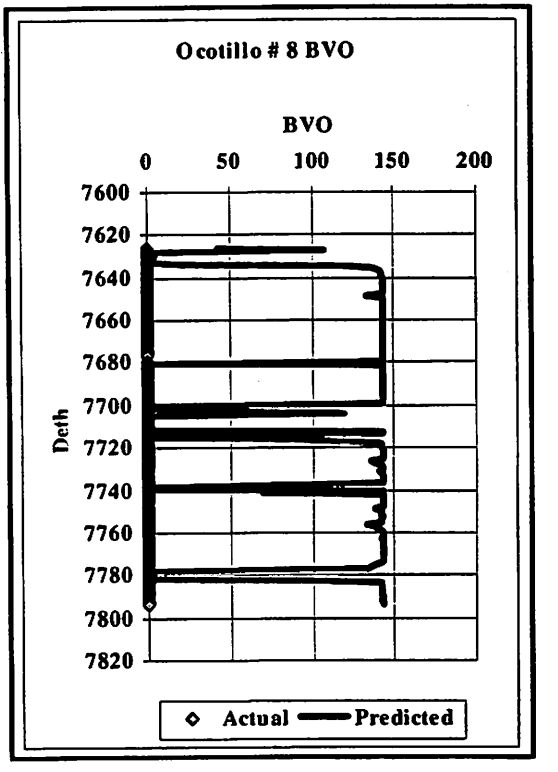

Figure 6.40: Actual Vs Predicted values of Ocotillo # 1 Bulk Volume Oil based on Dagger Draw #12 trained network

We can conclude from all the above pseudo logs developed that Dagger Draw #12 has a good correlation established between the logs and the core measurements and this correlation will be extended for all the remaining wells in the field which is evident from the five wells that we have used for our testing.

6.4 Production Correlations

Intuitively, the parameters Bulk Volume Oil, Gas and Water should correlate with the well's oil, gas and water production rates. It also seems reasonable that statistical properties can be used to describe the patterns of a BVO, BVG and BVW logs. Indeed, this was the situation that arose from this work. Three statistical properties, sum, average and standard deviation of the six-wells are calculated using the rules discusses below.

6.4.1 Statistical Parameters

In this study, univariant plots for data are generated for different derived properties. In order to evaluate the data statistically, the shape of the distribution is important in order to calculate the mean, standard deviation and sum.

6.4.1.1 Mean and Median value

The sample mean or average of a set of n measurements, $x_1, x_2 \ldots\ldots x_n$, is the sum of measurements divided by n. The mean is denoted by $\bar{x}$, which is expressed by

$$\bar{x} = \frac{\sum_{i=1}^{n} x_i}{n} \qquad (6.1)$$

6.4.1.2 Standard Deviation

In order to calculate the sample variance for the data, the following equation can be applied;

$$s^2 = \frac{\sum_{i=1}^{n} (x_i - \bar{x})^2}{n-1} \tag{6.2}$$

By calculation of sample variance the unit is squared. In order to arrange variance in the same unit as x_i and $\bar{x}$ a square root execution can be performed. The square root of the variance is defined as standard deviation.

$$s = \sqrt{\frac{\sum_{i=1}^{n} (x_i - \bar{x})^2}{n-1}} \tag{6.3}$$

If the data is exponential distributed, standard deviation is defined as the same as the sample mean. Then standard deviation simplifies to,

$$s = \bar{x} \tag{6.4}$$

The magnitude of standard deviation expresses how extensively the data are scattered. With only one single data set the numerical value of standard deviation is not so clear. Comparing two or more data sets, of the same quantity, a larger standard deviation means that data are more scattered [8].

6.5 Univariant Plots

6.5.1 Bulk Volume Oil

The statistical parameters of all the predicted Bulk Volumes of Oil, Gas and Water were calculated. Different univariant plots were plotted to check any correlation exists between the statistical parameters and the annual production rates. Figure 6.41 below suggests that the sum of BVO through the dolomite zone does correlate with the initial oil rate defined as the average of the first 12 producing months.

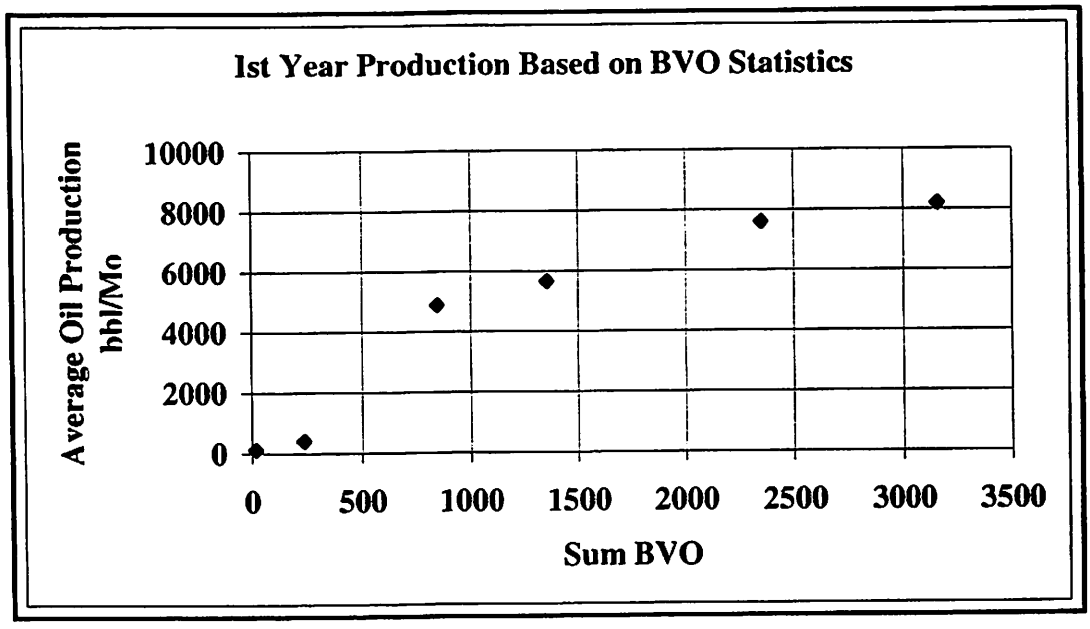

Figure.6.41: Statistical property "Sum" of the BVO logs in the 6-well dataset correlates with the initial oil rate.

Since the analysis is based on statistics, the dataset was enlarged to 14 wells. The Dagger Draw #12 neural network was used to develop statistical BVO log values given the caliper, shallow resistivity and density porosity logs from an additional eight non-cored wells. The statistical properties of each BVO log are included in Table IV.

No.	Name	Oil, bbl/mo	Sum	Average	STD
1	Dagger Draw #12	5954	1881	16.6	30.5
2	Marathon Federal #5	5650	1339	13.7	26.2
3	Barbara Federal #12	4400	1937	16.7	25.0
4	Ocotillo Federal #1	94	22	0.1	1.7
5	Cooper AHH #1	2576	269	5.9	14.6
6	Saguaro Federal #8	7458	4014	19.7	24.5
7	Diamond AKI #1	13409	65143	119	104
8	Hinkle ALD #3-H	8020	12432	22.8	49.0
9	Patriot AIZ #10	23603	65143	119	108
10	Preston Fed #5	5274	41237	75.5	99.2
11	State K #3	27513	23367	42.8	75.4
12	Walt Canyon # 2-H	3	7296	8.7	0.0
13	Binger AKU #4	332	49980	76.9	104.4
14	Rodke AOY # 1-H	0	30266	42.4	75.2

Table 6.2 Statistical properties and average values for first 12 producing months

A sum of BVO and standard deviation (STD) of BVO versus the initial oil rate crossplot with the 14-well dataset is plotted in Figures 6.42, 6.43. From these two plots we see that the distribution of points between the statistical parameters (sum, STD BVO) and the initial oil rates was impressive. Therefore, a proposal to develop a neural network using the statistical parameters was made, using the trend, to predict the production rates of the 8 non-cored wells.

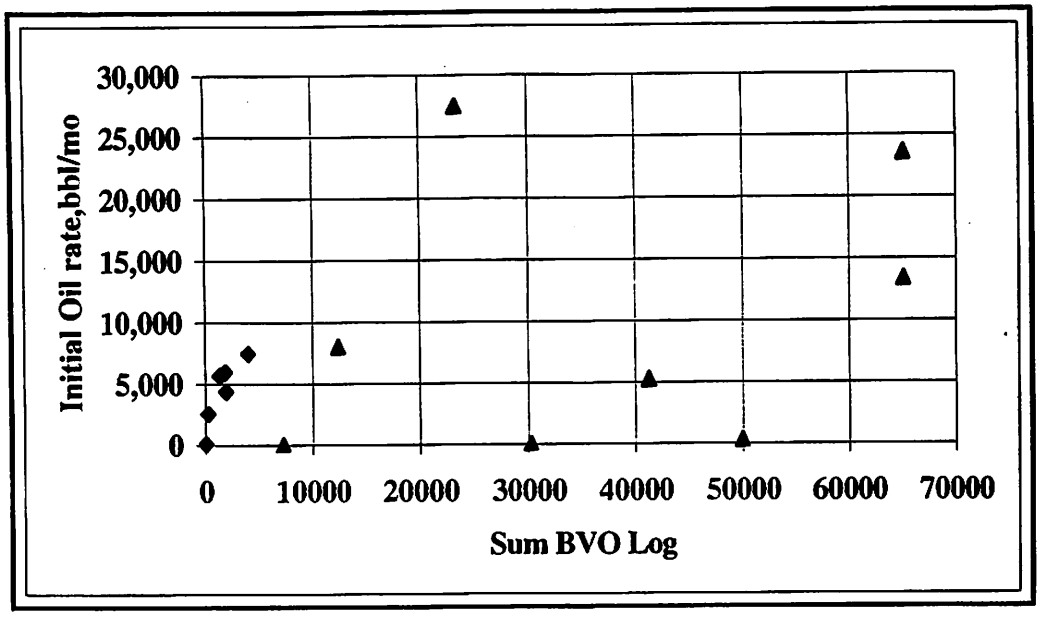

Figure 6.42: Statistical property "Sum" of the BVO logs in the 14-well dataset crossploted with initial oil rate.

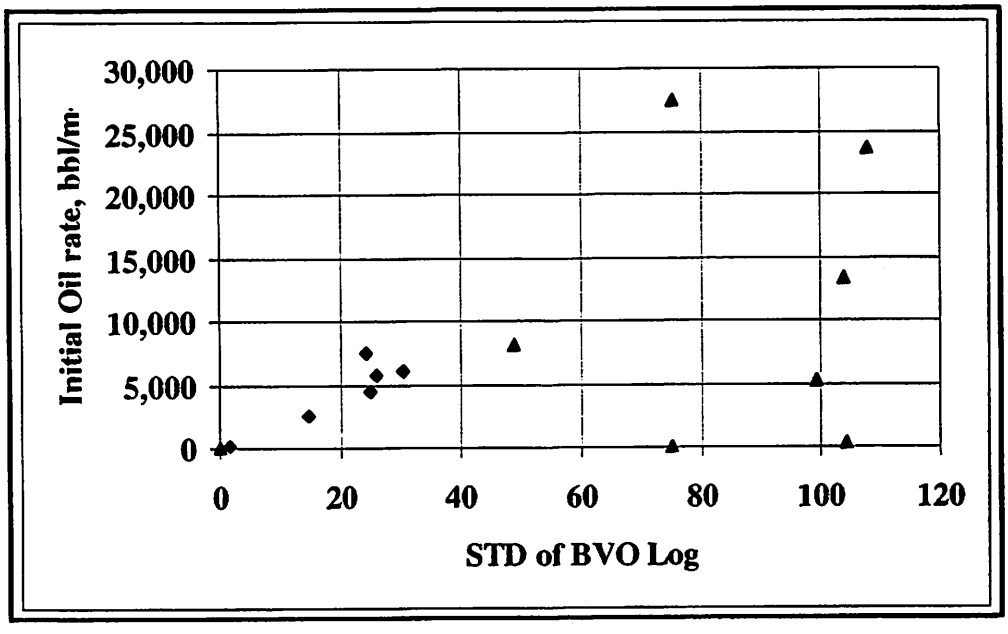

Figure 6.43: Statistical property standard deviation of the BVO logs in the 14-well dataset crossploted with the initial oil rate.

The available statistical parameters like sum, average, and STD of BVO were fuzzy ranked and sum, STD were selected as inputs for training the neural network. It was determined by trial and error that a 2-1-2-1 neural network with a 95% training correlation would correlate the two statistical properties with the initial oil-producing rate, and this network was used to predict the initial oil rate of the remaining 8 non-cored wells and the results are shown in Figure.6.44. The trained network wells are represented by "rombus points" and the tested values are represented by "triangle points".

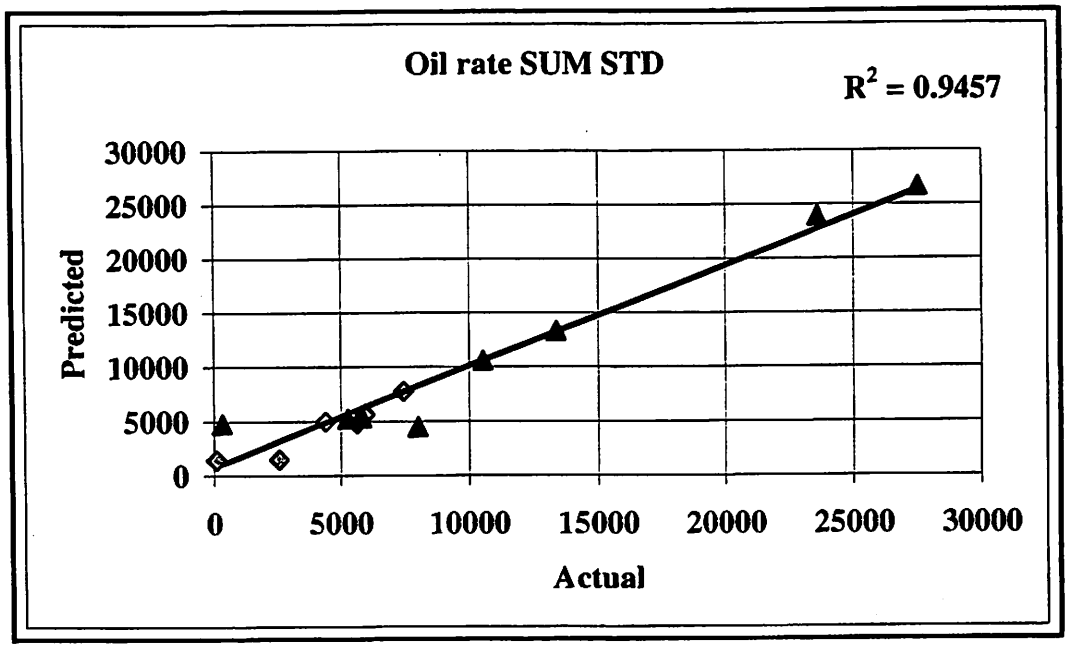

Figure 6.44: Goodness of multivariate correlation between predicted and actual oil rate developed with 2-1-2-1 neural network.

As we can see from Figure 6.44, a very good production correlation (94.5%) was developed. This neural network can be used to predict the initial oil rates of the rest of the wells in the Dagger Draw filed provided the well log data is available.

6.5.2 Bulk Volume Gas

In the same way as described earlier, the statistical parameters sum, average (Avg) and standard deviation (STD) of Bulk Volume Gas were calculated and produced in Table 6.2 . Different univariant plots were plotted to determine if any correlation exists between the statistical parameters and the initial gas rates.

Well	Sum BVG	Average Gas ProductionMMscf/mo	STD	Average
MOC Federal #5	29995	41236.5	129.01	306.01
Dagger Draw #12	41655.24	20415	161.448	218.093
Sagurao #8	34066.9	16484.5	110.09	228.63
Cooper#1	9945.6	8457.3	128.8	216.2
Ocotillo#1	22918.9	16031	109.17	138.06
Barbara#12	14497.7	12769	162.43	233.53

Table 6.3: Statistical parameters and the actual gas production rates of all the six wells

Figure 6.45 below suggests that the sum of BVG through the dolomite zone does correlate with the initial gas rate defined as the average of the first 12 producing months.

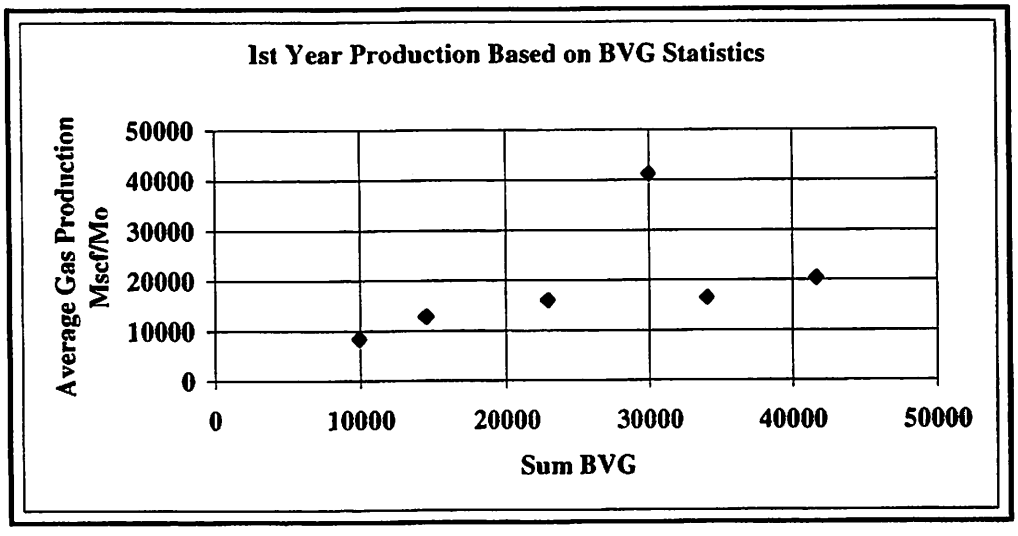

Figure 6.45: Univariant plot of the sum of Bulk Volume Gas and initial gas rate

The standard deviation (STD) and average(Avg) of Bulk Volume Gas versus the initial gas rate crossplot with the 6-well dataset was developed. But, only a noisy trend is recognized for both these statistical parameters as evident from Figures 6.46,6.47.

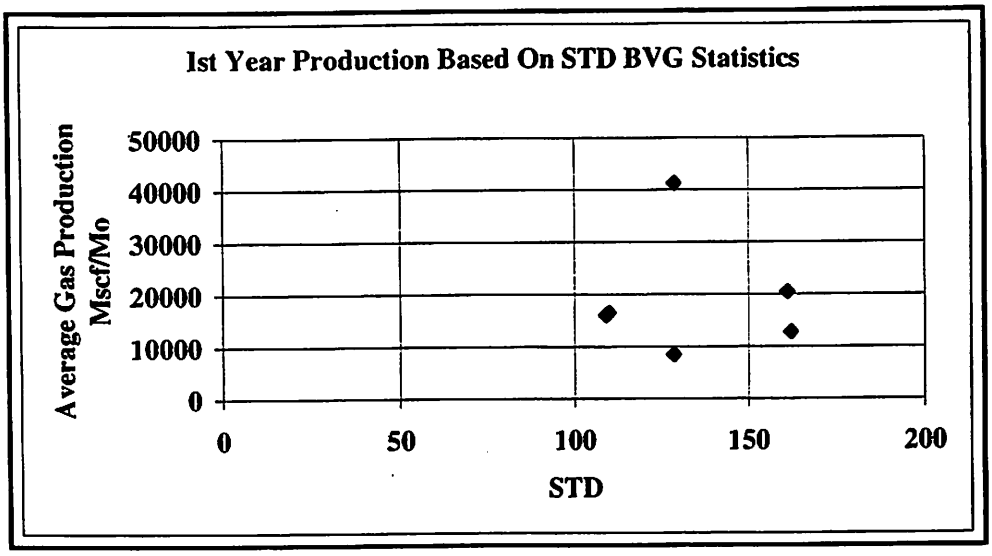

Figure 6.46: Univariant plot of the STD of Bulk Volume Gas and initial gas rate

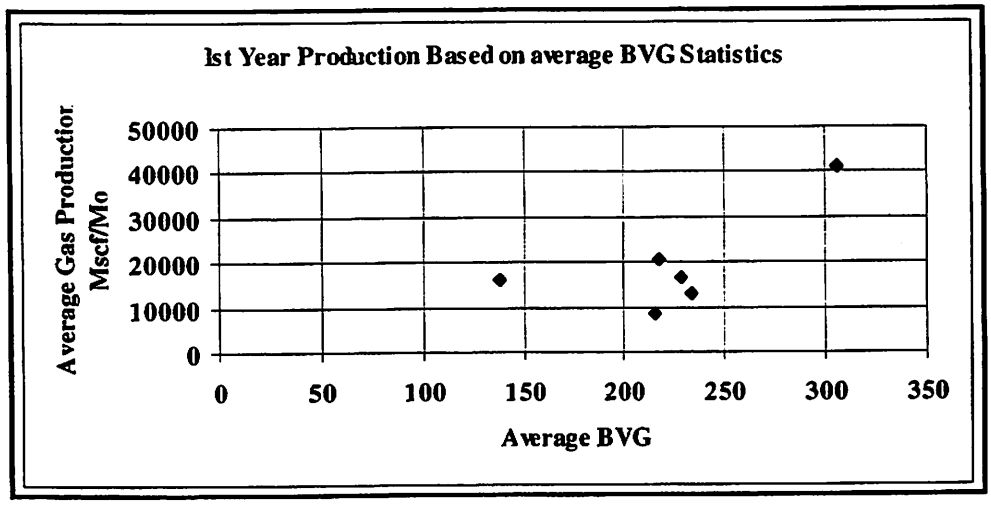

Figure 6.47: Univariant plot of the average of Bulk Volume Gas and initial gas rate

A proposal to develop a neural network was made and when the statistical parameters sum and standard deviation of Bulk Volume Gas were used as inputs to a train the neural network, it was determined by trial and error that a 2-1-1 neural network would correlate the two statistical properties with the initial gas-producing rate with a 97% production correlations Figure 6.48.

This dynamic neural network can be used to predict the initial gas rates for the rest of the wells in the Dagger Draw filed provided the statistical parameters are available.

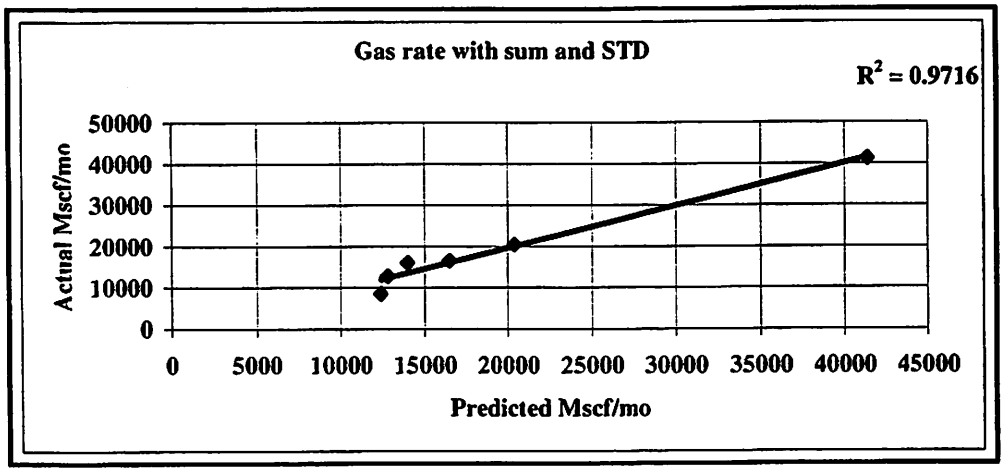

Figure 6.44: Goodness of multivariate correlation between predicted and actual gas rate developed with 2-1-1 neural network.

In the same way a neural network for initial water rate is established using sum and Avg with 1 (2-1-1) architecture and a production correlation of 75% was achieved Figure 6.45.

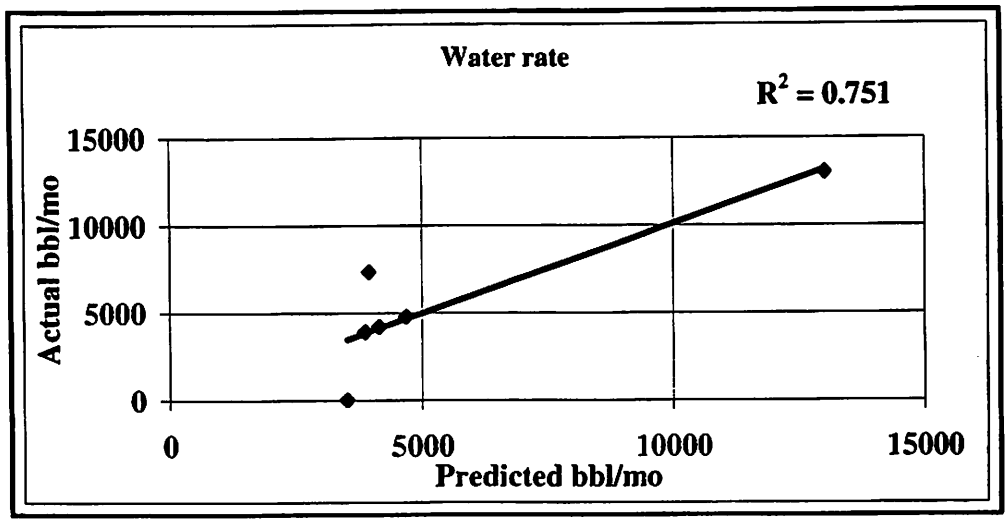

Figure 6.45: Production correlation of actual and predicted water rates for all the six wells.

Although this neural network was not as good as those developed for oil and gas this network can still be used for prediction of initial water rates as water is not our main concern.

Chapter VII

Conclusions

Artificial intelligence tools, fuzzy ranking and neural networks were used to correlate carbonate reservoir logs with laboratory core measurements of bulk volume oil, gas and water. The caliper, shallow resistivity and density porosity logs demonstrated the strongest relationship with BVO and BVW (highest fuzzy rank) of the eight available logs and similarly photo electric factor, shallow resistivity and density porosity logs demonstrated the strongest relationship with BVG of all the available logs.

Six wells with both log and core information were in the dataset. Neural Networks with caliper, shallow resistivity and density porosity logs as inputs and BVO as output were developed for each of the wells. Of the six single well datasets, the neural network with 200 core measurements, Dagger Draw #12 was particularly robust.

The robust neural network was used to predict BVO, BVG and BVW logs using the remaining six wells with caliper, shallow resistivity, density porosity, photo electric factor logs as input. The correlation coefficients resulting from crossplots of the predicted BVO ,BVG and BVW values versus the measured values were quite similar to training values of the respective datasets suggesting that the robust Neural Network could be applied to other non-cored wells in the field.

The robust Dagger Draw #12 neural network was used to generate BVO, BVG and BVW logs from the caliper, shallow resistivity, photo electric factor and density porosity logs of eight other logs in the field. The statistical properties, sum and standard deviation of the six wells BVO, BVG and BVW logs were used to generate a neural network correlation with the initial oil-producing rate. This production correlation was used to predict the initial oil rates of the 8 non-cored wells and the results seem to be good.

Thus, caliper, shallow resistivity, photo electric factor and density porosity logs from any well in the Dagger Draw Field can be used to locate potential oil and gas behind pipe [7].

REFERENCES

[1] Weiss W.W., Balch R.S., Wo S., Welch D. "Predicting Core Porosity using Wire-Line logs at Dagger Draw Field, SE New Mexico," SPE Permian Basin oil and gas recovery conference, Midland. SPE 59554 (March 2000).

[2] Ronald F. Broadhead. "Underdeveloped oil fields in Upper Pennsylvanian and Lower Permian carbonates of southeast New Mexico: Initial development missed major Reserves," The Leading Edge (September 1999)

[3] Ronald F. Broadhead. "Underdeveloped oil fields-Upper Pennsylvanian and Lower Wolf campian carbonate reservoirs of southeast New Mexico," Carbonates and Evaporates, v. 14, no. 1,1999,p. 84-105.

[4] Zhong H., Linyu Y., John Y., Ching W."Neural-Network approach to Predict Well Performance using available Field Data," SPE Western Regional Meeting held in Bakersfield, California. SPE 68801 (March 2001).

[5] Doraiswamy H., "Methods of Neuro-Simulation for Field Development," SPE Rocky Mountain /Low Permeability Reservoir Regional Meeting held in Denver. SPE 39962 (April 1998).

[6] Thomas W Engler., "Well Log Interpretations," Course notes Spring 2001.

[7] W.Weiss., V.Gottumukkala., R.Balch. "A New Method of Calibrating Wireline Logs with Carbonate Core Measurements To Recognize Pay Zones," SPE Annual Technical Conference, San Antonio. SPE 77330(September 2002).

[8] Arild Sunde. "Producing Characteristics and Drainage Volume of Dakota Wells, San Juan Basin, New Mexico." Thesis May 2000.

[9] William Weiss., Dr. Ron Broadhead., Dr. Andrew Sung. "Risk reduction with a fuzzy expert exploration tool." DOE Annual report June 30, 2000.

[10] Lin Y., and Cunniham G.A. "A new approach to Fuzzy-Neural System Modeling," IEEE Transactions on Fuzzy Systems, (v3 no 2,1995), 190-198.

[11] http://www-ra.informatik.uni-tuebingen.de/SNNS.

ADDITIONAL REFERENCES

[1] Stundner. M., Al-Thuwaini J.S. "How Data-Driven Modeling Methods like Neural Networks can help to integrate different Types of Data into reservoir Management," SPE Middle East Oil Show in Bahrain. SPE 68163 (March 2001).

[2] Cheng Z., Xi-Ling W., Ju-An C., Jianghan Petroleum Inst."Determining Reservoir Properties in Reservoir studies Using a Fuzzy Neural Netwrok," SPE 68th Annual Technical conference and Exhibition held in Houston,TX. SPE 26430 .

[3] Soto B., Holditch S.A. "Development of Reservoir Characterization Models Using Core, Well Log, and 3D Seismic Data and Intelligent Software," SPE East Regional Conference in Charleston, WV. SPE 57457

[4] Shahab M.,Andrel P.,George K.,David H.,Advanced Resources International. "Reducing the Cost of Field –scale Log Analysis Using Virtual Intelligence Techniques," 1999 SPE Eastern Regional Meeting held in Charleston. SPE 57454 (October 1999).

[5] Lopez R., Perez J.R., Dassori C.G., Ranson A." Artificial Neural Networks Applied to the Operation of VGO Hydrotreaters," SPE Latin America and Caribbean Petroleum Engineering Conference in Buenos Aires, Argentina. SPE 69500.

[6] Shahab M." Neural Network: What It Can Do for Petroleum Engineers," Journal of Petroleum Technology, SPE 29919.

[7] Caers J., Journel A." Stochastic Reservoir Simulation Using Neural Networks Trained on Outcrop Data," SPE Annual Technical Conference held in New Orleans. SPE 49026 (September 1998).

[8] Hart M., Balch R., Weiss W., Wo S." Time-to-Depth Conversions of Nash Draw "L" Seismic Horizon Using Seismic Attributes and Neural Networks," SPE Permian Basin Oil and Gas Recovery Conference held in Midland, TX. SPE 59555 (March 2000).

[9] Tapias O., Soto C., Perez H., Bejarano A."Reservoir Engineer and Artificial Intelligence Techniques for Data Analysis," SPE Asia Pacific Oil and Gas Conference held in Jakarta Indonesia. SPE 68743 (April 2001).

[10] Ali J.K., "Neural Networks: A New Tool for the Petroleum Industry?," SPE European Petroleum Computer Conference in Aberdeen, UK. SPE 27561 (March 1994).

[11] Kunmoluyi A.O., Daltaban .T.S. "Higher –Order Neural Networks in Petroleum Engineering," SPE Western Regioanl Meeting held in Longbeach, California. SPE 27905 (March 1994).

[12] Shahab M., Scott R., David H., Advanced Resources International. "Development of an Intelligent Systems for Restimulation Candidate Selection," 2000 SPE Gas Technology Symposium held in Calgary, Alberta, Canada. SPE 59767 (April 2000).

Appendix A

Fuzzy Curves

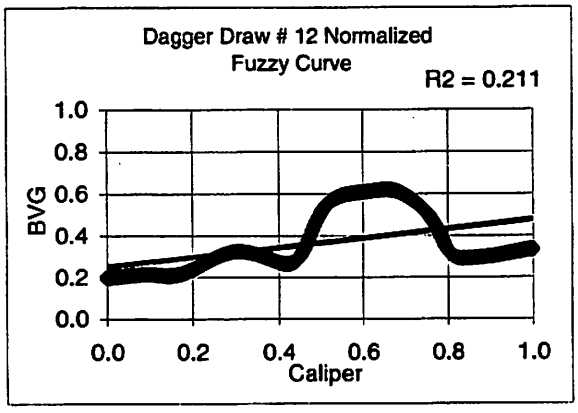

Figure A-1: Fuzzy Curve BVG vs Calip

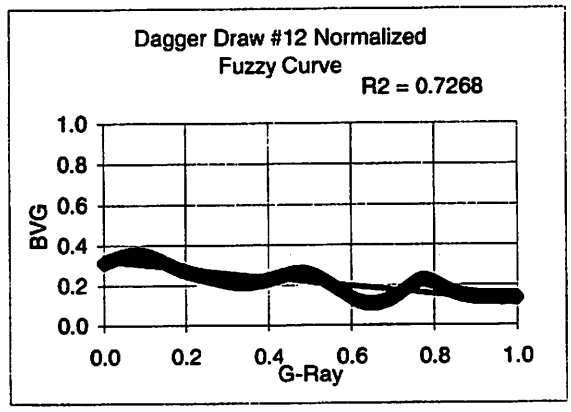

Figure A-2: Fuzzy Curve BVG vs G-Ray

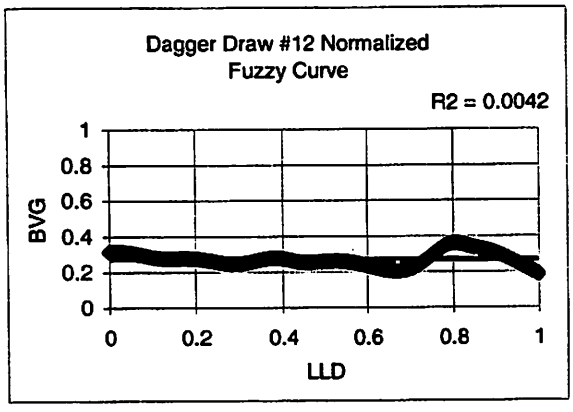

Figure A-3: Fuzzy Curve BVG vs LLD

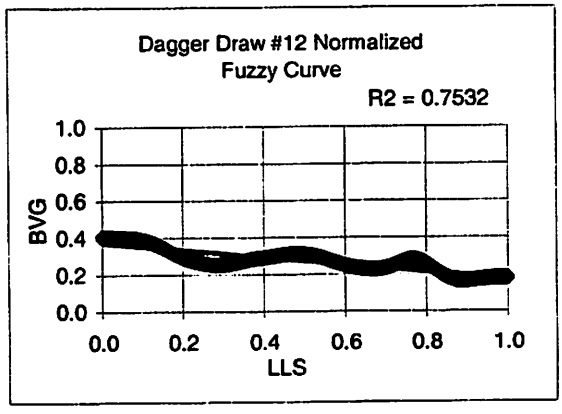

Figure A-4: Fuzzy Curve BVG vs LLS

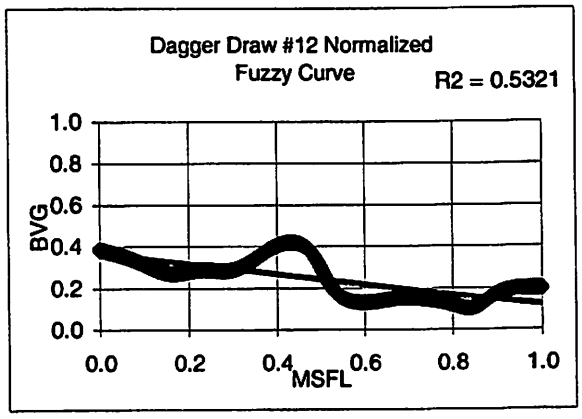

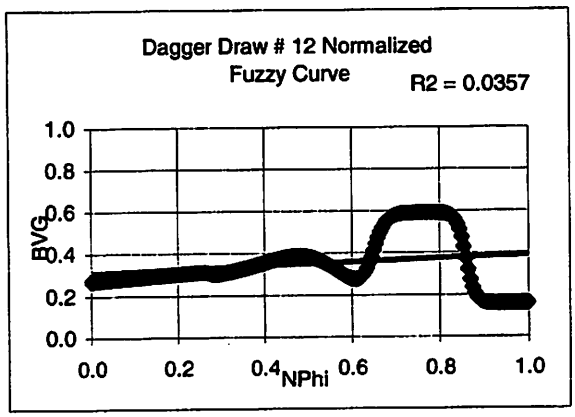

Figure A-5: Fuzzy Curve BVG vs MSFL **Figure A-6: Fuzzy Curve BVG vs Nphi**

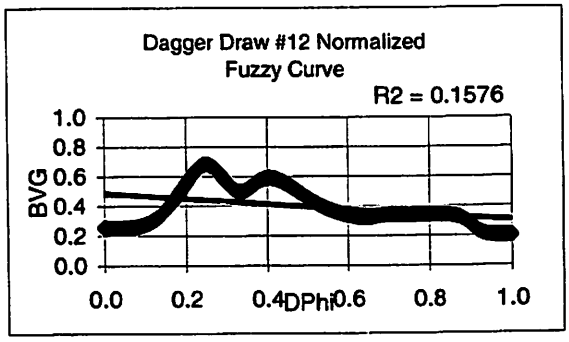

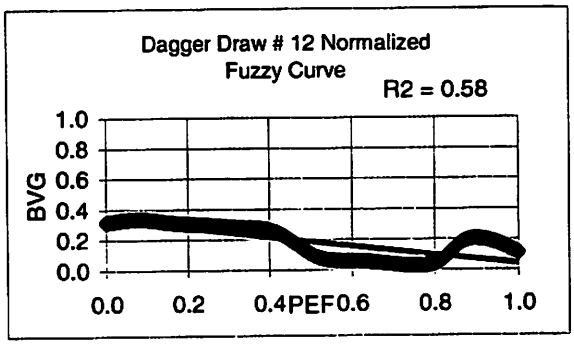

Figure A-7: Fuzzy Curve BVG vs Dphi **Figure A-8: Fuzzy Curve BVG vs PEF**

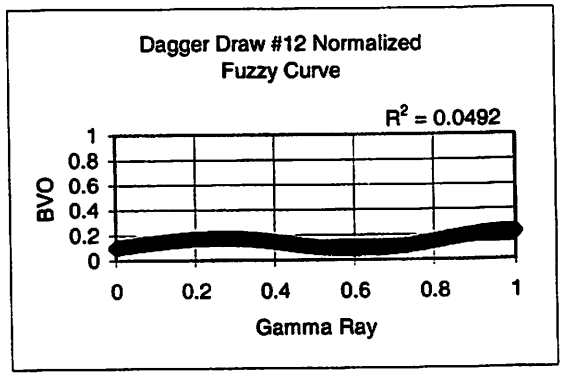

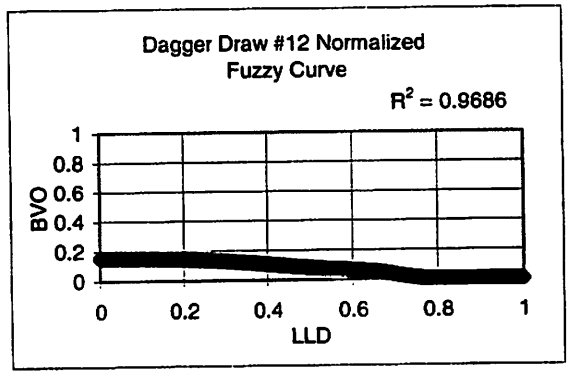

Figure A-9: Fuzzy Curve BVO vs G-Ray **Figure A-10: Fuzzy Curve BVO vs LLD**

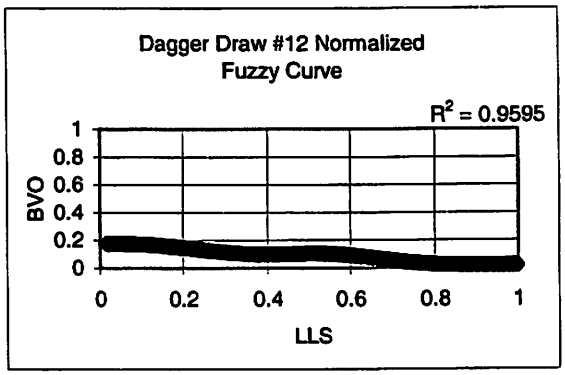

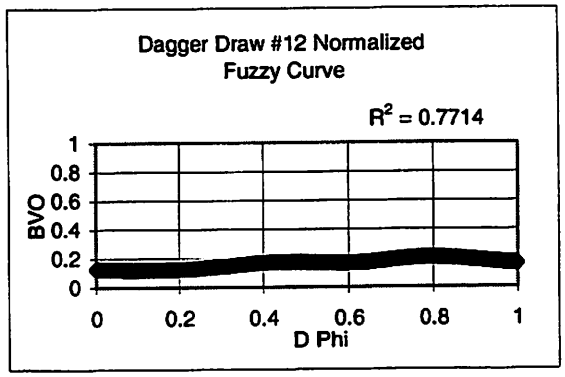

Figure A-11: Fuzzy Curve BVO vs LLS **Figure A-12: Fuzzy Curve BVO vs Dphi**

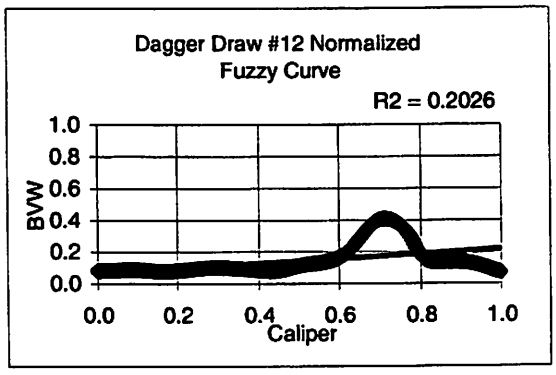

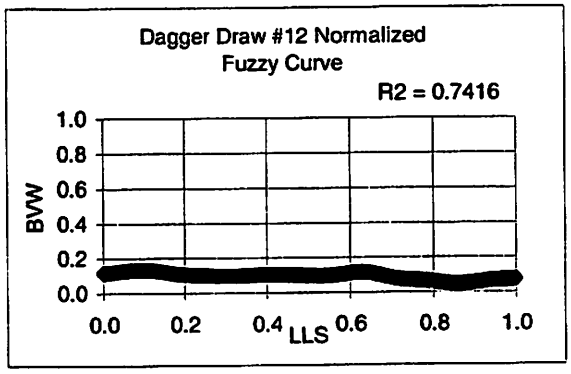

Figure A-13: Fuzzy Curve BVW vs Calip **Figure A-14: Fuzzy Curve BVW vs LLS**

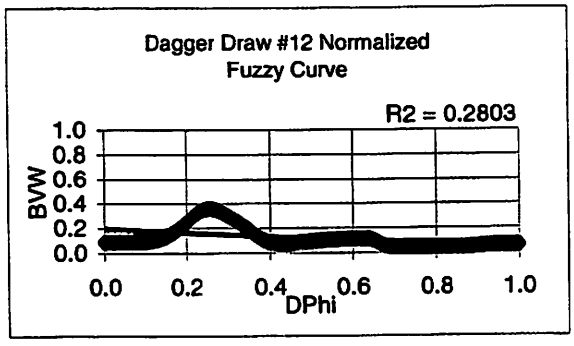

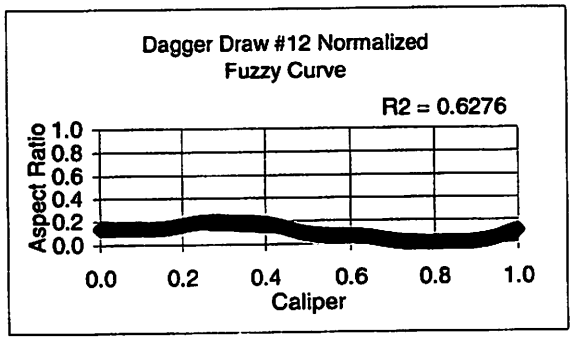

Figure A-15: Fuzzy Curve BVW vs Dphi **Figure A-16: Fuzzy Curve Aspect vs Calip**

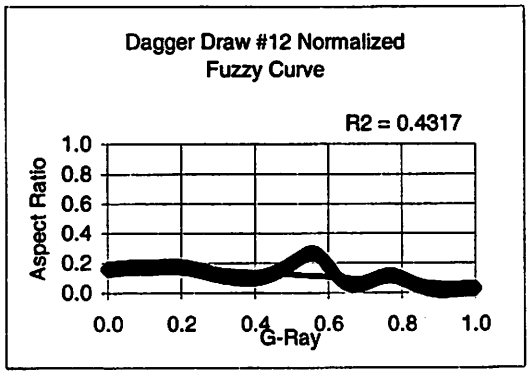

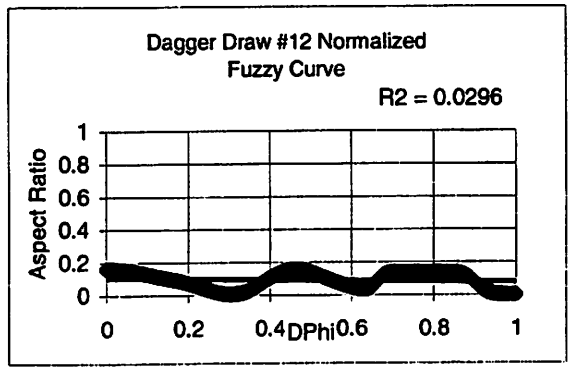

Figure A-17: Fuzzy Curve Aspect vs GR **Figure A-18: Fuzzy Curve Aspect vs Dphi**

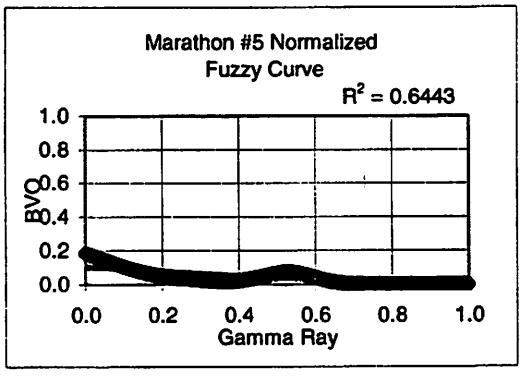

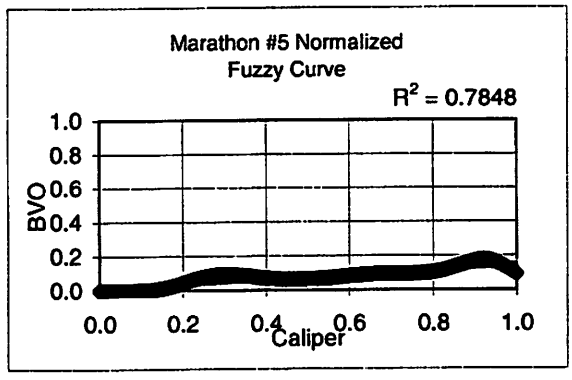

Figure A-19: Fuzzy Curve BVO vs GR **Figure A-20: Fuzzy Curve BVO vs Calip**

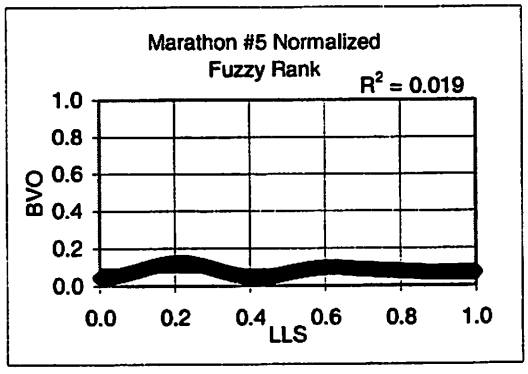

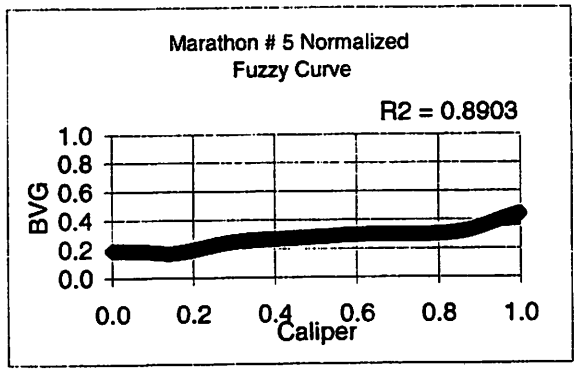

Figure A-21: Fuzzy Curve BVO vs LLS **Figure A-22: Fuzzy Curve BVG vs Caliper**

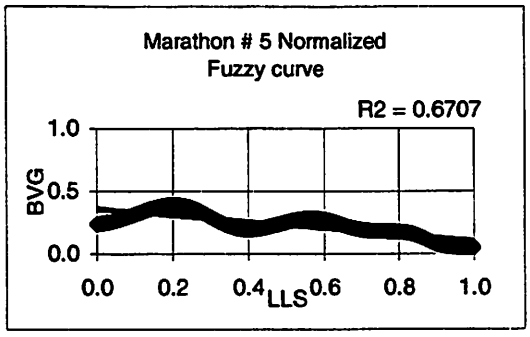

Figure A-23: Fuzzy Curve BVG vs LLS

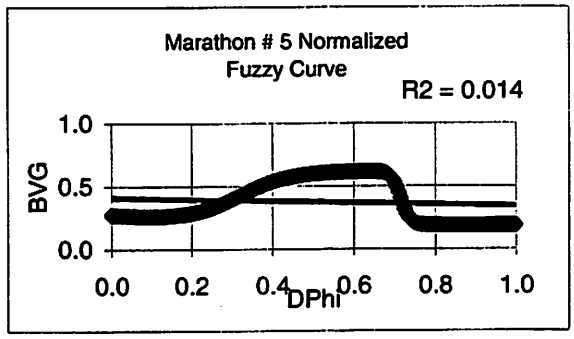

Figure A-24: Fuzzy Curve BVG vs Dphi

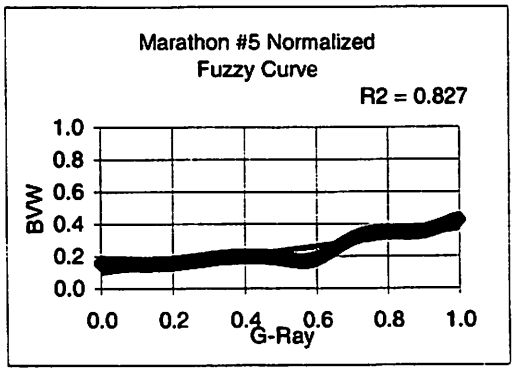

Figure A-25: Fuzzy Curve BVW vs GR

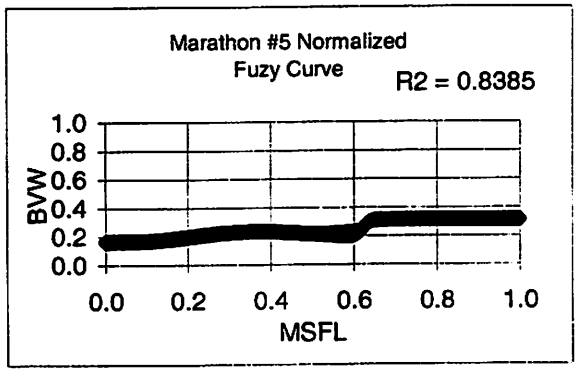

Figure A-26: Fuzzy Curve BVW vs MSFL

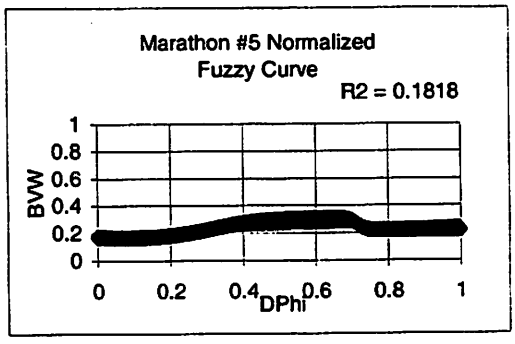

Figure A-27: Fuzzy Curve BVW vs Dphi

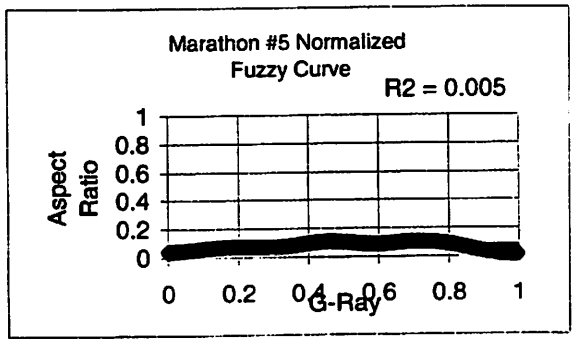

Figure A-28: Fuzzy Curve Aspect vs GR

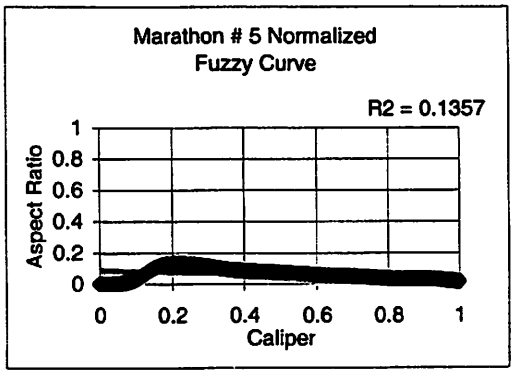

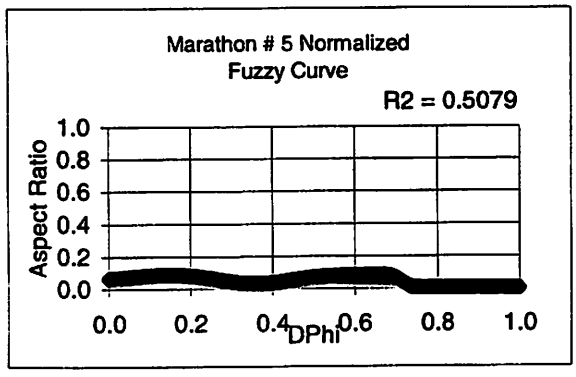

Figure A-29: Fuzzy Curve Aspect vs Cali Figure A-30: Fuzzy Curve Aspect vs Dphi

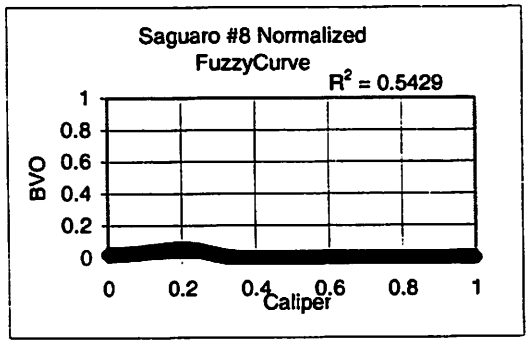

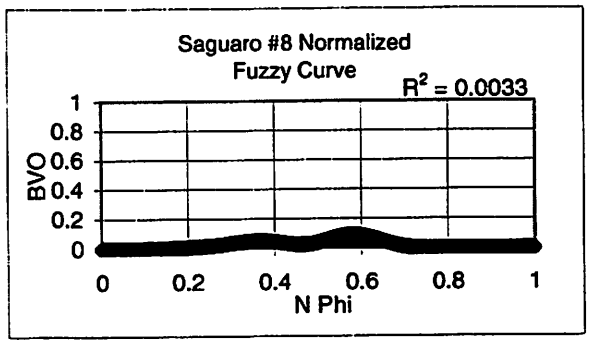

Figure A-31: Fuzzy Curve BVO vs Calip Figure A-32: Fuzzy Curve BVO vs Nphi

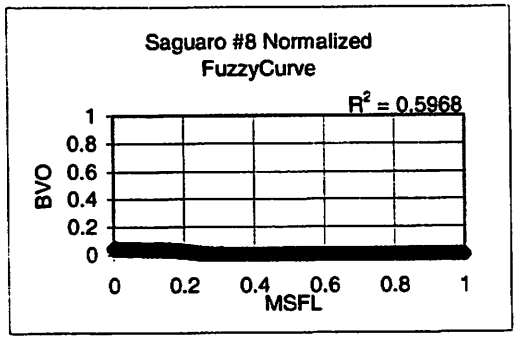

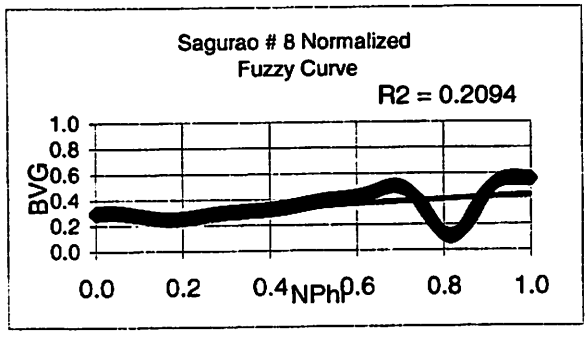

Figure A-33: Fuzzy Curve BVO vs MSFI Figure A-34: Fuzzy Curve BVG vs Nphi

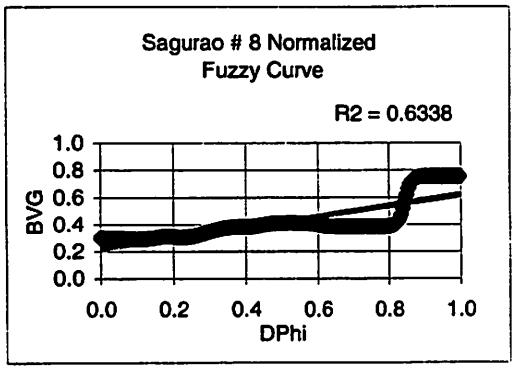

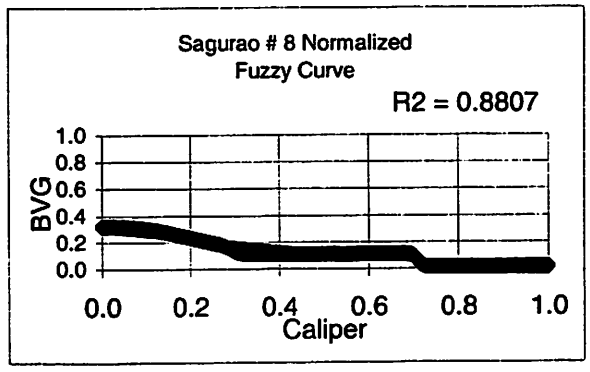

Figure A-35: Fuzzy Curve BVG vs Dphi Figure A-36: Fuzzy Curve BVG vs Calip

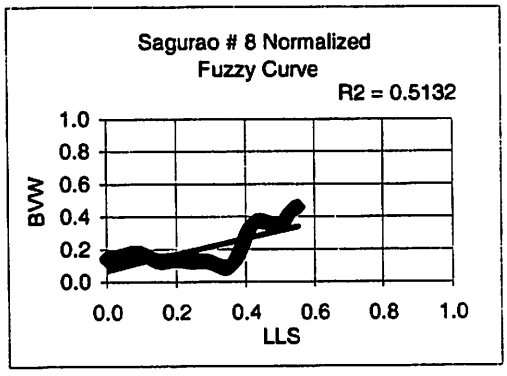

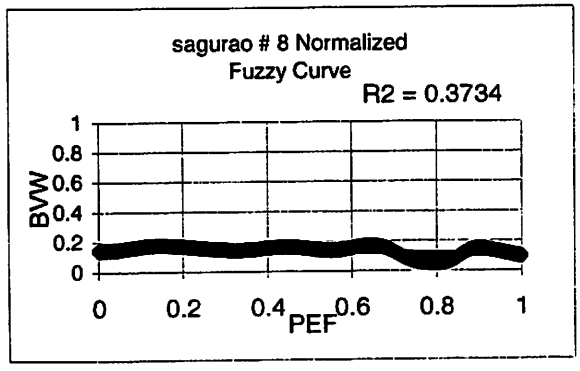

Figure A-37: Fuzzy Curve BVW vs LLS Figure A-38: Fuzzy Curve BVW vs PEF

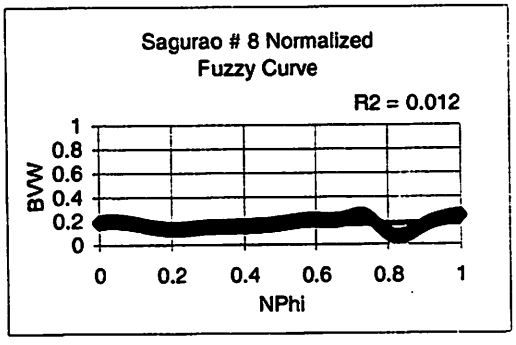

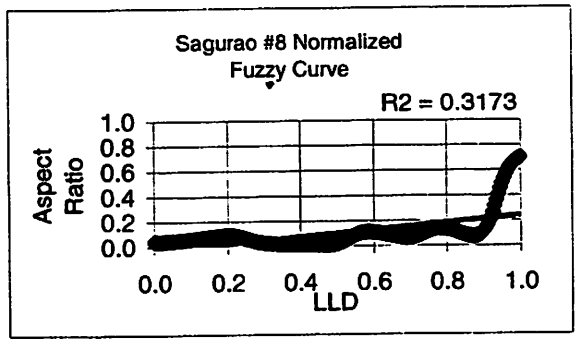

Figure A-39: Fuzzy Curve BVW vs Nphi Figure A-40: Fuzzy Curve Aspect vs LLD

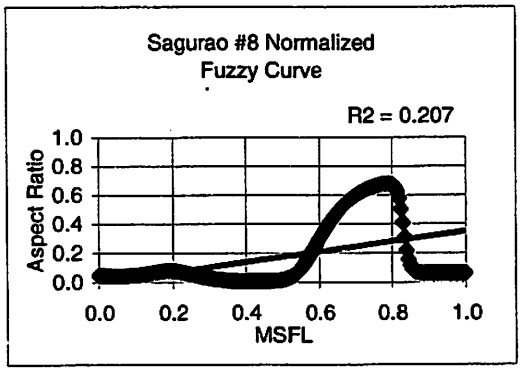

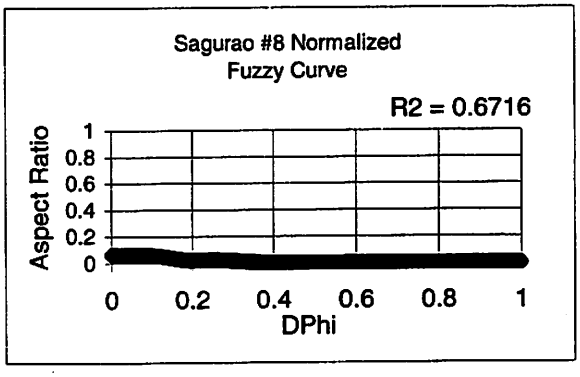

Figure A-41: Fuzzy Curve Aspect vs MSI **Figure A-42: Fuzzy Curve Aspect vs Dphi**

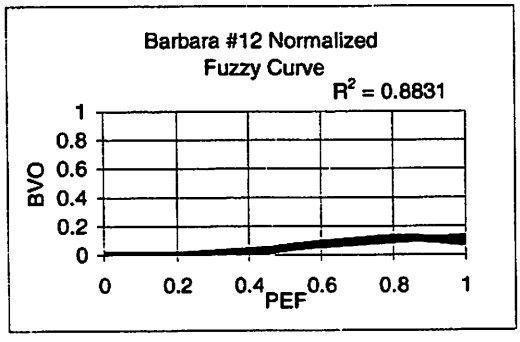

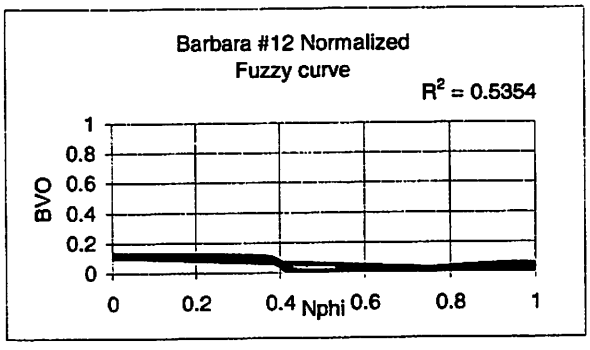

Figure A-43: Fuzzy Curve BVO vs PEF **Figure A-44: Fuzzy Curve BVO vs Nphi**

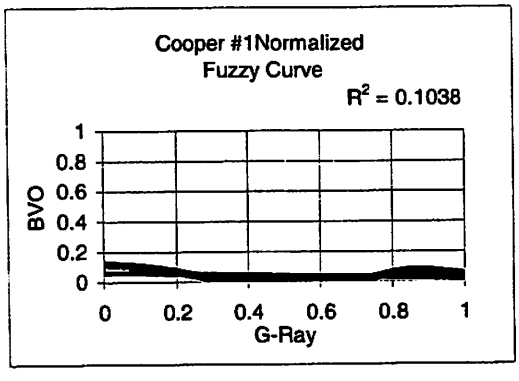

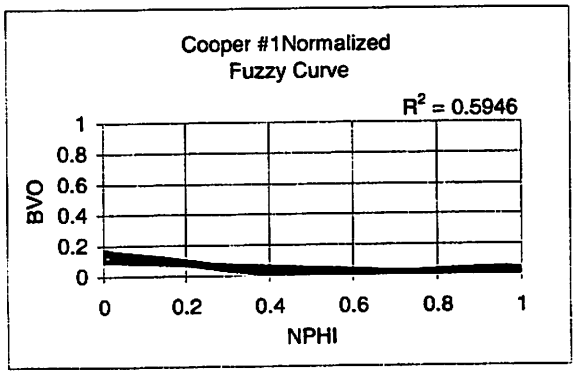

Figure A-45: Fuzzy Curve BVO vs GR **Figure A-46: Fuzzy Curve BVO vs Nphi**

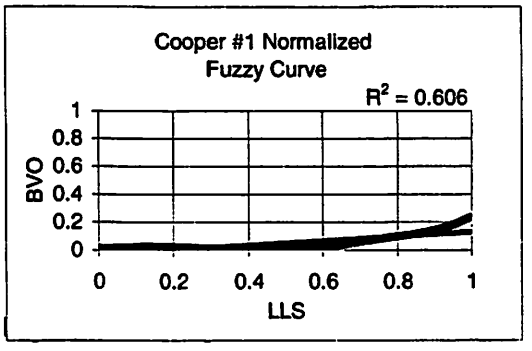

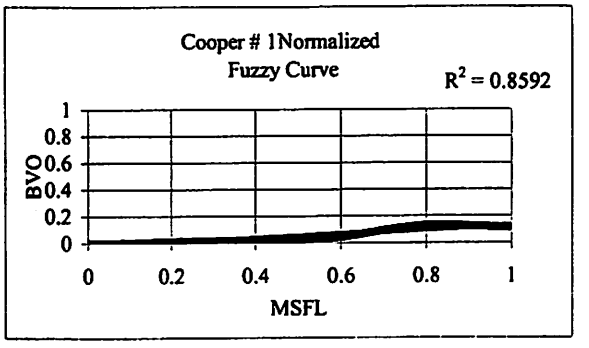

Figure A-47: Fuzzy Curve BVO vs LLS **Figure A-48: Fuzzy Curve BVO vs MSFL**

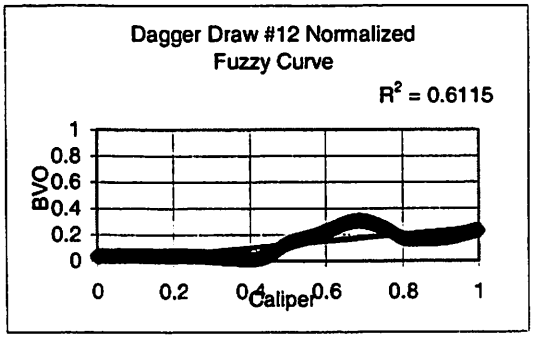

Figure A-49: Fuzzy Curve BVO vs Calip

Appendix B

Univarinat Plots

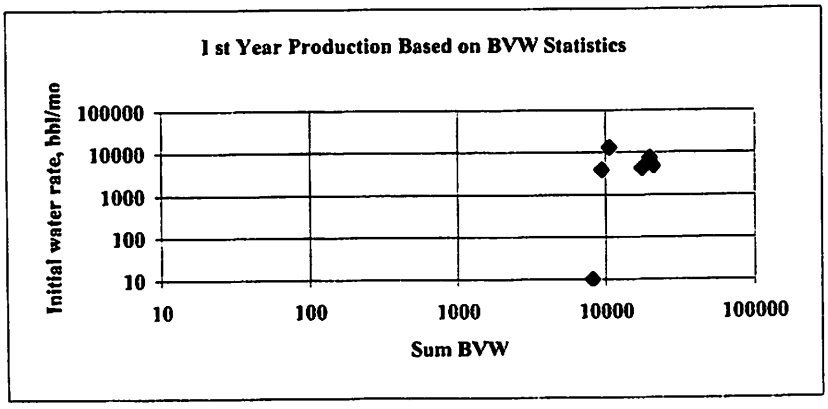

Figure B-1: Univariant plot of sum BVW and initial water rate

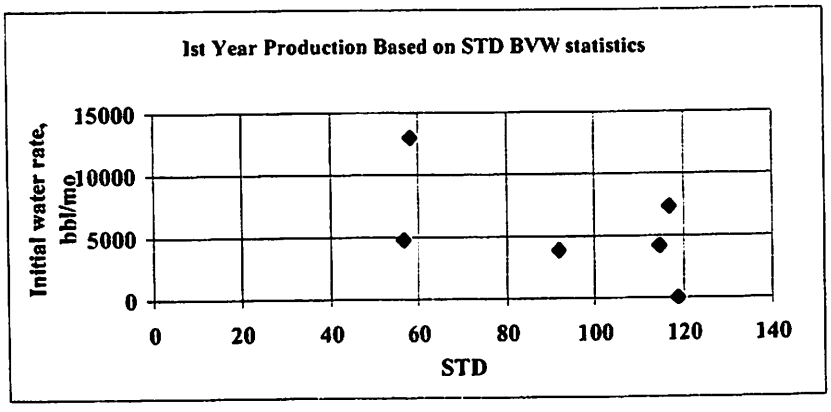

Figure B-2: Univariant plot of STD BVW and initial water rate

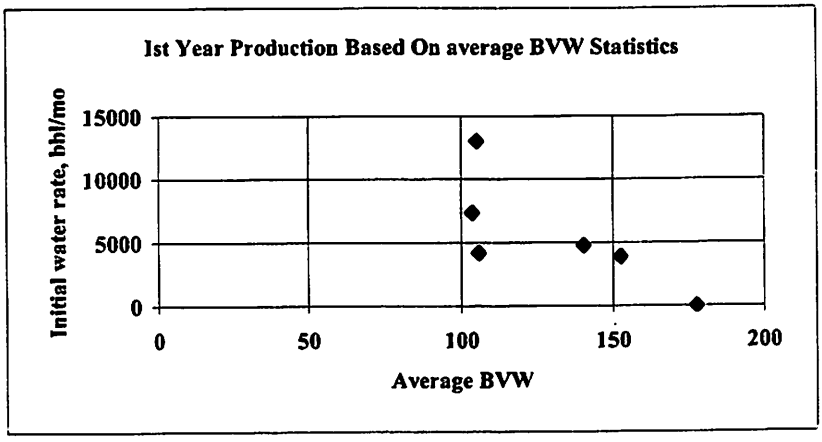

Figure B-3: Univariant plot of average BVW and initial water rate

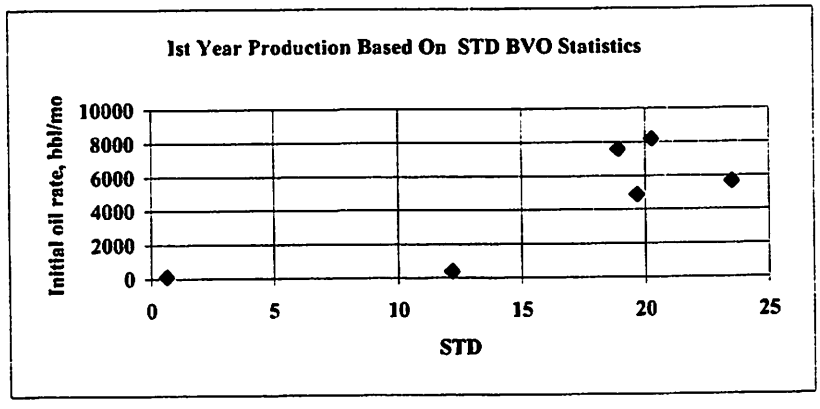

Figure B-4: Univariant plot of STD BVO and initial oil rate

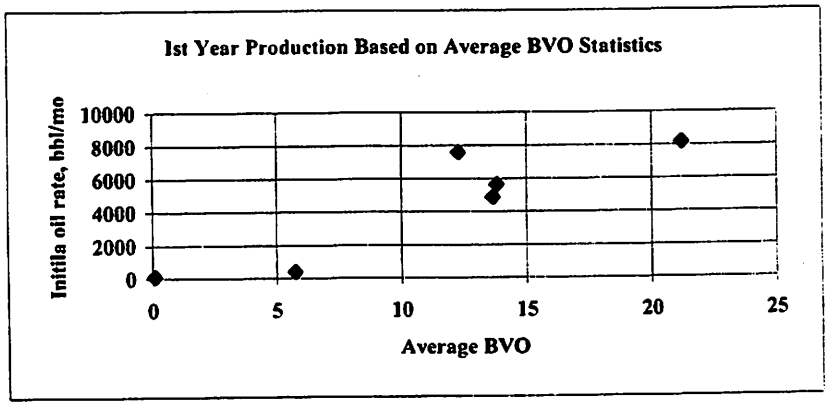

Figure B-5: Univariant plot of average BVO and Initial oil rate

Appendix C

Fuzzy Rank Plots

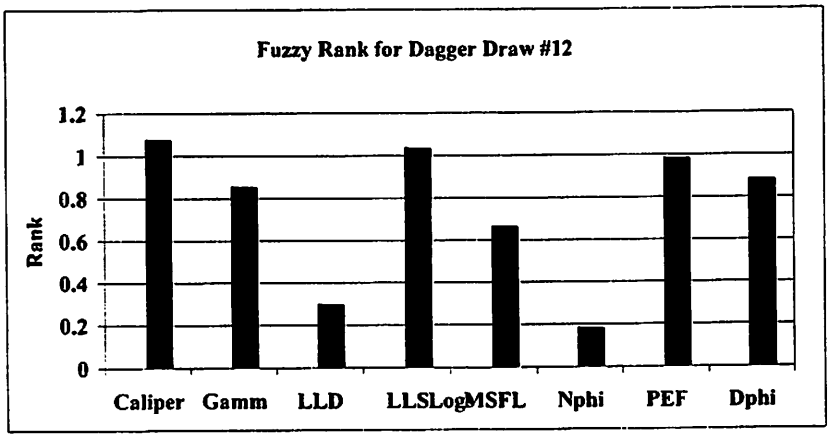

Figure C-1: Fuzzy ranks of Dagger Draw # 12 logs

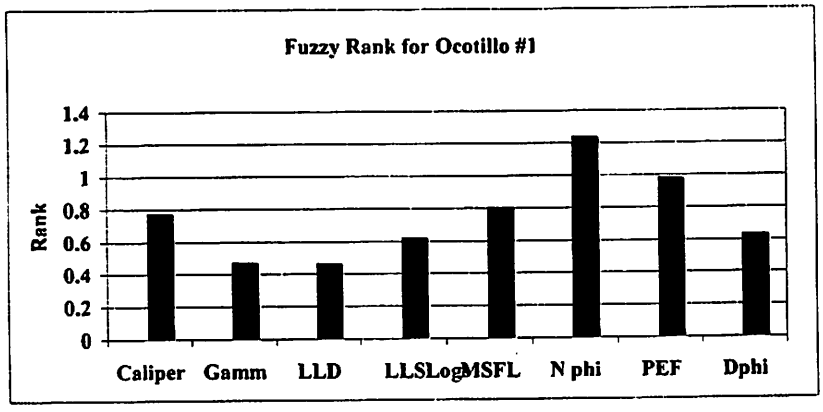

Figure C-2: Fuzzy ranks of Ocotillo # 1 logs

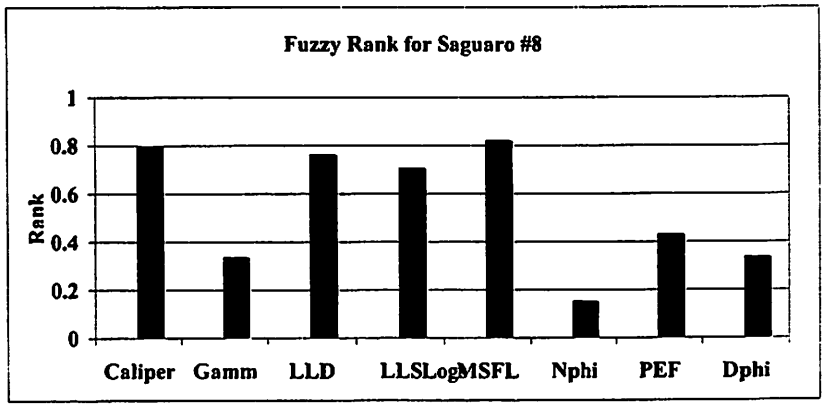

Figure C-3: Fuzzy ranks of Saguaro # 8 logs

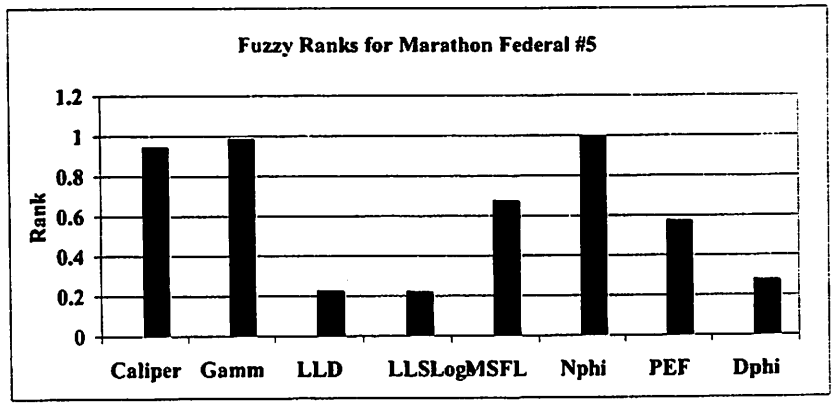

Figure C-4: Fuzzy ranks of Marathon # 5 logs

Appendix-D

Tables showing the rank and correlation coefficient of all logs

Bulk Volume Oil

Well	Architecture	CC	Input Logs for Training
MOC Federal #5	3-6-4-1	0.86	G-Ray, Caliper, LLS
Dagger Draw #12	3-8-4-1	0.95	Caliper, LLS, Dphi
Sagurao #8	3-6-4-1	0.80	Caliper, MSFL, Nphi
Cooper#1	3-4-2-1	0.62	G-Ray, LLS, Dphi
Barbara#12	3-4-4-1	0.69	Caliper, PEF, Nphi

Table D-1: Table showing the architecture, input logs used for training and training correlations for the Bulk Volume Oil of all the six wells.

Bulk Volume Gas

Well	Architecture	CC	Input Logs for Training
MOC Federal #5	3-6-4-1	0.6	G-Ray, MSFL, Dphi
Dagger Draw #12	3-6-4-1	0.92	PE, LLS, Dphi
Sagurao #8	3-8-4-1	0.7	Nphi, Caliper, Dphi
Cooper#1	3-3-2-1	0.75	Nphi, LLS, G-Ray
Ocotillo#1	3-6-4-1	0.68	Nphi, LLS, Dphi
Barbara#12	3-4-2-1	0.68	Nphi, LLS, Dphi

Table D-2: Table showing the architecture, input logs used for training and training correlations for the Bulk Volume Gas of all the six wells.

Bulk Volume Water

Well	Architecture	CC	Input Logs for Training
MOC Federal #5	3-6-4-1	0.72	Caliper, G-ray, Dphi
Dagger Draw #12	3-6-4-1	0.93	Caliper, LLS, Dphi
Saguaro #8	3-6-4-1	0.5	LLS, PEF, Nphi
Cooper#1	3-5-2-1	0.73	Nphi, LLS, G-Ray
Ocotillo#1	3-6-4-1	0.65	Caliper, PEF, Nphi
Barbara#12	3-4-2-1	0.79	LLD, MSFL, Nphi

Table D-3: Table showing the architecture, input logs used for training and training correlations for the Bulk Volume Water of all the six wells.

Dagger Draw #12 Bulk Volume Oil

Logs	Range	R^2	CC	Rank
Caliper	0.29	0.61	0.78	1.07
LLS	0.10	0.87	0.93	1.03
PEF	0.09	0.79	0.89	0.98
Dphi	0.21	0.44	0.67	0.88
G-Ray	0.06	0.62	0.79	0.85
MSFL	0.10	0.32	0.56	0.66
LLD	0.07	0.05	0.23	0.29
Nphi	0.09	0.01	0.10	0.19

Table D-4: Shows the range, correlation coefficient, and Fuzzy Rank

Dagger Draw #12 Bulk Volume Gas

Logs	Range	R^2	CC	Rank
LLS	0.24	0.75	0.87	1.11
G-Ray	0.25	0.73	0.85	1.1
PEF	0.31	0.58	0.76	1.07
MSFL	0.31	0.53	0.73	1.04
Caliper	0.42	0.21	0.46	0.88
Dphi	0.44	0.16	0.40	0.84
Nphi	0.43	0.04	0.20	0.62
LLD	0.17	0	0.06	0.23

Table D-5: Shows the range, correlation coefficient, and Fuzzy Rank

Dagger Draw # 12 Bulk Volume Water

Logs	Range	R^2	CC	Rank
LLS	0.09	0.74	0.86	0.95
PEF	0.13	0.61	0.78	0.91
MSFL	0.09	0.62	0.79	0.87
G-Ray	0.09	0.6	0.77	0.86
Dphi	0.27	0.28	0.53	0.8
Caliper	0.32	0.2	0.45	0.77
Nphi	0.14	0.07	0.26	0.41
LLD	0.08	0.04	0.20	0.28

Table D-6: Shows the range, correlation coefficient, and Fuzzy Rank

Dagger Draw #12 Aspect Ratio Fuzzy Ranks

Logs	Range	R^2	CC	Rank
Nphi	0.16	0.76	0.87	1.03
Caliper	0.19	0.63	0.79	0.98
G-Ray	0.24	0.43	0.66	0.89
MSFL	0.19	0.2	0.45	0.63
LLS	0.16	0.18	0.42	0.58
Delta LL	0.21	0.12	0.35	0.56
PEF	0.16	0.06	0.24	0.41
Dphi	0.16	0.03	0.17	0.33
LLD	0.19	0.01	0.10	0.28

Table D-7: Shows the range, correlation coefficient, and Fuzzy Rank

Saguaro # 8 Bulk Volume Oil Fuzzy Ranks

Logs	Range	R^2	CC	Rank
MSFL	0.045	0.597	0.77	0.82
Caliper	0.056	0.543	0.74	0.79
LLD	0.055	0.494	0.70	0.76
LLS	0.045	0.432	0.66	0.70
Dphi	0.066	0.132	0.36	0.43
G-Ray	0.111	0.049	0.22	0.33
PEF	0.255	0.006	0.08	0.33
Nphi	0.091	0.003	0.06	0.15

Table D-8: Shows the range, correlation coefficient, and Fuzzy Rank

Saguaro # 8 Bulk Volume Gas Fuzzy Ranks

Logs	Range	R^2	CC	Rank
Dphi	0.46	0.63	0.79	1.26
Caliper	0.31	0.88	0.94	1.25
PEF	0.24	0.79	0.89	1.13
Nphi	0.45	0.21	0.46	0.91
G-Ray	0.31	0.12	0.35	0.66
MSFL	0.18	0.21	0.46	0.64
LLS	0.37	0.07	0.26	0.63
LLD	0.31	0.01	0.10	0.41

Table D-9: Shows the range, correlation coefficient, and Fuzzy Rank

Saguaro # 8 Bulk Volume Water Fuzzy Ranks

Logs	Range	R^2	CC	Rank
LLS	0.37	0.51	0.71	1.08
Caliper	0.12	0.74	0.86	0.98
G-Ray	0.09	0.57	0.75	0.84
PEF	0.12	0.37	0.61	0.73
MSFL	0.22	0.22	0.47	0.69
Dphi	0.28	0.15	0.39	0.67
LLD	0.25	0.03	0.17	0.42
Nphi	0.17	0.01	0.10	0.27

Table D-10: Shows the range, correlation coefficient, and Fuzzy Rank

Saguaro # 8 Aspect Ratio Fuzzy Ranks

Logs	Range	R^2	CC	Rank
LLD	0.69	0.32	0.57	1.25
MSFL	0.49	0.21	0.46	0.95
PEF	0.07	0.71	0.84	0.92
Dphi	0.06	0.67	0.82	0.88
Caliper	0.07	0.58	0.76	0.84
G-Ray	0.11	0.31	0.56	0.66
LLS	0.18	0.16	0.40	0.58
Nphi	0.11	0.17	0.41	0.52

Table D-11: Shows the range, correlation coefficient, and Fuzzy Rank

Marathon # 5 Bulk Volume Oil Fuzzy Ranks

Logs	Range	R^2	CC	Rank
Caliper	0.160	0.785	0.89	1.05
Nphi	0.080	0.832	0.91	0.99
G-Ray	0.180	0.644	0.80	0.98
MSFL	0.070	0.362	0.60	0.67
PEF	0.060	0.267	0.52	0.58
Dphi	0.060	0.045	0.21	0.27
LLS	0.080	0.019	0.14	0.22
LLD	0.130	0.009	0.09	0.22

Table D-12: Shows the range, correlation coefficient, and Fuzzy Rank

Marathon # 5 Bulk Volume Gas Fuzzy Ranks

Logs	Range	R^2	CC	Rank
caliper	0.25	0.89	0.94	1.19
LLS	0.3	0.67	0.82	1.12
G-Ray	0.28	0.5	0.71	0.99
PEF	0.17	0.49	0.70	0.87
Nphi	0.1	0.58	0.76	0.86
LLD	0.27	0.06	0.24	0.50
Dphi	0.37	0.01	0.10	0.49
MSFL	0.02	0.01	0.10	0.12

Table D-13: Shows the range, correlation coefficient, and Fuzzy Rank

Marathon # 5 Bulk Volume Water Fuzzy Ranks

Logs	Range	R^2	CC	Rank
G-Ray	0.27	0.83	0.91	1.18
MSFL	0.15	0.84	0.92	1.06
Caliper	0.25	0.48	0.69	0.94
Nphi	0.02	0.65	0.81	0.83
LLS	0.2	0.26	0.51	0.71
LLD	0.17	0.17	0.41	0.58
PEF	0.1	0.19	0.44	0.55
Dphi	0.12	0.18	0.42	0.54

Table D-14: Shows the range, correlation coefficient, and Fuzzy Rank

Marathon # 5 Aspect Ratio Fuzzy Ranks

Logs	Range	R^2	CC	Rank
LLS	0.08	0.86	0.93	1.01
Dphi	0.09	0.51	0.71	0.80
LLD	0.09	0.44	0.66	0.75
Nphi	0.07	0.44	0.66	0.73
PEF	0.12	0.34	0.58	0.70
caliper	0.12	0.14	0.37	0.49
MSFL	0.05	0.1	0.32	0.36
G-Ray	0.09	0.01	0.10	0.16

Table D-15: Shows the range, correlation coefficient, and Fuzzy Rank

Ocotillo # 8 Bulk Volume Oil Fuzzy Ranks

Logs	Range	R2	CC	Rank
Caliper	0.533	0.730	0.039	0.769
Gamma	0.157	0.396	0.068	0.463
LLD	0.203	0.450	0.009	0.459
LLS	0.133	0.364	0.253	0.617
MSFL	0.576	0.759	0.041	0.800
Nphi	0.715	0.846	0.388	1.233
PEF	0.754	0.868	0.108	0.977
Dphi	0.108	0.328	0.303	0.631

Table D-16: Shows the range, correlation coefficient, and Fuzzy Rank

Cooper # 1 Bulk Volume Oil Fuzzy Ranks

Logs	Range	R2	CC	Rank
LLS	0.606	0.778	0.238	1.016
MSFL	0.859	0.927	0.132	1.059
Nphi	0.595	0.771	0.146	0.917
G-Ray	0.1038	0.322	0.116	0.438

Table D-17: Shows the range, correlation coefficient, and Fuzzy Rank

Barbara # 1 Bulk Volume Oil Fuzzy Ranks

Logs	Range	R2	CC	Rank
LLS	0.061	0.248	0.179	0.427
PEF	0.883	0.940	0.117	1.057
Nphi	0.535	0.732	0.107	0.839
G-Ray	0.689	0.830	0.144	0.974

Table D-18: Shows the range, correlation coefficient, and Fuzzy Rank

This thesis is accepted on behalf of the
Faculty of the Institute by the following committee:

Bill Weiss

Advisor

Sept. 9, 2002

Date

I release this document to the New Mexico Institute of Mining and Technology.

Student's Signature

09/09/2002

Date